THE EFFECT OF OPERATING PARAMETERS ON THE WEAR BEHAVIOUR OF DISC POPPET VALVES IN RECIPROCATING SLURRY PUMPS

by

S.H.D. Joffe

A thesis submitted to the Faculty of Engineering, University of Cape Town in the fulfilment of the degree of Masters of Science in Engineering.

Department of Materials Engineering
University of Cape Town

July 1988

ABSTRACT

An investigation has been carried out to determine the factors controlling the wear characteristics of disc poppet valves in reciprocating slurry pumps used in the transportation of quartzite slurries. A laboratory test rig has been designed and built which closely simulates the operating conditions experienced by slurry pump valves.

Experiments have been conducted to determine the effect of the design parameters, namely - slurry constitution, valve closure velocity and valve angle, on the wear resistance of a low alloy steel, as a function of its mechanical properties.

It has been shown that the wear of the valves is a sensitive function of the operating parameters. Significant improvements in the life of the valves can be achieved through increasing material hardness, reducing valve closure velocity, slurry density and valve angle.

A detailed study has been made of the mechanisms contributing to valve wear. It has been established that both percussive impact and three body abrasion wear mechanisms predominate. The influence of each mechanism has been shown to to be a function of the slurry constitution and the material hardness.

ACKNOWLEDGEMENTS

I would like to thank all those in who assisted me during the course of this research project.

I am grateful to Professor Colin Allen for his guidance and support.

I am thankful to Mrs Helgard Böhm, Miss Suzie Betz and Mrs Anne Ball for their assistance. Bernard Greeves and James Petersen are thanked for their help with equipment and photographic work.

I wish also to thank Mrs Shirley and Miss Heidi van der Meulen for their assistance in the preparation of this manuscript.

The work of Mr Glen Newins and Mr Nick Dreze of the workshop is gratefully acknowledged.

Special thanks are extended to my colleagues in the department of Materials Engineering.

In addition I would like to thank the Chamber of Mines Research Organization (COMRO), both for their sponsorship and co-operation.

CONTENTS **Page**

1. INTRODUCTION

The hydraulic filling of stopes in deep level mines with comminuted waste slurries, is regarded as an attractive means of controlling the convergence of stopes, absorbing energy released from the surroundings and increasing the percentage extraction of gold from wide reefs (45).

The Chamber of Mines Research Organization (COMRO) is currently developing a backfilling system for deep level South African gold mines. The concept of backfilling essentially involves the communition of waste rock underground and its return by hydraulic transport to the working face or stope to provide underground support, so improving mining conditions. Although hydraulic stope filling or backfilling has been practiced in other parts of the world for at least 25 years, it had not been used to a large extent in South Africa prior to 1977 (81). The reason primarily was that the technology required to pump the high concentration slurries, which developed the high backfill strengths in the stopes, was inadequate.

The comminuted waste rock consists primarily of quartzite which has been crushed to a diameter of 6mm or less. Water is then added to the crushed rock to produce a slurry which consists of approximately 80 per cent solid (specific gravity of 2.1 g/cm^3) by mass. The viscous slurry is pumped at high pressure and low velocity for distances of over a kilometer. The high pressure gradients necessitate the use of high pressure reciprocating slurry pumps.

Schwing positive displacement or reciprocating slurry pumps, originally designed to pump concrete, are used to pump backfill slurries. The Schwing valve assembly is illustrated in fig.1.

The Schwing slurry pump is an hydraulically powered twin-cylinder reciprocating pump. The slurry flow is controlled by means of disc poppet valves. Each pumping cylinder has one suction and one pressure valve. The poppet valves are actively controlled, being operated in such a manner that on the side of the intaking piston the suction valve is opened and the pressure valve is closed. During the pumping stroke the suction valve is closed and the pressure valve open. At the end of a stroke, reversal of the valves ideally takes place in such away that the formerly open valves are closed before the closed valves are re-opened.

Fig.1 Cast Schwing valve housing showing the positions of the pressure valve (a) and suction valves (b).

Although similar pumps are used abroad to pump backfill (19,46), it would appear that the service-life of valve bodies and discs in South Africa is considerably lower due to the highly abrasive nature of the quartzite slurry. Experience to date has shown that the useful life of the valve poppet and seat can be as low as 30 hours, corresponding to 700 tonnes of dry solids (6). A valve is usually classified as a failure when an excessive loss in pumping pressure occurs due to improper sealing of the worn valve. The delivery or pressure valves reportedly wear much faster than the suction valves. An example of a pressure valve failure can be seen in fig.1.1 where both abrasive and erosive wear are evident.

Abrasive wear is caused when particles are trapped between the valve poppet and the seat on valve closure. The hard particles indent the valve material leading to surface deformation and material removal. An extensive investigation of the pressure valve by Barnett (9), concluded that the particularly severe preferential wear of the pressure valve was caused by a stationary bed of abrasive quartz at the base of the valve which became trapped between the poppet and seat on closure. This uneven wear, coupled with the high differential pressures across the valve, caused slurry to flow rapidly through the gap which formed, resulting in flow erosion of the valve material.

Fig.1.1 A typically worn pressure valve showing both abrasive and erosive wear.

Since the high wear could be attributed to the valve orientation, Barnett suggested that the problem could be remedied by redesigning the valve chamber so that none of the valves closed in the horizontal plane. It was also established by Barnett that the suction valve in contrast to the pressure valve only suffered general wear. Consequently it was decided to simulate the operation of this valve in a laboratory test rig in order to study the parameters affecting wear rate and to facilitate a better understanding of the wear mechanisms.

2. AIMS AND OBJECTIVES

The general aims of this research programme of work were to establish the important operating parameters controlling the life of disc poppet valves in a Schwing pump used in the transportation of quartzite slurries, and to correlate the valve wear resistance with microstructural parameters. The overall objective was to suggest modifications to the design of reciprocating or positive displacement pumps to maximize wear resistance.

The specific objectives were to:

(i) Establish the effects of different design parameters, namely slurry constitution, valve closure velocity and valve geometry on the wear of disc poppet valves.

(ii) Ascertain the wear mechanisms.

(iii) Investigate the effect of valve hardness on wear.

3. LITERATURE REVIEW

3.1 Introduction

In addition to the high wear rates which are typically experienced in slurry pipelines as a result of the transportation of the highly abrasive quartzite slurries, severe wear is also experienced in valves, pistons and cylinder liners of the reciprocating slurry pumps. An extraordinary number of basic wear modes have been identified by Miller (46) acting either individually or in combination during the pumping of slurries.

However it was established by Barnett (9) that the two predominant wear modes responsible for wear of disc poppet valves in reciprocating slurry pumps are abrasive and impact wear.

Although the wear of disc poppet valves by quartzitic slurries is a specific problem, an examination of fundamental wear knowledge from research by others can significantly contribute to the interpretation of test results and ultimately lead to a better understanding of the problem.

3.2 Abrasion

A broad range of definitions exist for abrasive wear but probably the most useful is the one proposed by McQueer (44) in her discussion, which states that abrasive wear should be regarded as *any damage or alteration occurring at the surface of a solid component, due to the relative motion across that surface of particles capable of cutting or grazing it*.

This definition not only considers the removal of material by the mechanical action of the abrasive but draws attention to the fact that other surface damage or changes in the surface layers as a result of exposure to an abrasive environment should also be considered. Such alterations include plastic deformation, phase changes and recrystallisation, which, while not causing the loss of surface material directly, interact with the mechanisms which produce such loss. Resistance to abrasive wear is not an intrinsic material property but is dependent upon the variables in the system. The response to abrasive wear depends on the interaction of material properties, the properties of the abrasive and the environmental conditions (63).

3.2.1 Classification of Abrasive Wear

Abrasive wear processes are traditionally divided into two groups namely two body and three body abrasive wear according to Finnie and Misra (47,48).

Two body abrasive wear *occurs when a rough surface or fixed abrasive particles move relative to a second surface resulting in damage to that surface.* In contrast, three body abrasive wear arises when *loose abrasive particles capable of moving freely relative to one another cause damage to the wearing surface.* The loose abrasive particle trapped between the two surfaces constitute the three bodies in the later case.

Finnie and Misra (47) maintain that two body abrasive wear is a relatively clearly defined process in contrast with three body abrasive wear where several subdivisions may arise. In three body abrasion, two surfaces are not necessarily required as they may be so far apart that the mechanical properties of one surface have no influence on the wear of the other. Three-body abrasive wear was thus classified as being either "closed" or "open".

Closed three body abrasive wear occurs when loose abrasive particles are trapped between two sliding or rubbing surfaces which are relatively close to one another. In this type of wear, particles may indent or embed into the softer surface. Embedded particles may subsequently cause wear of the other harder surface through two body abrasion.

Open three body abrasive wear occurs when the two surfaces are far apart or when only one surface is involved in the wear process. Finnie and Misra (47) used Avery's (3) classification to further subdivide *open* three body abrasion into three categories:

1) Gouging: A condition in which coarse abrasive particles cut deep into the wearing surface with considerable force, producing deep gouges and removing macroscopic particles from the surface.

2) High stress: This occurs when two wearing surfaces (e.g. grinding balls and the liner of a ballmill) come together in a gritty environment with enough mechanical force to crush the abrasive particles entrapped between them.

3) Low stress: This is defined as a condition in which the stresses imposed on the abrasive particles do not exceed the crushing strength i.e. particles are transported along the surface with a rolling or sliding action.

This classification of abrasive wear is summarized below,

- Abrasive wear
  - two body
  - three body
    - closed
    - open
      - gouging
      - high stress
      - low stress

However care should be exercised when attempting to classify the abrasive wear since it is possible that a combination of more than one type of abrasion may be responsible for the actual wear of the component in service.

An additional problem exists with the above classification of abrasive wear, because consensus regarding the definition of three body and two body wear has not been reached. Misra's (47) classification of open low stress three body abrasion for instance is equivalent to two body abrasive wear as defined by Eyre (17).

A comparison should not be made on the basis of the classification system alone since each wearing system is unique. Instead, a classification should only be attempted after careful assessment of both the internal and external variables governing the wear process.

3.2.2 Models

Mathematical models of abrasion are necessarily oversimplifications of a very complex process and are used to predict the effect of certain variables on the wear process.

Consider an abrasive particle in contact and moving across the surface of a ductile material as shown in fig.3.1. According to Moore (55) two major processes occur namely :

1) The formation of grooves i.e the material is displaced laterally to form ridges. No direct material removal occurs.

2) The separation of material in the form of primary wear debris or microchips.

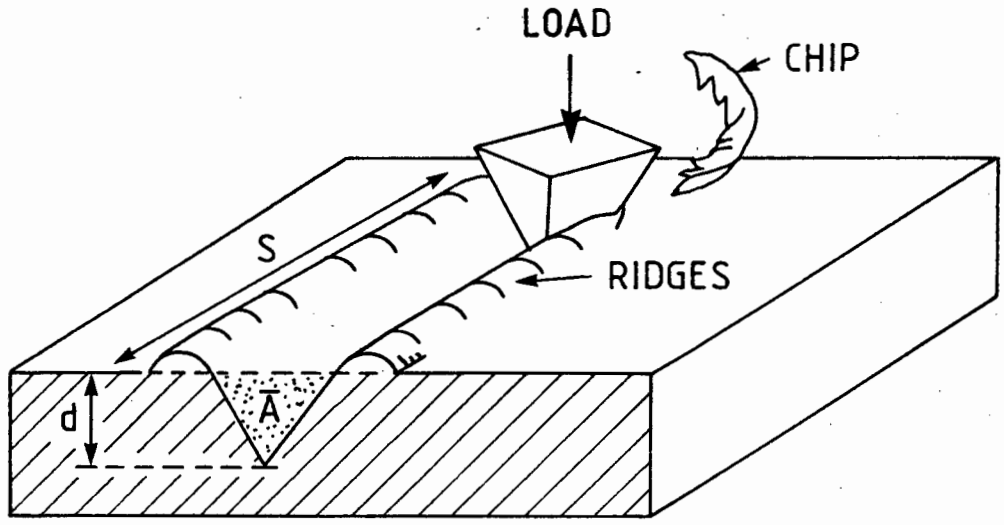

Fig.3.1 A simple model of abrasive wear (53)

A model for abrasive wear resistance similar to that used by Khruschov (34) in his pioneering work was later used by Rabinowicz, Dan and Russell (64) to predict a linear relationship between hardness and wear resistance for commercially pure and annealed metals (fig.3.2). The wear rate is described by the equation,

$$\frac{dV}{dS} = L\left(\frac{\tan\theta}{\pi H}\right) \qquad \ldots\ldots\ldots 3.1$$

where H - hardness of material
dV - volume removed
dS - relative movement
L - load

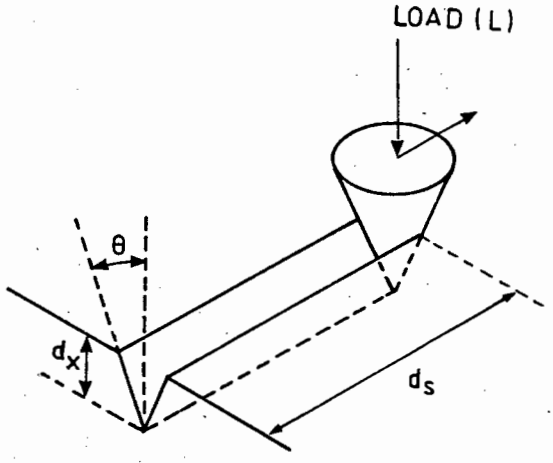

Fig.3.2 Schematic illustration of a conically ended grain which removing material from a metal surface (64).

Earlier Khruschov and Babichev (34) had postulated that for heterogeneous materials such as steels, the wear resistance was proportional to the volume fraction of the individual components,

$$\epsilon = \alpha\epsilon_1 + \beta\epsilon_2 \qquad \ldots\ldots\ldots 3.2$$

where α and β are volume fraction of phases ϵ_1 and ϵ_2 having bulk wear resistance ϵ_1 and ϵ_2 respectively

This model fails to explain why materials of the same hardness have different wear properties under similar conditions, nor does it describe why steels exhibit a lower wear resistance than pure metals.

Larsen-Badse and Mathew (39) modified equation (3.1) in an effort to include the effects of work hardening. They proposed the equation,

$$\epsilon = CHe^n \qquad \ldots\ldots\ldots 3.3$$

Where
- ϵ abrasion resistance
- H hardness of the material
- C is constant
- n normal strain exponent from true/strain curve

Mutton and Watson (59) identified a problems with equation (3.3). It is assumed that all metals can be fitted equally well to a single stress strain curve.

Mutton and Watson (59) identified a problem with equation (3.3). It is assumed that all metals can be fitted equally well to a single stress strain curve.

Probably the best model to date, is the model presented by Moore (53), which shows that for a number of successive particles the volume removed may be represented by the following equation,

$$V = K_1.K_2.K_3.S.\sigma/H \qquad \ldots\ldots\ldots 3.4$$

Thus the volume of material removed during abrasion depends on the variables in the equation (3.4) which can be classified into three main groups:

Material properties : K_1 - The proportion of groove volume removed
H - Hardness of the material

Abrasive properties : K_2 - Particle shape and size

External variables : K_3 - The proportion of abrasive particles making contact with the surface
S - abrasion path length
σ - The applied load per unit area

The most recent models have attempted to link wear mechanisms to various microstrutures and properties, but have achieved only moderate success (24,90).

The inability of these simple models to explain the results for heat treated steels and the contradictory nature of some of the models, suggest that abrasion resistance is not an intrinsic mechanical property and therefore it cannot be modelled by a simple mathematical model. The entire tribological system must be considered.

3.2.2 Material Properties influencing abrasive wear

3.2.2.1 Hardness and Composition

The hardness of the abraded material is generally considered to be the most important parameter in the selection of an alloy because it controls the depth of penetration of the abrading particle (23,25,58).

It was Khruschov (34), in his pioneering work, who established that the relative abrasion wear resistance (Px/V) was proportional to the bulk hardness of pure and annealed metals. Khruschov (35) later extended his work

(fig.3.3). This work was further extended to include sand slurries as the abrasive medium (fig.3.4).

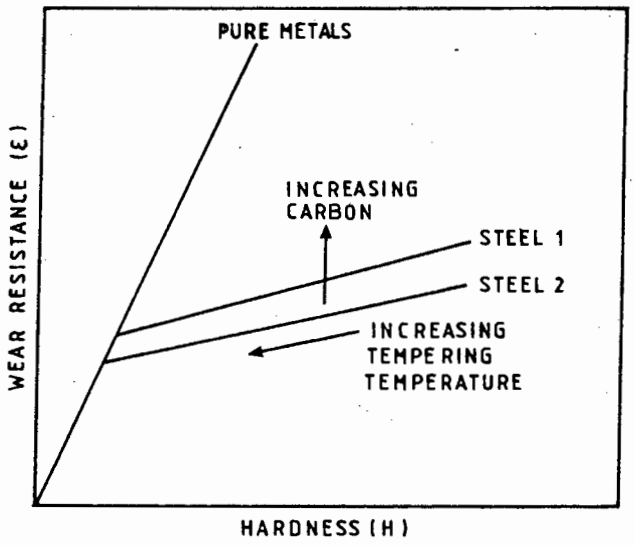

Fig.3.3 The effect of hardness of metals on abrasive resistance (34).

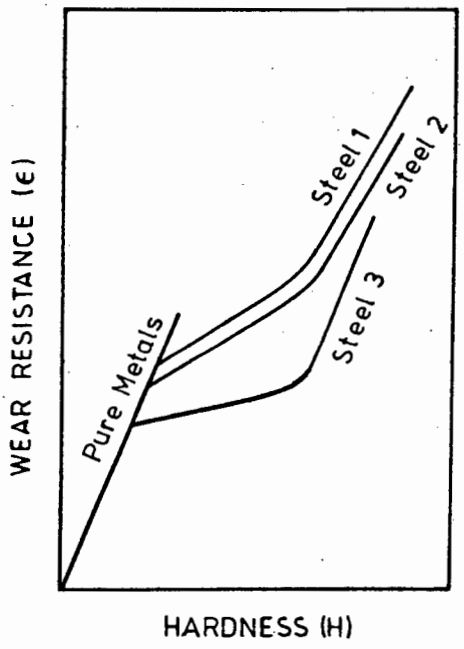

Fig.3.4 Heat treated steels subjected to wear by sand slurries (35).

Khruschov (34) reached the following conclusions:

1. At a given hardness, the wear resistance of a heat treated steel is significantly less than that of a pure metal of equivalent hardness.

2. As the carbon content of the steel is raised the wear resistance versus hardness curve is displaced to higher values of wear.

Several researchers extended the investigation of abrasive wear properties to commercially pure annealed metals and carbon steels (35,38,69).

Mutton and Watson (59) showed (fig.3.5) that the relationship between wear resistance and hardness for different steels is better described by a series of sigmoidal curves and suggested that the relatively low slope obtained for carbon steels is not simply related to the hardness, but to microstructure also.

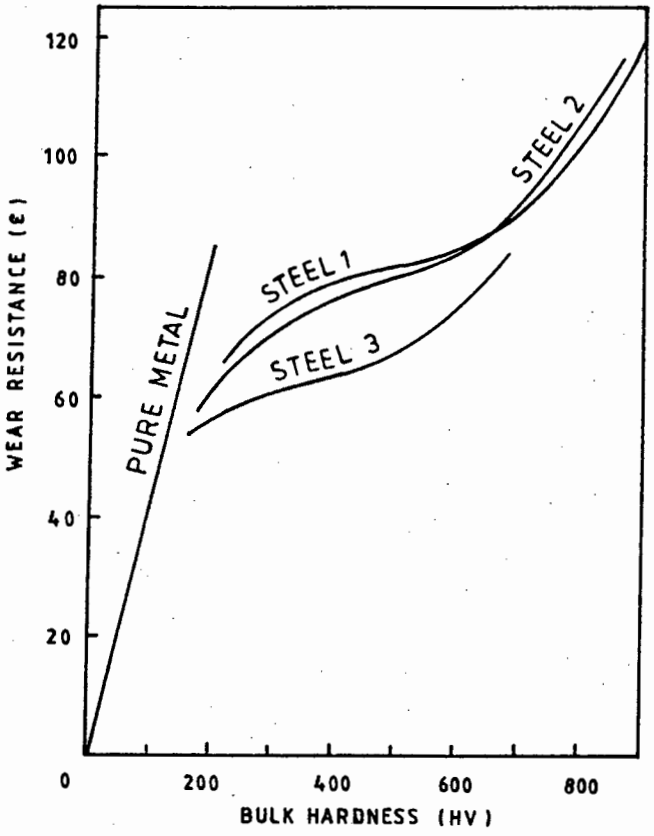

Fig.3.5 Wear resistance as a function of hardness for three quenched and tempered steels (59).

Since it is well established that abrasive wear resistance is a function of the particle abrasivity (45), reference should not be made directly to material bulk hardness but to relative hardness (Ha/H) i.e. the ratio of the abrasive hardness (Ha) to that of the wearing

material (H). Elkholy (16) clearly took cognizance of this when he plotted his slurry abrasive test results (fig.3.6). His results compare favorably with those of other workers (35,59).

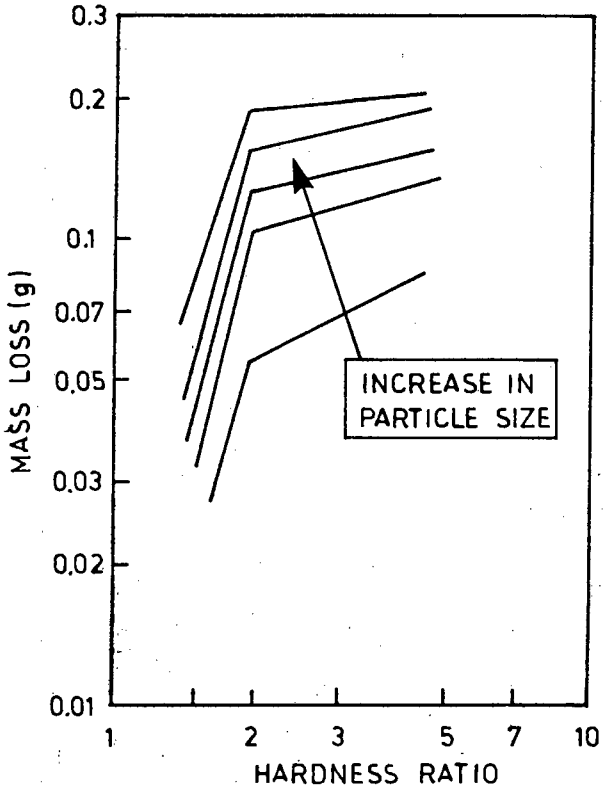

Fig.3.6 Relative hardness (Ha/H) vs. mass loss for a number of quench and tempered steels in sand slurries (16).

A number of workers including Richardson (69) have attempted to explain the deviation in the wear resistance curve for steels by relating it to surface hardening characteristics rather than bulk hardness but they have experienced only moderate success.

Prasad and Kulkarini (62) have concluded that neither hardness nor morphological characteristics alone can explain abrasive wear resistance and that it would be better to consider a broader range of mechanical properties.

3.2.2.2 Work hardening

According to Angus (2) it is not the initial bulk hardness which is important but rather the hardness of the work hardened surface layer. However Khruschov and Babichev (34) showed that wear resistance is relatively independent of prior cold working. They proposed that

this was because the material reached a limiting hardness and flow stress during abrasion, irrespective of any work hardening applied previously. Richardson (68) also studied the effects of prior cold working on metals but could not find a satisfactory relationship between wear resistance and strained surface hardness.

Moore and Richardson (50) ascribed the limiting strength of the worn surface to the microstructure and the addition of alloying elements. Zum-Gahr and Mewes (87) showed that the abrasive wear resistance is proportional to the shear strength of the abrading surface, which explains why a better correlation between abrasive wear resistance and hardness of the worn surface has been found experimentally.

Garrison (23) related the mechanism of material removal to the work hardening capacity (fig.3.7). He illustrated with reference to pile up geometry that material is more easily ploughed in an alloy with a low work hardening capacity (n). This is in agreement with Ball (5) who argued that the optimal alloy is one with a moderate yield strength but a high work hardening capacity.

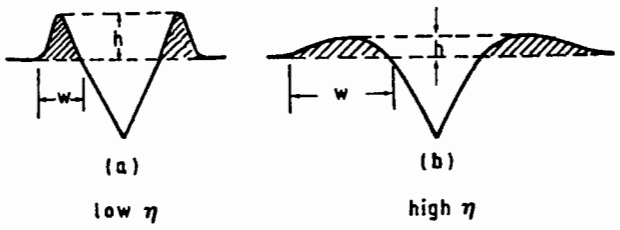

Fig.3.7 The effect of workhardening capacity on the pile up geometry of a steel (23).

3.2.2.3 Properties of the wearing Material

Although hardness is an important parameter, it is not always true that the hardest material offers the most wear resistance. It is therefore important to consider other metallurgical variables which influence wear resistance. Various attempts have been made to relate wear resistance to other properties including Young's modulus and yield strength. However these relationships are no better than those related to hardness. This is not surprising according to Eyre (17) because all mechanical properties are related. Allen, Protheroe and Ball (5) suggest that the microstructural approach to wear

of abrasion resistance than those based only on simple mechanical properties such as hardness.

Moore (52) divided the role of microstructure in abrasive wear into two major effects:

1) Bulk properties - this includes bulk matrix structure and grain size

2) Inclusions - i.e. distribution of dispersed phases, their coherency, size, shape and hardness

It is generally recognized that most ferrous martensitic materials exhibit abrasive wear resistance superior to ferritic, pearlitic or bainitic materials. Moore (52) has shown that it is the structure that determines the hardness and flow stress and hence the abrasion resistance (fig.3.8).

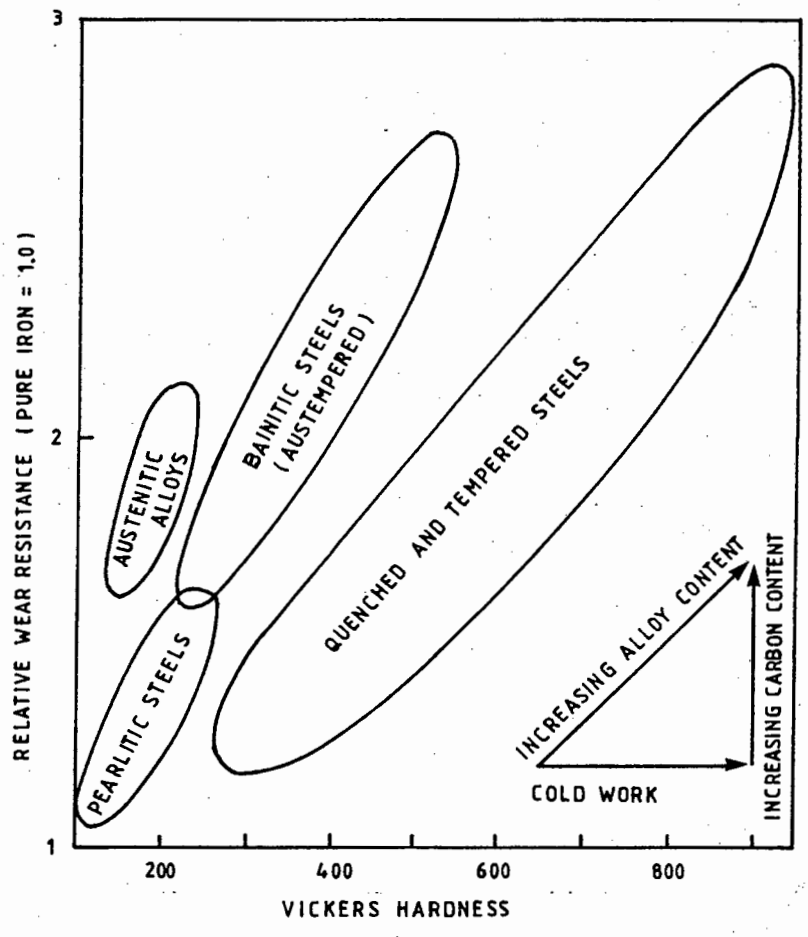

Fig.3.8 Effect of structure, heat treatment and alloy content on the wear of steels (Worn on 90μm Al_2O_3 abrasive, 1 MN/M^2 applied Load) (52).

Additions of alloying elements can improve hardenability and hence wear resistance if they alter the microstucture

significantly (31,70). Increasing the carbon content increases the hardenability, bulk hardness and volume fraction of alloy and iron carbides. Abrasion resistance decreases after the addition of more than 1% carbon (22). The addition of chromium to steel improves both strength and toughness but has only a moderate effect on abrasive wear resistance (37). The addition of molybdenum may reduce the severity of temper embrittlement, during heat treatment, which sharply reduces fracture toughness and wear resistance in Fe-Cr-Mn-C alloys, as continuous films of high carbon interlath retained austenite transform to iron carbide and thus promotes unstable crack propagation. At higher tempering temperatures carbides continue to grow and eventually spheroidize, resulting in a reduced stress concentration and hence a reduction in the crack tendency (13). The addition of manganese decreases the interlameller spacing in pearlite resulting in an increase in the impact and fracture toughness without a loss in strength which in turn results in improved wear resistance.

Several investigators have observed that retained austenite appears to enhance wear resistance in steels (22). Kar (30) studied a series of secondary hardening steels, and found bainitic microstructures containing a substantial amount of retained austenite, generally exhibited better wear resistance than quenched and tempered microstructures at similar hardness levels. Khruschov (34) suggested that the lower wear resistance of quenched and tempered steels may be related to the presence of high internal stresses in the quenched steel, which contributes to their poor fracture toughness compared to bainitic structures containing retained austenite.

Kwok and Thomas (37) ascribed the enhancement of wear by the retained austenite to:

1. The transformation induced plasticity (TRIP) of austenite to martensite which can absorb energy for fracture and produce local compressive stresses that impede microcrack formation.

2. The presence of a ductile austenite film between the martensite laths discouraging microcrack nucleation and propagation.

3. An increase in the work hardening coefficient (n) through TRIP.

4. The retention of retained austenite at lath boundaries preventing brittle lath boundary carbide formation. In the case of low carbon steels the distribution and morphology of retained austenite may be more important than the relative amount present.

Salesky and Thomas (73) have suggested that a high strength/toughness microstructure such as an austentic-martensitic microduplex structure is the optimum steel for reducing wear, which is agreement with Fogel (37).

Most engineering materials used in abrasive wear environments, have structures of hard carbides in either hardened or soft matrices.

The carbides in the microstructure of the metal should be harder than the abrasive and the matrix should be strong enough to support the carbides and prevent fracture. In low stress abrasion, the presence of massive carbides (harder than the abrasive) in the matrix of martensite is preferable to a carbide-free martensitic structure of similar bulk hardness (2). Larsen-Badse and Mathew (39) found that a finely dispersed hard phase influences the flow stress of the material and thereby increases the abrasion resistance according to a Hall-Petch type relation (i.e. the abrasion resistance is inversely proportional to the square root of the distance between the dispersed particles). They conclude that coarse particles only contribute to abrasion resistance because they directly offer a hard surface. Thus ideally a fine distribution of spherical carbides is required for abrasion resistance. However the nature of the carbide/matrix interface bond controls the wear resistance (30).

The coherency between precipitates and matrix increases as the shape of the carbides change from spheroids to needles, which resist pullout most efficiently but produce planes of weakness in the bulk material leading to macro-fracture and spalling (44,62). Thus a high volume of fine acicular coherent carbides strongly bonded to the matrix will improve abrasive wear resistance. Fogel (22) notes that a too high volume fraction can have adverse effects.

Sare (74) concludes that the wear rate is a balance between carbide removal and matrix removal, the slower of the two governing the overall wear rate. In low-stress abrasion, the carbides will retain sufficient support to resist pullout and fracture as preferential wear of the matrix will be slight, and gradual attrition of the carbides will thus control the wear rate. Preferential wear of the matrix becomes more significant under high-stress conditions, and carbides will more easily be pulled out and fracture - implying that the removal of the matrix governs the wear rate.

3.2.3 Abrasive Characteristics

3.2.3.1 Abrasive hardness

It has been well established that a material must be significantly softer than an abrasive if it is to wear to any extent. Richardson (69) showed that, for many combinations of metals and abrasives, abrasive wear decreases rapidly when the abrasive hardness is less than 1.25 times the hardness of the metal, H i.e. the relative hardness Ha/H must be greater than 1.25 for substantial wear to occur. Torrance (80) showed by applying a simple slip line field model to the abrasive metal contact, that abrasive wear should become significant when Ha/H ≈ 1.16 and should increase rapidly to a maximum and level out when Ha/H ≈ 1.26. This result was verified experimentally by Misra and Finnie (48) (fig.3.9).

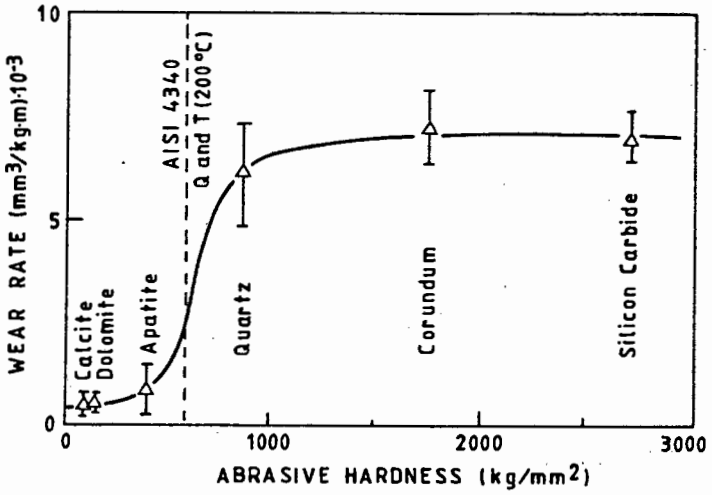

Fig.3.9 Wear rate as a function of abrasive hardness (Ha) for AISI 4340 steel quenched and tempered at 200°C, and abraded by 250μm size particles (48).

Richardson (70) reported that scratching of a material by an abrasive continues even when the relative hardness (Ha/H) drops below unity and only ceases when the flow stress of the the material equals that of the abrasive.

It was generally found that for a relative hardness of Ha/H >2, the relative wear resistance was almost independent of hardness of the metal matrix (fig.3.10). In martensitic steels the presence of carbides increased the wear resistance but this effect was suppressed with harder abrasives. It was Moore (52) who reported that wear resistance is almost independent of particle size when relative hardness is less than 1.2, and is sensitive to particle size when Ha/H is greater than 1.2. This

effect was ascribed to blunting and fracture of abrasive grains as a result of plastic flow.

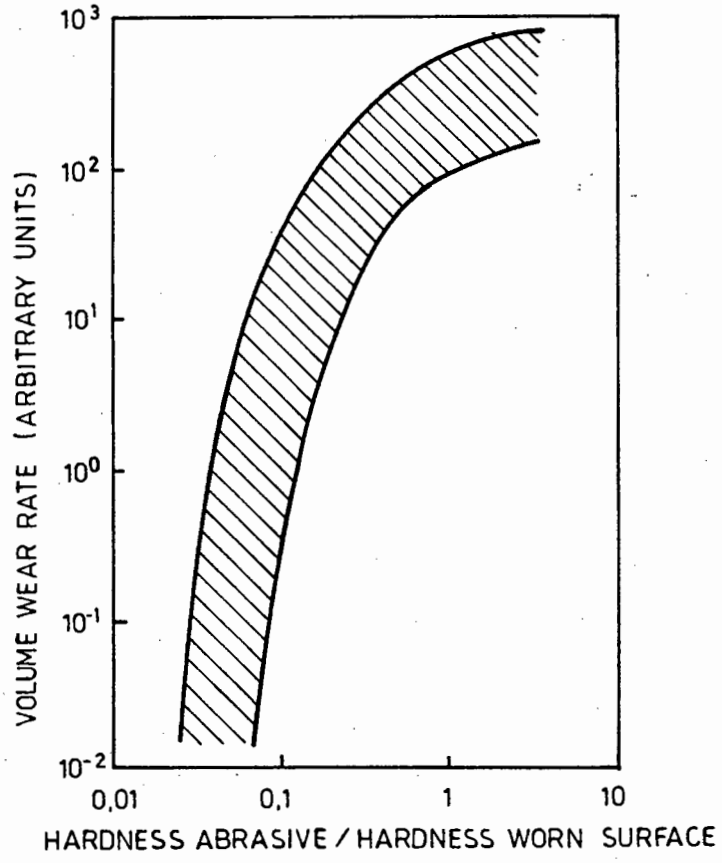

Fig.3.10 The effect of relative hardness (Ha/H) on a metallic material by a range of different abrasives (70).

3.2.3.2 Geometric properties

It is generally agreed that in addition to hardness, the size and shape of the abrasive particle are important factors influencing abrasion wear rates.

It has been found typically that volume wear is greater for coarse abrasives (43,48,64). The observed decrease in the abrasion rate with decreasing abrasive particle size below some critical size, which is generally considered to be about 100 microns, is termed the size effect. Above the critical size the abrasion rate is approximately constant (fig.3.11), although some studies have shown an increase in abrasion rate with size above the critical size (fig.3.11) (48).

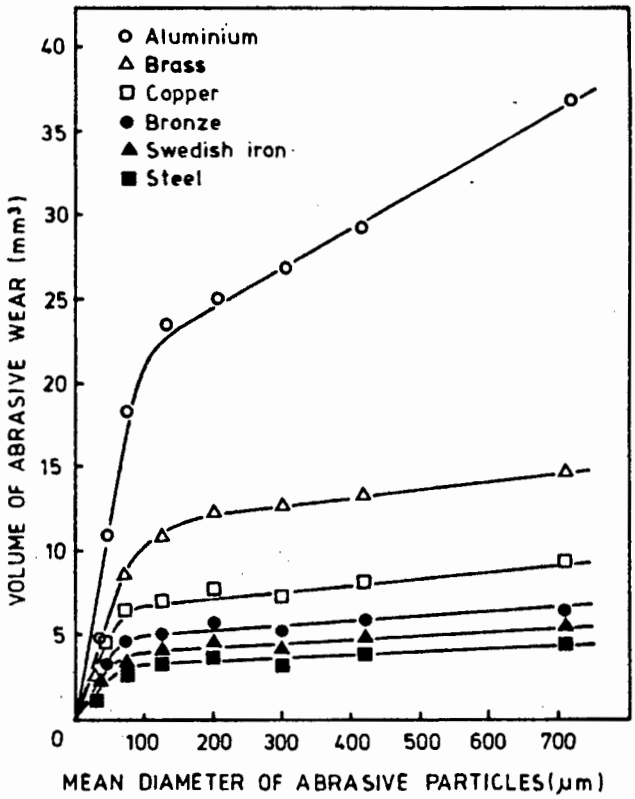

Fig.3.11 The effect of particle size of an alumina abrasive on different metal surfaces (52).

It has been suggested that the surface layers 50-100μm thick work harden more than the bulk of the material. Thus when small particles abrade the surface, they only influence the workhardened layer and thus encounter much harder material than do larger particles which will deform the material to a greater depth. After some critical particle size, the influence of the outer workhardened layer will be slight, and thus there will only be a small increase in wear rate for a further increase in particle size (49,64).

When the ratio of material hardness to the abrasive hardness exceeds unity, blunting of the abrasive by plastic flow can occur. Whilst plastic flow tends to blunt the abrasive, fracture may well regenerate cutting facets. The probability of an abrasive having a suitably oriented defect increases with particle diameter and load. These larger particles are more likely to fracture than fine or lightly loaded abrasive particles.

Moore (51) also attempted to explain the increase in wear with particle size. He concluded that greater loads are carried by fewer particles and as a result wear is more severe.

The shape of the particle rather than the size determines wear rates, as only a fraction of the abrasive particles

according to Vingsbo (83) which is in agreement with Wang (84).

Abrasivity of a particle has been defined by Miller (45) as being a function of hardness and shape of the abrasive particles. He has developed an ASTM standard known as the Miller number to classify slurries according to abrasivity.

It is generally agreed that particle shape and size have a significant effect on the material removing mechanism.

3.3.3.2 Concentration

Elkholy (16) has found that wear increases with increasing solid particle concentration and with increasing abrasive particle size for sand slurries. He does not attempt an explanation.

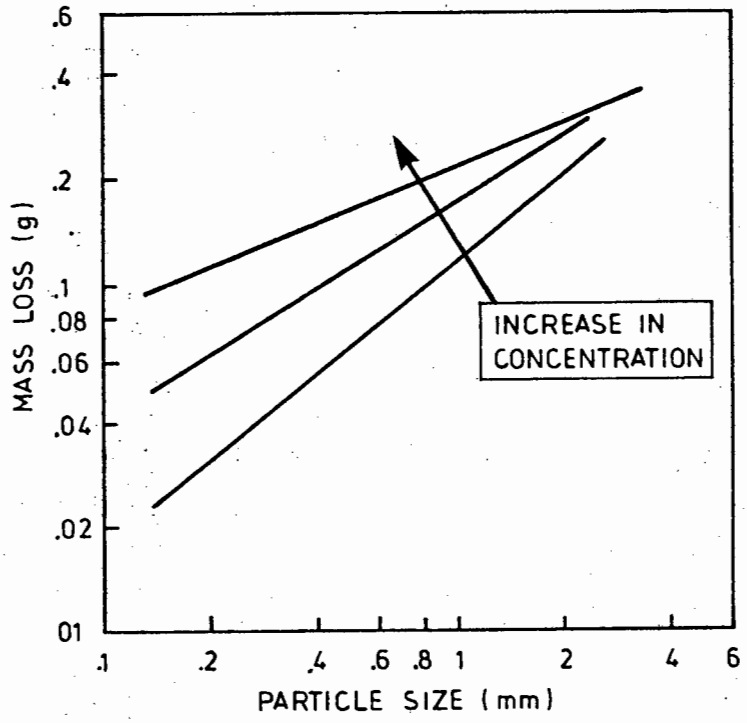

Fig.3.12 The concentration/wear relationship for a range of particle sizes in a sand slurry (16).

3.3.3 Mechanisms of abrasive wear

Wear mechanism is the collective name for micro events, by which wear occurs (83).The interaction between an abrasive and a wearing surface can be divided into four categories (89,90). The processes are shown schematically in fig.3.13.

1) Microploughing — In the ideal case microploughing due to a single pass of one abrasive particle does not result in any detachment of material from a wearing surface. A prow is formed ahead of the abrading particle and material within the wear path is plastically deformed and pushed to both sides of the wear groove.

2) Microfatigue — When volume loss occurs in micro ploughing due to the action of many abrasive particles or repeated action of a single particle it is known as microfatigue. Material may be ploughed aside repeatedly by passing particles and may break off by a low cycle fatigue (microfracture). In practice, wear in this situation would probably occur through a mechanism of delamination (78).

3) Microcutting — Microcutting results in a volume loss by chips, equal to the volume of wear grooves. The grooves are sharply defined and the chips usually resemble machining chips. Total removal of this sort gives rise to the most severe rate of abrasive wear in ductile materials.

4) Microcracking — This occurs when highly concentrated stresses are imposed by abrasive particles, particularly on the surface of brittle materials. In this case wear debris is detached from the surfaces due to crack formation and propagation.

In ductile materials microploughing and microcutting are the dominant wear mechanisms. When the hardness of the abrasive is much higher than that of the specimen, microcutting is the predominant wear mechanism (86).

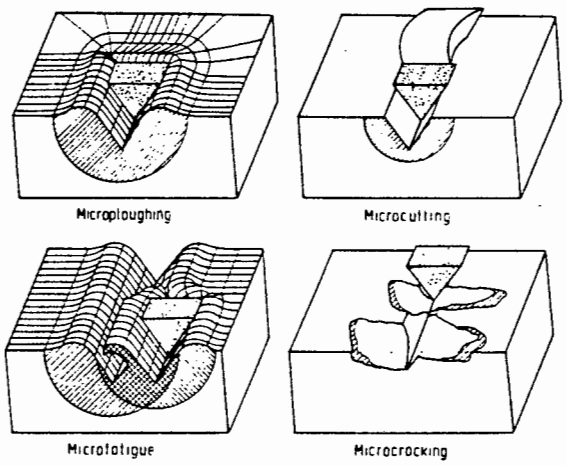

Fig.3.13 Physical interaction between abrasives particles and the surface of materials. Note the plastically deformed subsurface (90).

Spurr (77) demonstrated the nature of deformation occurring during ploughing by sliding indentors against specimens made up of laminae of different colour platicines (fig.3.14), which correlated well with the subsurface deformation actually observed in metals.

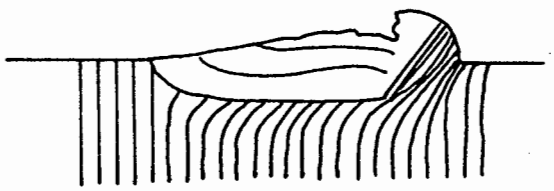

Fig.3.14 Sketch showing the nature of deformation during ploughing (77).

Murray, Mutton and Watson (58) explained the sigmoidal behaviour of heat treated steels observed earlier by Mutton and Watson (59), in terms of a transition in wear mechanisms from a predominantly ploughing mode to a predominantly cutting mode at higher hardness values (fig.3.15).

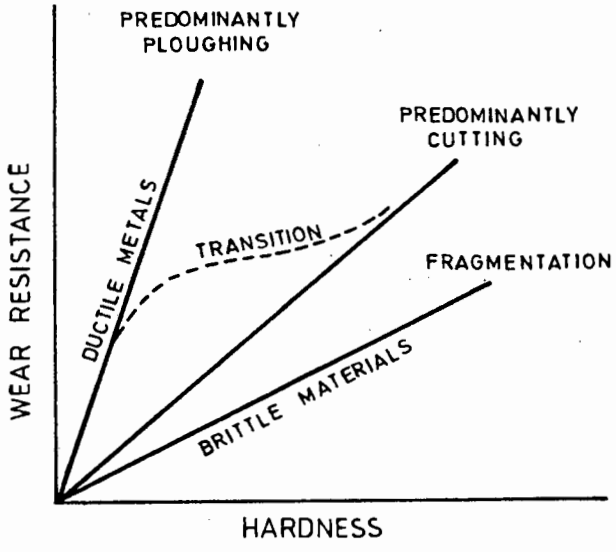

Fig.3.15 Three possible relationships between hardness and wear resistance predicted by consideration of ploughing, cutting and spalling mechanism of groove formation. The dotted curve shows the transitional behavior formed for steels (58).

Murray, Mutton and Watson (58) have shown that, as the hardness of a steel is increased, the number of particles suitably deposed to cause cutting or machining, increases. They therefore suggest that in the fully annealed state, steels behave in a similar manner to pure metals displaying a wear mechanism that is predominantly ploughing, while in the fully hardened condition wear takes place predominantly by cutting (32). This result has been confirmed by Hokkirigawa and Li (25). They show that the degree of cutting increased with an increase in hardness, but that the critical degree of penetration for the transition between ploughing mode and wedge-forming mode was independent of the material hardness.

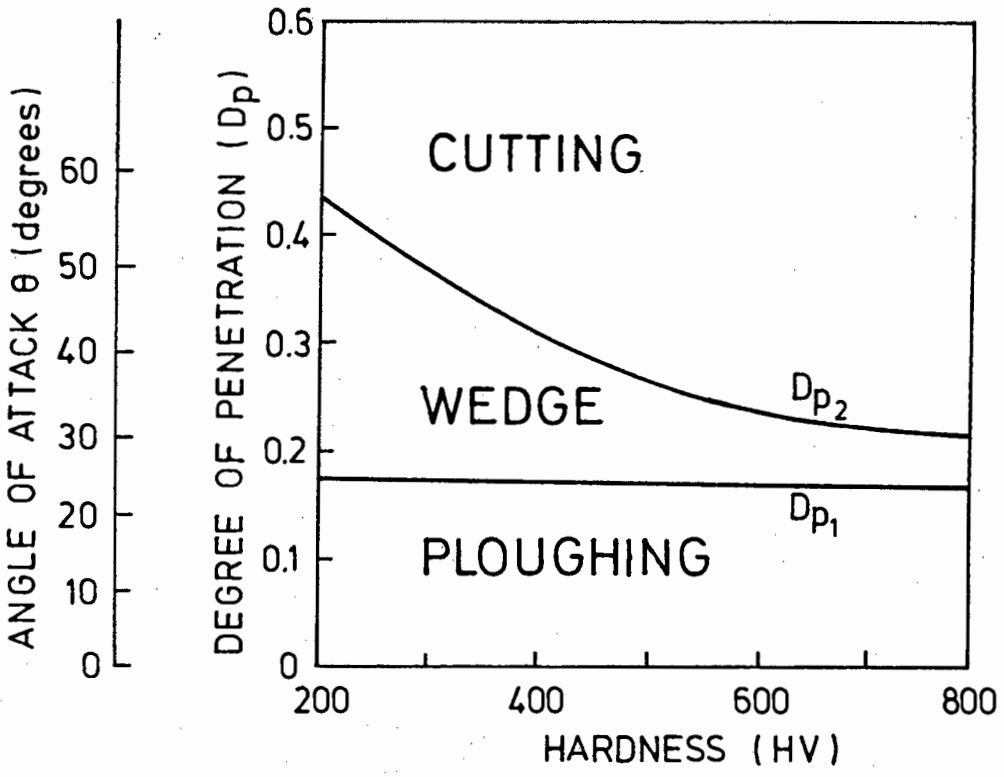

Dp1 - critical degree of penetration which corresponds to the transition from ploughing mode to wedge forming mode.

Dp2 - critical degree of penetration which corresponds to the transition from wedge forming mode to cutting mode.

Fig.3.16 The transition in wear mode with degree of penetration and attack angle (25).

3.3.4 Effect of sliding velocity

The effect of velocity on wear against fixed abrasive is associated with the wearing material's dynamic properties through strain rate sensitivity, resulting in changes in the wear mechanism (61). Velocity variations may also cause the particle loading to change, either through contacting particle flow dynamic effects or through larger range effects associated with strain rate stiffening of the abrasive medium.

In spite of the importance of velocity in abrasive wear there is very little quantitative information in the literature for velocities exceeding 1m/s. Moore and Mclees (54) have compared their results with other workers and found that there is an applicable increase in wear from speeds of 0.25 to 2m/s.

3.4 Impact Wear

Engel (15) has defined impact wear as *the mechanical damage to the surface of solid bodies resulting from repetitive impacting by particles, as either erosive or percussive wear.* Erosive wear results from the *action of a stream of small solid particles and/or liquids,* whilst percussive wear *is caused by solid body impact.* This review will consider the latter type. Rabinowicz (65) noted that since both processes involve dependencies on the energy of incidence, the erosion mechanism may aid in the understanding of impact wear where overlaps occur.

3.4.1 Classification of Impact Wear

Impact wear is caused by repetitive solid body interaction and can be divided into near-surface and sub-surface phenomena (41).

Sub-surface phenomena are typified by high energy impacting, dominated by a large normal velocity. The contact stress (σ_0) in relation to the yield stress σ_y of the material in compression, is very much greater than unity i.e $\sigma_0/\sigma_y < 0$.

Near surface or surface phenomena are characterized by low energy oblique impacts in which frictional effects are more influential. Low energy impacts result from impacts when $\sigma_0/\sigma_y < 1$.

3.4.2 Mathematical Model of Impact Wear

Few attempts have been made to model the impact wear process. Most workers have limited their studies to experimental aspects, supported by empirically derived relationships based on the conservation of energy and momentum and measured wear characteristics (41).

The first systematic study of percussive impact wear was carried out by Wellinger and Breckel who suggested that wear from solid particle impingement could be regarded as the result of independent normal and horizontal impact forces equal to the components of the actual impact (15). According to the model, a material exhibited a weight loss, W, proportional to the normal approach velocity, V,

$$W = NKV^{\phi} \qquad \ldots\ldots\ldots 3.5$$

Where N is number of cycles
K,ϕ are material and geometric constants

Engel (14) utilized a zero wear criterion on the basis of the amount of wear necessary to halve the initial surface roughness. The Engel model shows a strong dependence on the applied forces and, in the case of contacts that produce relative slip during impact, on the role of sliding speeds and distances .

Hutchings (27) developed a model based on the criterion of critical plastic strain to explain several features of impact of metals by spherical particles at normal incidence.

A limited number of models have considered oblique angles of incidence. Recent workers have attempted to relate crater volume to wear resistance (76,79). Finnie (21) demonstrated a relationship between impact wear resistance (W) and indentation hardness for pure and annealed metals. The Finnie model assumes crater volume will diminish as the plastic flow resistance of the material increases and gives the relationship

$$W \approx 1/\sigma^m \qquad \ldots\ldots\ldots \quad 3.6$$

where σ is the effective flow stress or hardness value of the target material.
m is a constant

However, the relationship does not hold for high angles of incidence, alloys or work hardened pure metals.

Although impact wear behavior can be related to some physical or mechanical property for a carefully defined set of materials, none of the models hold for material in all conditions of heat treatments or plastic deformation.

Hovis, Talia and Scattergood (26) suggest several reasons why a satisfactory model has not been developed.

1. Models do not account for the lip of displaced material at impact craters (fig.3.17), although they assume that some average fraction of this lip must be removed during an impact.

2. While flow stress or hardness can give adequate predictions, at least one other material parameter is needed when dealing with specific alloy systems.

3. Particles are seldom spherical but instead have a sharp angular geometry.

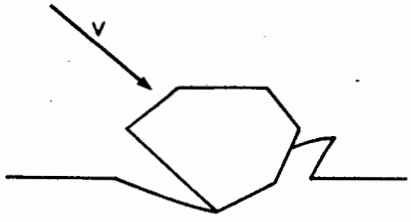

Fig.3.17 Schematic diagram of an impact crater showing a lip of displaced material. The impact crater volume is normally measured with respect to the initial flat surface (26).

3.4.3 The effect of material variables

3.4.3.1 Properties of the wearing material

The removal of material from metallic surfaces occurs by deformation and fracture of wear particles. Thus the impact wear rate must depend on the microstructure and the mechanical properties such as - the flow stress, hardness, strain hardening capacity, ductility and toughness of the wearing material.

The effect of hardness on the wear rate has been the subject of many experimental investigations and is generally assumed to be inversely proportional to the wear resistance. However, this relationship may only be used if the increased hardness does not extensively affect other mechanical properties (29).

Jahanmir (29) found that the inter-particle spacings of a hard second phase or inclusions affected the rate of impact wear in an alloy. He explained that in a material with small inter-particle spacing, the crack propagation between inclusions or the microvoids occurs faster than in a material of equal hardness but larger particle spacing. The material containing large particles or precipitates and hence a large inter-particle spacing contains fewer microcracks than a material with finer precipitates. Thus the smaller number of microcracks will result in better wear resistance. The importance of a hard second phase was discussed by Sare (75), who also observed the fracturing of the carbides in a martensitic steel matrix under particle impacts.

Wayne (85) found that duplex steel microstructures offer much higher wear resistance than spheroidized carbide structures in steels. In addition it appeared that the volume fraction of martensite in a duplex microstructure is an important factor in impact wear resistance.

microstructure resisting wear through the containment of cracking.

3.4.3.2 Geometric factors

Few studies have considered the effect of particle size or shape on impact wear. Although Hutchings (27) did not consider these effects he did predict that particle size and shape would have a significant effect on the strain rate and the dynamic hardness of the target material.

Many investigators have shown an increase in crater volume with increased particle size, but unfortunately crater volume does not provide an indication of the impact wear resistance (76), and hence no satisfactory relationship exists for particle size. Crater volume may be defined as the size of the impression which results after a single particle impact on the target material relative to the original unworn surface.

Hovis (26) reported that particle shape (i.e.spherical versus angular) appears to influence the amount of displaced material from a damaged crater during an impact event and hence the wear mechanism. For angular particles, at shallow impact angles, wear occurs by a cutting process. As the rake angle increases, fewer particles are orientated correctly to remove material by the cutting process and hence the dependency on angularity decreases at higher angles (29).

3.4.4 Mechanisms

Wear by solid particle impingement is believed to occur by a combination of two mechanisms, namely cutting wear and deformation wear (10). The cutting mechanism dominates at low or oblique impact angles (fig.3.18a), whilst the deformation mechanism dominates at higher angles (fig.3.18b).

The cutting mechanism which is responsible for oblique impact wear, occurs in a manner similar to abrasive wear (29). Not all impacting particles are capable of removing material by a cutting action because they may not have the correct rake angle (fig.3.17) or sufficient energy. These non-cutting particles will plough the surface after impact and deform the surface layers plastically (83). In impact wear the surface damage may not directly produce any wear particles - it may only weaken the surface layers. Any surface material which contains microcracks and voids can then be removed more easily by the cutting action of subsequent impacting particles.

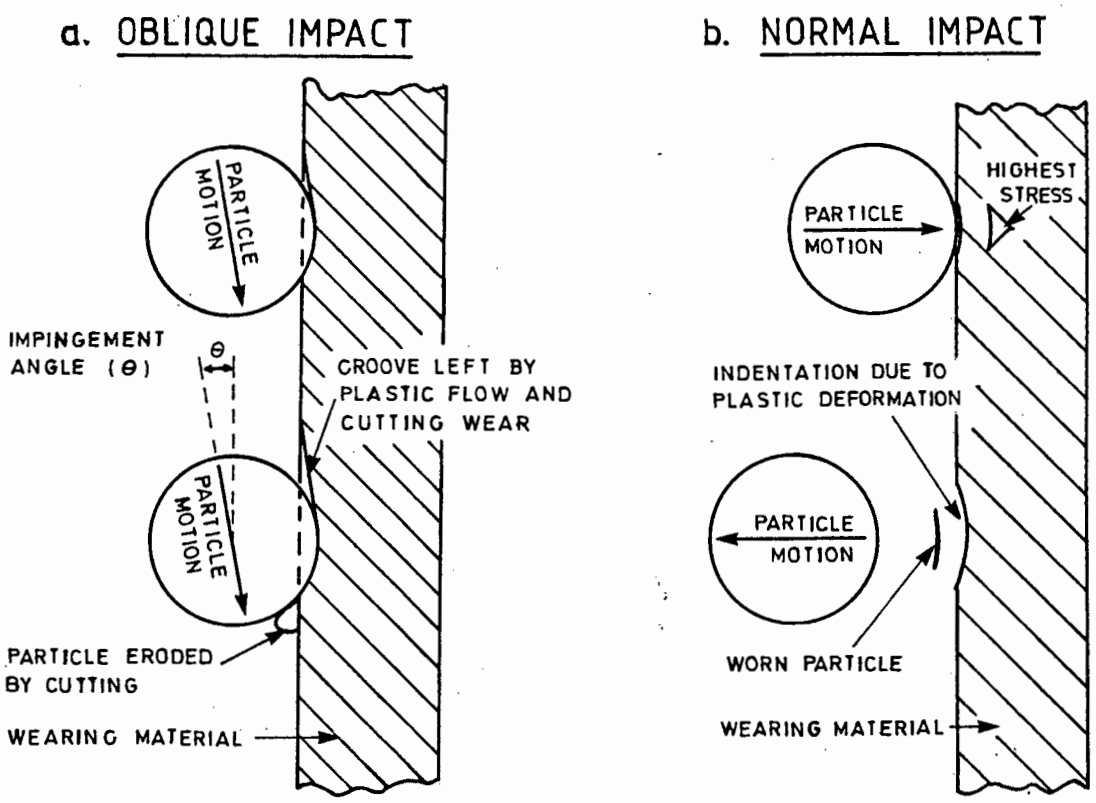

Fig.3.18 Cutting (a) and deformation impact wear (b) (28).

Impacting particles act as a cutting tool and remove material from target surfaces by the formation of microchips. At larger impact angles the impacting particles cannot remove material by the cutting process. Under these conditions the cutting angle or the rake angle is too large for chip formation. Thus there is a substantial lateral displacement of material by a ploughing mode of deformation, which leads to the formation of a raised rim ahead of the particle. Eventually the deformed material separates from the surface in the form of thin platelets (fig.3.19).

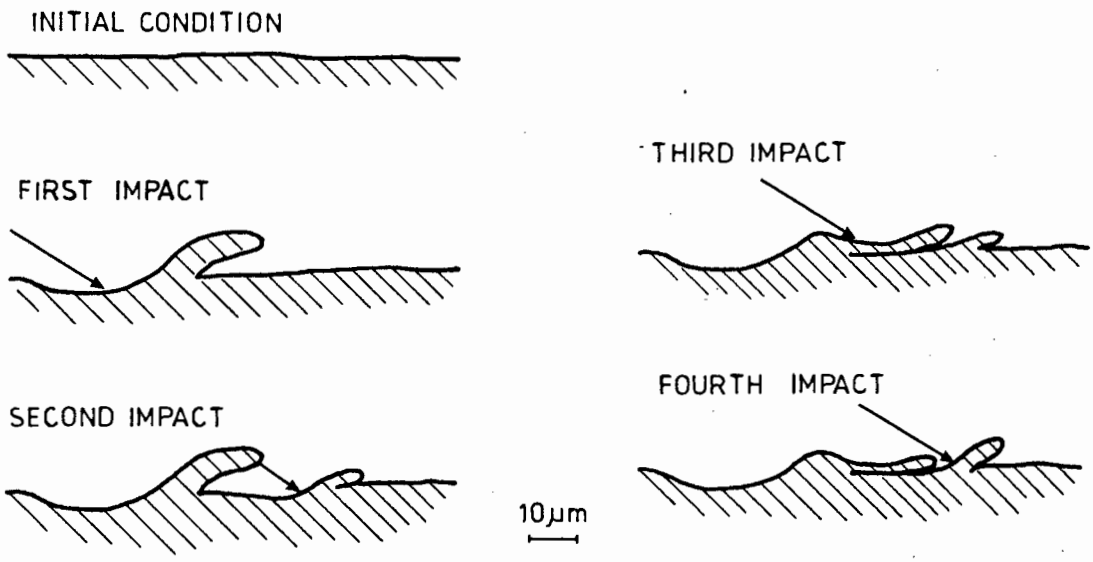

Fig.3.19 Sequence of platelet formation (42).

The substantial plastic deformation which occurs below the surface can cause microvoid and microcrack formation. In the presence of microcracks the deformed surface material can fracture from the surface by crack propagation between microvoids and cracks. Since inclusions and precipitates are potential sites for nucleation of voids, it has been suggested the wear rate may be inversely proportional to the interparticle spacings (29).

At high impact angles the mechanism of wear differs from the cutting and ploughing observed at shallower impact angles. A feature observed under multiple normal impacts at high angles is the development of ridges where craters overlap (72). These regions extrude in the direction of the impact in the form of thin platelets which undergo ductile fracture to produce wear particles (75). According to Hutchings (27) the major mechanism of metal removal at high angles occurs when disc-shaped or flat platelets which are usually smaller in thickness become detached parallel to the impact surface. Hutchings suggests further that material will only become detached at high angles in this manner after a number of impact cycles.

The exact nature of the deformation mechanism has not been clearly explained in the literature. Some proposals have been made such as - cold working and subsequent fracture after several impacts (29); fatigue crack propagation leading to final separation of loosened wear

particles; generation of platelets by plastic deformation of surface protrusions, but none have been absolutely proven. Levy and Morri (41) believe that the subsurface flow (rotational not translational) that occurs beneath impacts, results in the incorporation of the oxidized surface layers within the highly plastically deformed metal zone. These discontinuities or cracks coupled with additional surface flow generate shear stresses which are capable of producing crack propagation and eventual fracture.

In contrast, Sare (75) suggests that the interaction of compressive stress waves which are produced upon impact at the surface of a heterogeneous material, results in fracture of one of the phases and propagation of cracks parallel to the surface (fig.3.18b).

3.4.5 The effect of impact angle

It is well established that the wear of metals by solid particle impingement depends strongly on the angle at which particles strike the surface. For most ductile metal alloys, maximum impact wear occurs at shallow angles of incidence approximately 20° to 30°. Wear at normal incidence is about a third of the maximum (27). It can be seen from fig.3.20 that ductile materials are more susceptible to low-angle cutting wear. Steels are apparently more sensitive to heat treatments at higher impact angles than lower angles (60).

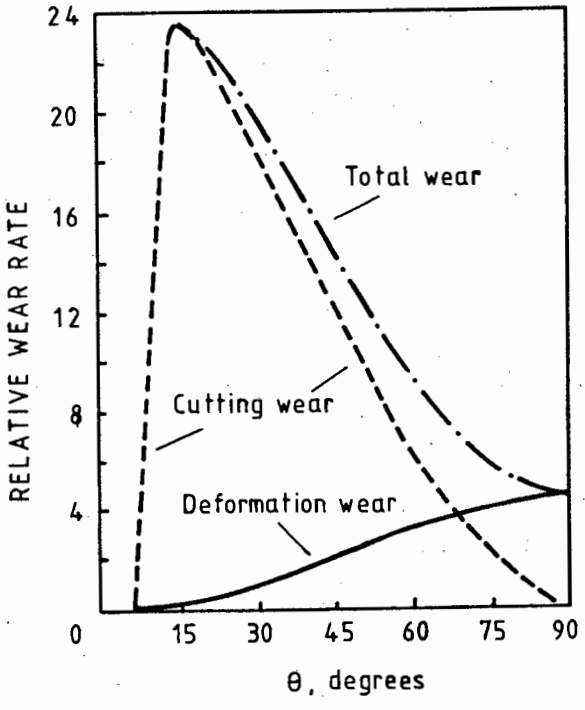

Fig.3.20 Influence of the angle of impingement on the relative rate of wear of a ductile alloy (10)

This phenomenon appears to be explicable in terms of the relative contribution of the lip and platelet mechanisms to the total material removal at different angles (71). Lip detachment during individual impact events is the dominant mechanism in both the single impact and multiple impact situations at low angles. The formation and detachment of platelets as a result of interaction between successive impacts accounts for the additional mass loss observed in the multi-impact situation at normal and near normal impacts (11). It has been suggested that at intermediate angles, impact wear occurs as a combination of possibly three mechanisms, that is, primary lip formation and detachment during a single impact, secondary removal of pre-existing lips by subsequent impacts, and detachment of platelets formed as a result of crater overlaps.

Jahanmir (29) attempted to explain impact angle wear in terms of microvoids and microcrack propagation. He found that void formation in a material occurs more readily at impact angles of 15 to 20 degrees, which corresponds to the impingement angle for peak impact wear in ductile metals. He concluded further that maximum wear should be expected at different angles for alloys with different degrees of ductility.

3.4.6 The effect of velocity

Wellinger and Breckel (15) showed with the aid of a simplified model that the target material exhibits a mass loss directly proportional to the normal approach velocity, which is in agreement with Rickerby and MacMillan (71).

Jahanmir (29) showed that a larger number of voids nucleate deeper below the target surface at higher impact velocities. These voids are potential nucleation sites for microcracks. Crack propagation between microvoids leads to the loss of material through fracture. Thus the wear rate is dependent on the depth of microvoids and hence on velocity of impact.

4. DESIGN AND DEVELOPMENT OF A LABORATORY TEST RIG AND SELECTION OF TESTING PARAMETERS

4.1 Introduction

Ideally, the wear behavior of materials should be monitored in situ (82). However it is not always practical or feasible to mount such an operation and as a consequence laboratory tests, which attempt to simulate the real operating conditions, are preferable to field tests (57). The three basic requirements for a meaningful test are according to Moore (57), reproducibility, differentiability and transferability. A relatively good applicability of the test results can be expected when the specimen and the original are similar (36). Moore (57) notes further that laboratory tests are comparative only, and should be used with extreme caution to predict the service life of the actual component because they simulate only some of the elements in the service environments.

In the present instance, it was considered that a laboratory rig could successfully reproduce the service conditions and allow process variables such as valve closure velocity, slurry constitution and valve design to be altered. Consequently a laboratory rig was designed and built by Barnett (8) in which full size valves could be tested under similar operating conditions and slurry densities as pump valves operating in the gold mines.

This design was subsequently modified by the author in an attempt to improve the mixing characteristics and to increase the pumpable concentration from a relative density of 1.6 to 1.9 g/cm^3.

4.2 Test rig

The test equipment consists of five major sections, namely:

1. The test cell
2. A slurry agitation and mixing system
3. A pipeline system
4. A pneumatic system and
5. A valve closure measurement system

A layout of the test rig is shown schematically in fig.4.1 and illustrated in fig.4.2.

A peristaltic pump delivers fresh slurry from an agitated supply tank to the test cell at a predetermined constant flow rate (appendix A). The closed loop system allows the slurry to be cycled continuously for the duration of the test. A pneumatic control system permits easy adjustment of the valve closure velocity, the number of impacts and the frequency of impact.

A detailed description of the operating procedure can be found in appendix B.

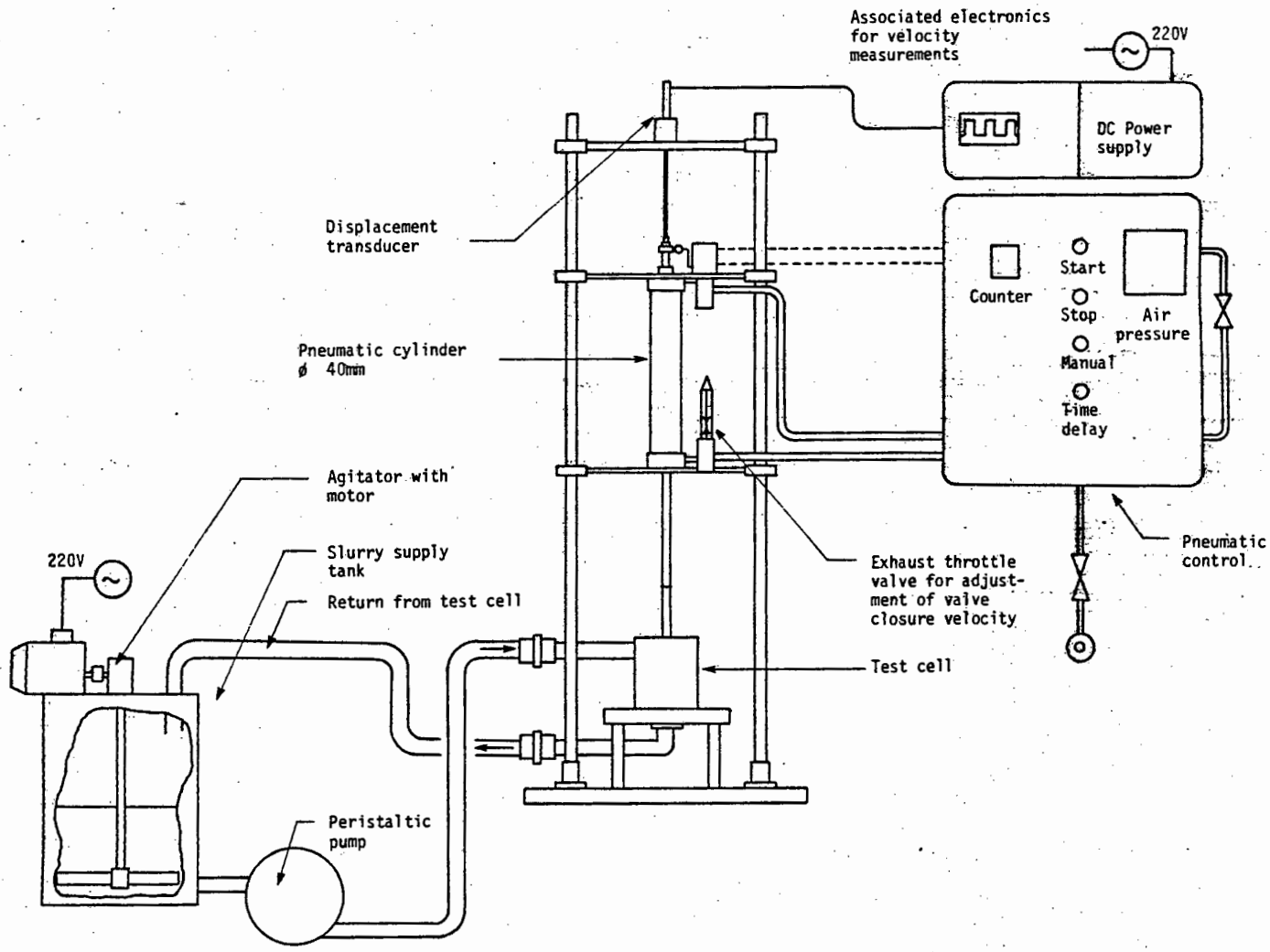

Fig.4.1 A schematic illustration of the test rig.

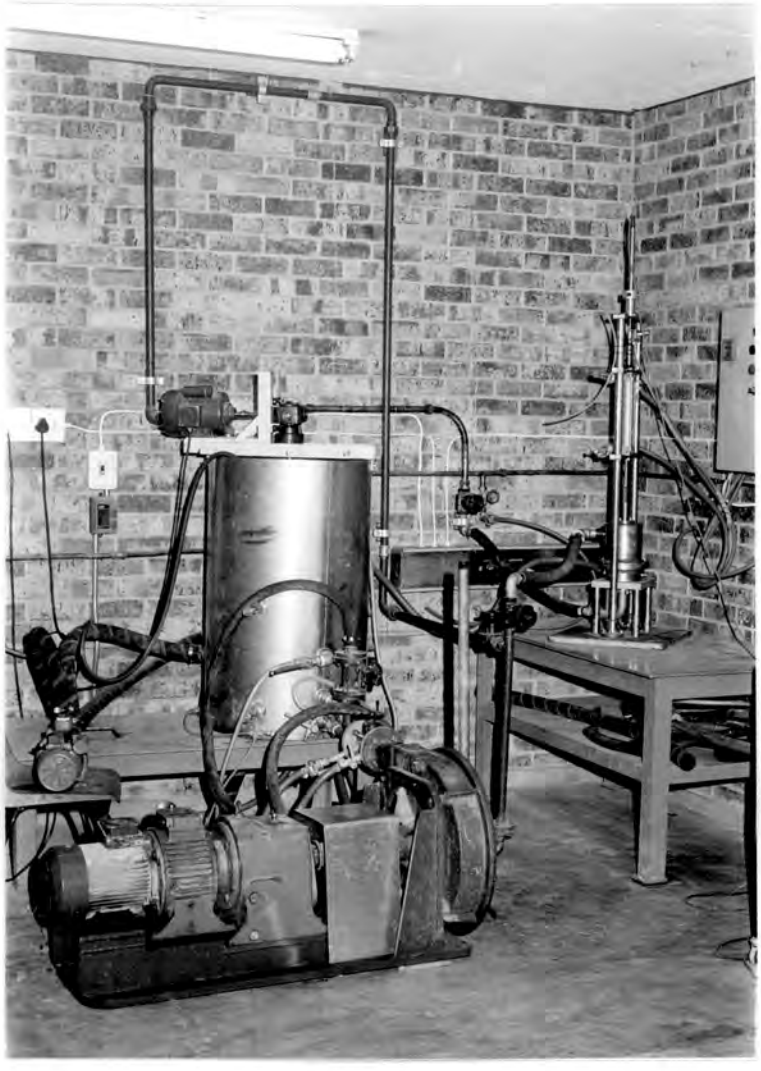

Fig. 4.2 Experimental test apparatus

4.2.1 The test cell

The test cell has been designed to simulate the service conditions of the disc poppet valve. The test cell consists primarily of a cylindrical chamber and flange which is clamped firmly against a rigid base to form a waterproof chamber. Slurry enters the test cell at the top and exits at the base (figs.4.3 and 4.4).

The seat or disc is positioned in the base of the test cell with the aid of an O-ring seal and the valve poppet is positioned by bolting it to the pneumatic plunger as illustrated in fig.4.4. The salient features of the test cell design are the ability to test full size valves of various designs, while remaining readily interchangeable.

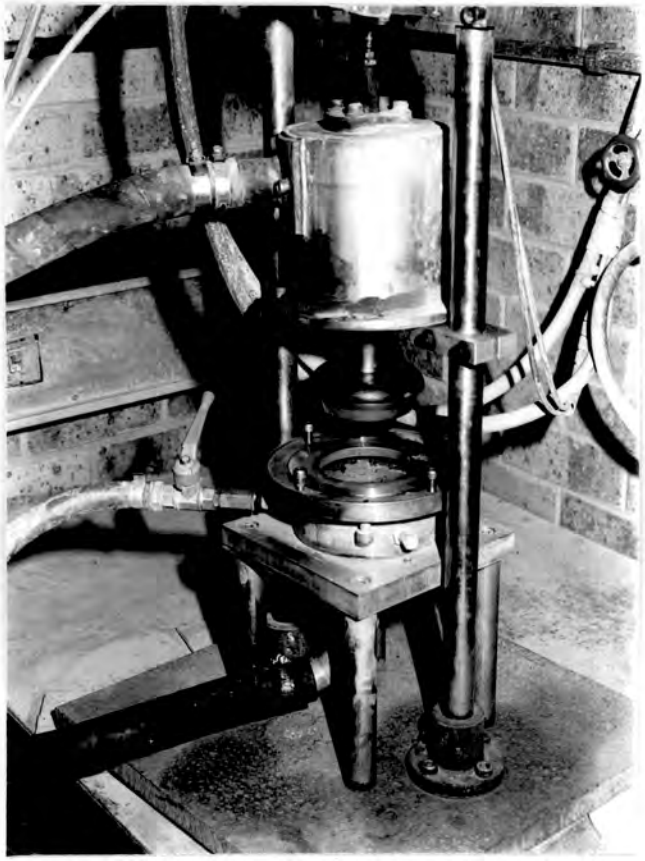

Fig.4.3 Test cell

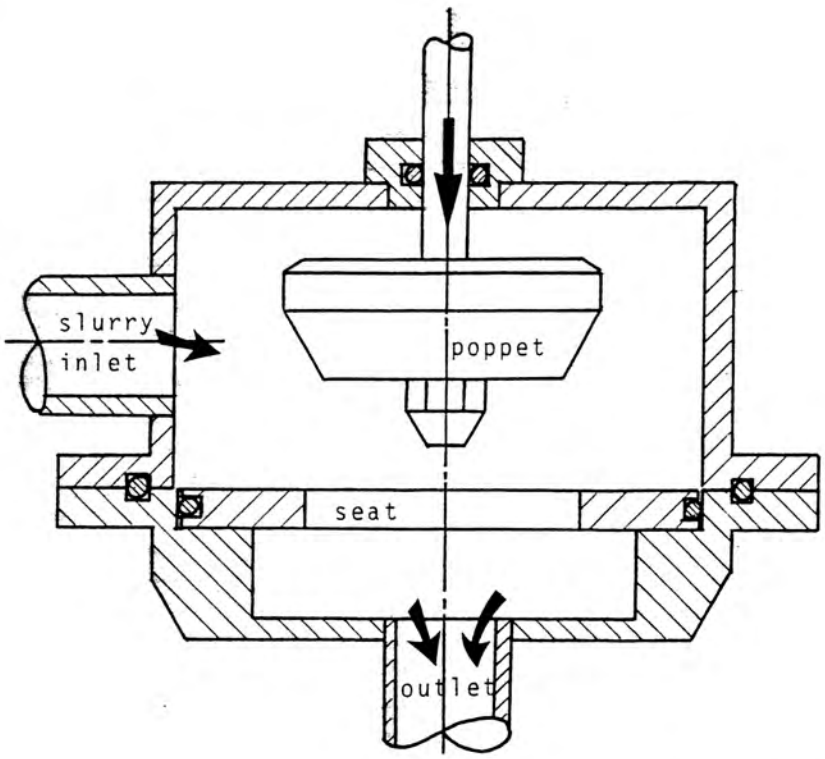

Fig.4.4 Schematic view of the test cell showing the position of the seat and poppet.

4.2.2 Slurry Agitation and Mixing

Since the coarser constituents of the slurry have a tendency to settle out, the slurry is mixed and agitated to ensure that a relatively constant particle size distribution is maintained for the duration of the test.

The original test rig design attempted to achieve mixing and agitation of the slurry by:

1. Injecting air at high pressure through several inlets at the base of the mix.
2. Stirring the mix with the aid of mixer blades at 25 revolutions per minute.

Unfortunately, because of clogging of the air inlets by the slurry and poorly designed mixer blades, only low concentrations could be mixed.

After extensive modifications by the author, the test rig consisted of three independent mixing systems designed to give improved agitation.

1. The mixing pump system

A 0.74 KW centrifuge pump was installed. The pump draws filtered slurry water near the surface of the mix and pumps the water back at the base of the mix resulting in violent agitation.

2. Stirring system

A more efficient 1KW splash proof electric motor with an overload facility was installed as well as a new gearbox (ratio 50:1) and a sophisticated spider couple. These modifications as well as the modified attack angle of the mixer blades delivered sufficient torque to mix the highly viscous slurry.

3. Air agitation

A lance coupled to the pneumatic supply was installed to probe the slurry manually which provided additional agitation. This modification proved particularly valuable for the finer more efficient packing slurries (belt filter tailings).

A schematic illustration of the modifications can be seen in fig.4.5.

4.2.3 Pipeline

One of the major problems associated with pumping slurry is that it tends to become hydrodynamically unstable, particularly at high concentrations. As a result

modifications were made to the test rig pipeline to improve the flow characteristics and hence to increase the pumpable concentrations. The radius of all the pipe bends was increased thus reducing friction and resulting in improved slurry flow. The pipeline route was also simplified by the removal of all unnecessary bends and fittings. Additionally a pipeline was fitted directly between the base of the test cell and the slurry drum. A schematic illustration of these modifications can be seen in fig.4.5.

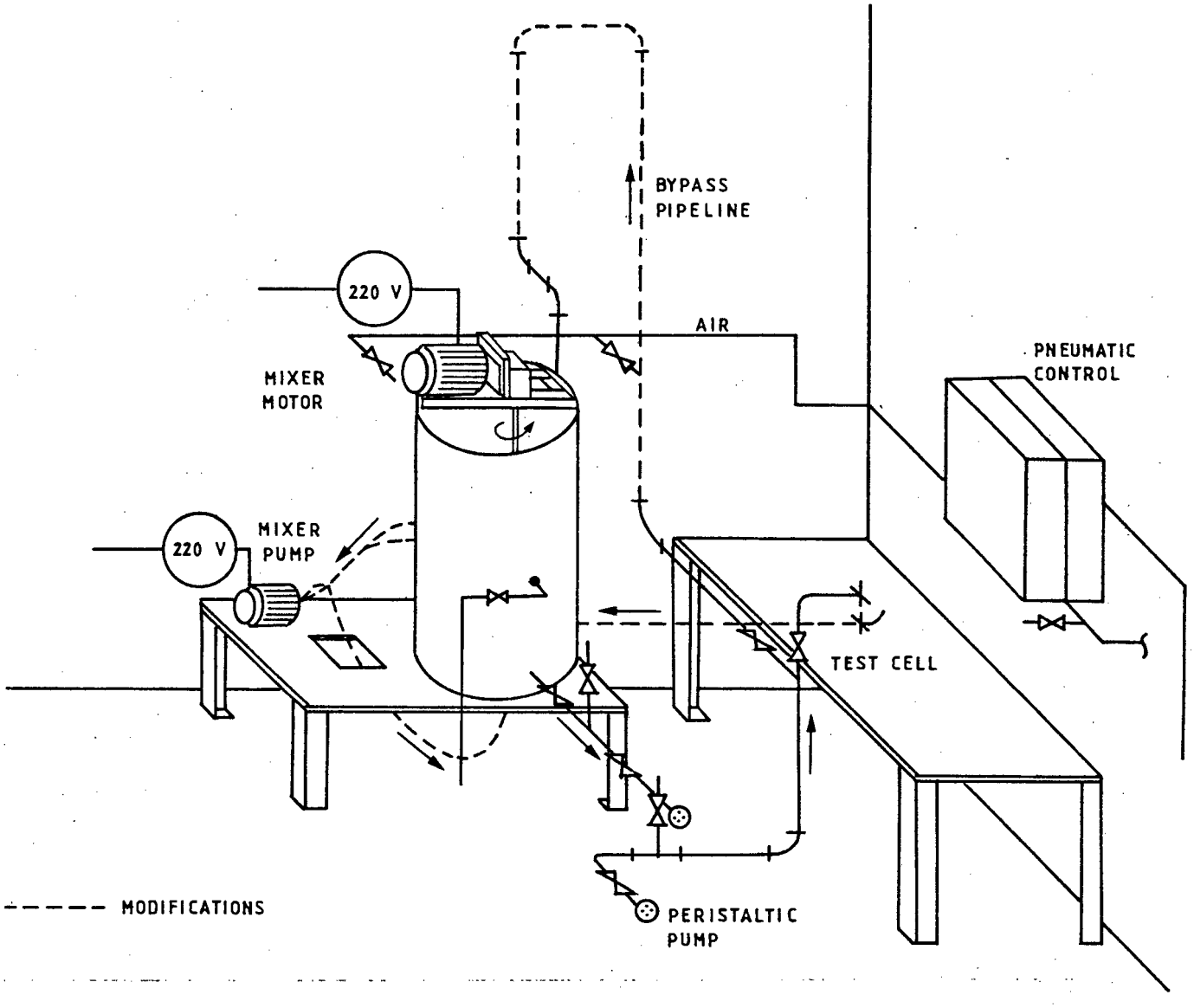

Fig.4.5 Schematic illustration of modifications to the mixing and pipeline system.

4.2.4 Pneumatic system.

A sophisticated pneumatic system controls the closure velocity, the frequency of closure, the number of cycles and the cycling waveform characteristics. A line pressure of 1.7 KPa was used to supply a reciprocating pneumatic cylinder thereby simulating valve opening and closure. The valve impacts typically with a force in excess of 70 N at a closure velocity of 1.9 m/s, but because the trapped quartzitic particles between the valve poppet and seat substantially reduce the bearing area, very high localized impact stresses can be expected.

An Atlas-Copco LT-730 compressor with a capacity of 350 liters and a maximum working pressure of 3.0 MPa was used as the pneumatic supply.

A water cooling system was attached to the pneumatic exhaust during this study to prevent overheating and detachment of the pneumatic rubber hosing.

4.2.5 Valve closure measurement

A LVDT (Linear Voltage Displacement Transducer) coupled to an oscilloscope was fitted to determine the valve closure characteristics and velocity.

4.3 Laboratory test parameters

4.3.1 Slurry types

Two common South African gold mine waste slurries, namely milled waste (6mm maximum particle size) and belt filter tailings (200μm maximum particle size) were tested. The particle size analyses of the milled waste and belt filter tailings are illustrated in figures 4.6 and 4.11 respectively.

4.3.2 Slurry quality

In order to ensure that the conditions during testing were kept relatively constant, slurry degradation tests were performed on both the milled waste and belt filter tailings slurries. The slurries were pumped continuously through the working system for a period of eight and twelve hours respectively. Slurry samples were taken at regular intervals and examined for shape and size changes. Particle size analyses were performed using the technique of wet sieving.

4.3.2.1 Milled waste

It was estimated that each test cycle using the milled waste slurry would take a total of 8 hours, hence a particle size degradation test was performed over a continuous period of eight hours.

The slurry degradation test showed that there was little alteration in the morphology and size distribution (fig.4.6) of the quartzite particles. A sample taken initially was compared to a similar sample which had undergone testing. Several different size ranges were analyzed from 63µm to 6mm.

No substantial changes in the morphology of the particles were observed except for slight blunting of the cutting edges for the large particles. Typical results are illustrated if figs.4.7 to 4.10. Similarly the particle size fraction did not change substantially during the eight hour period other than a small discrepancy for particles less than 0.5mm. This discrepancy was considered to be due to sampling technique or to the possibility that part of these fractions were washed away prior to the system being closed at the beginning of the test.

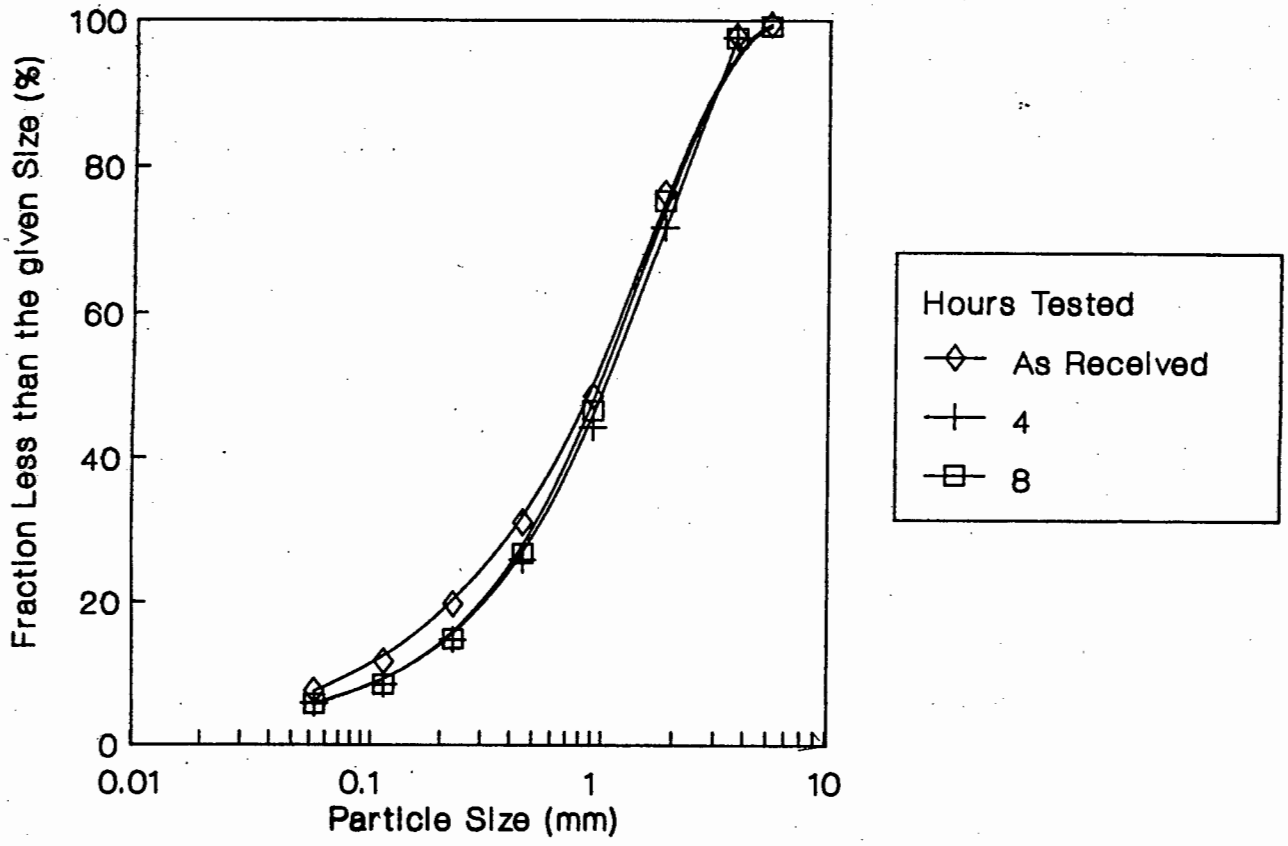

Fig.4.6 Milled waste particle distribution.

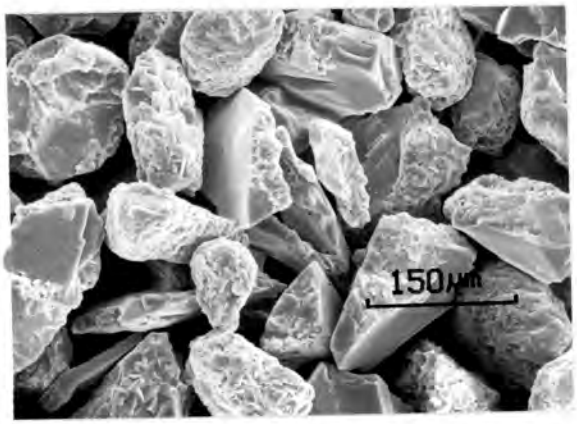

Fig.4.7 As received (unworn)
125-63µm

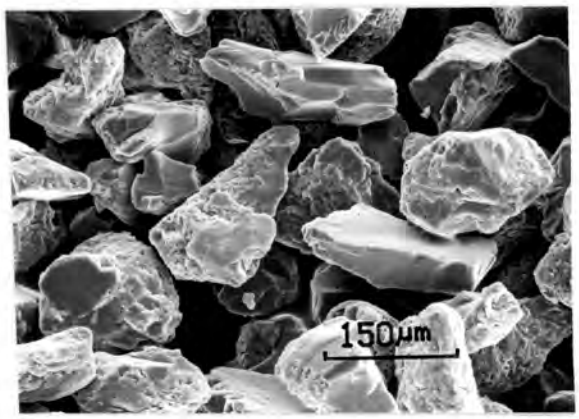

Fig.4.8 Worn particles
125-63µm

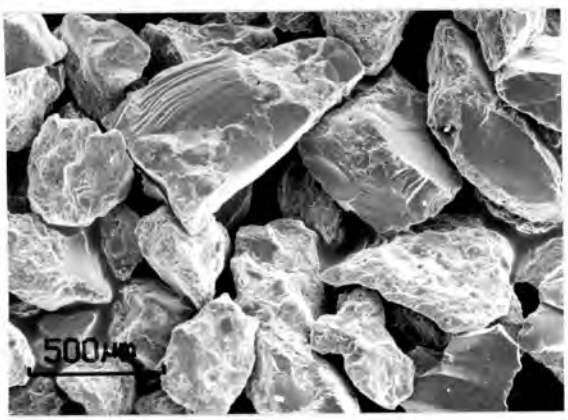

Fig.4.9 As received (unworn)
500-250µm

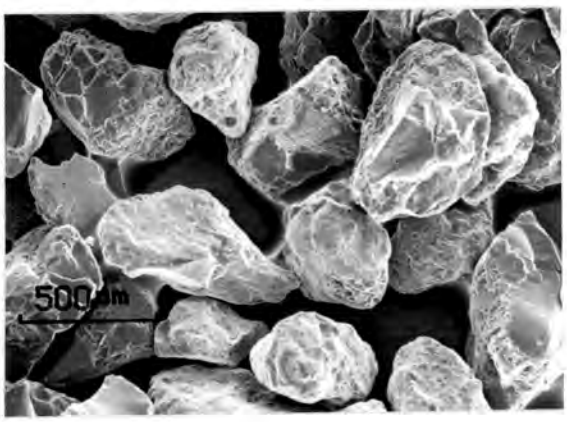

Fig.4.10 Worn particles
500-250µm

4.3.2.2 Belt filter tailings

The testing technique for the belt filter tailings was changed to ensure that none of the suspended fines were washed away. The changes included purging the system with as little fresh water as possible initially during start-up and keeping the the slurry drum overflow valve closed for the duration of the test. It was established that each test cycle using the belt filter tailings would take a total of 12 hours, hence a particle size degradation test over a continuous period of twelve hours was performed.

The slurry degradation test showed that there was little alteration in the morphology and the size distribution

(fig.4.11) of the quartzite particles. A sample, taken initially was compared to a similar sample which had undergone testing. Several different sizes were analyzed from 63µm to 2mm. No significant changes in the morphology were observed. Typical results are illustrated in figs.4.12 to 4.15.

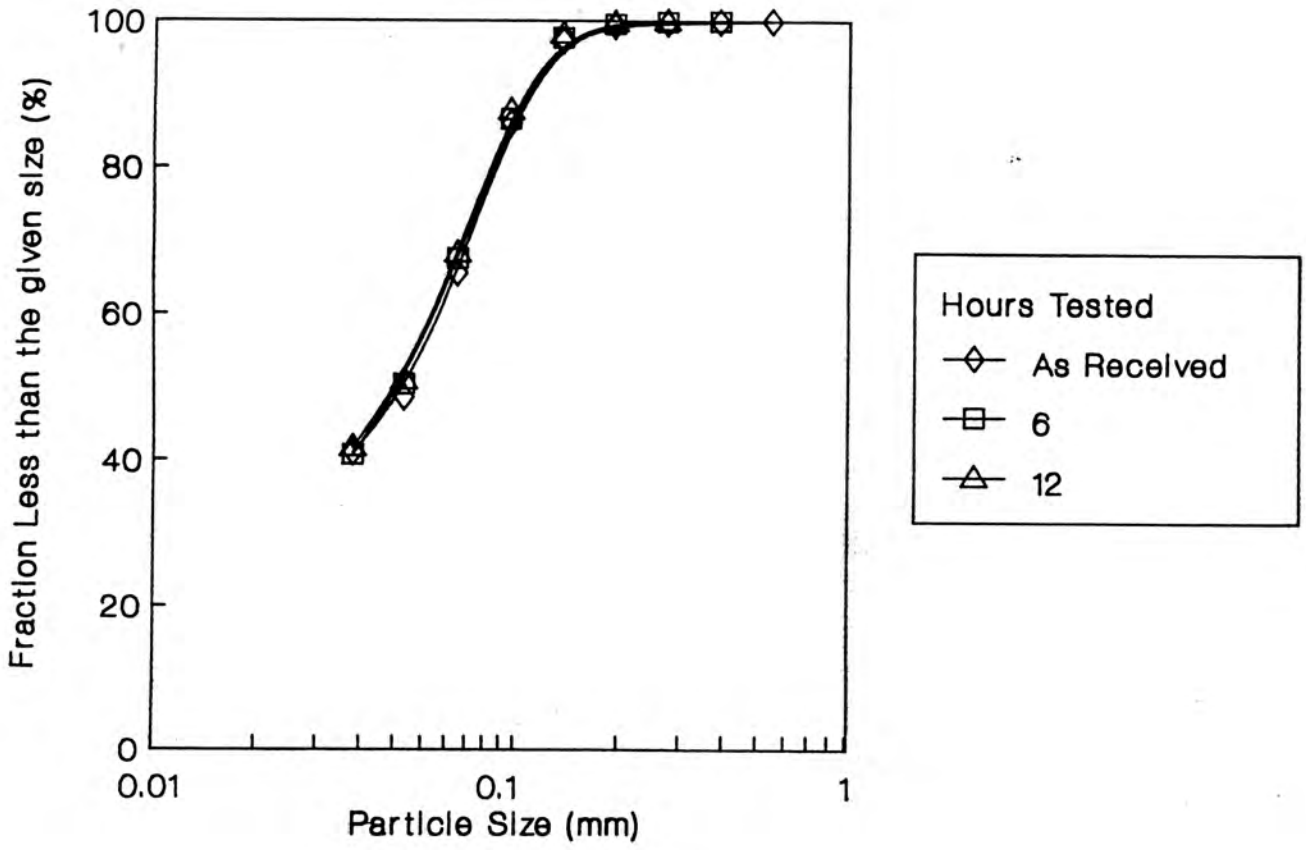

Fig.4.11 Belt filter tailing particle size distribution.

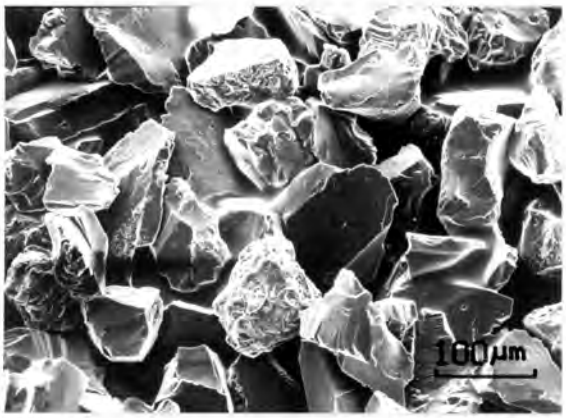

Fig.4.12 As received (unworn) 125-250μm

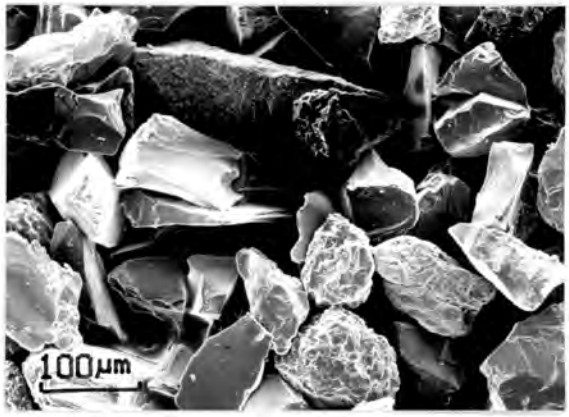

Fig.4.13 Worn particles 125-250μm

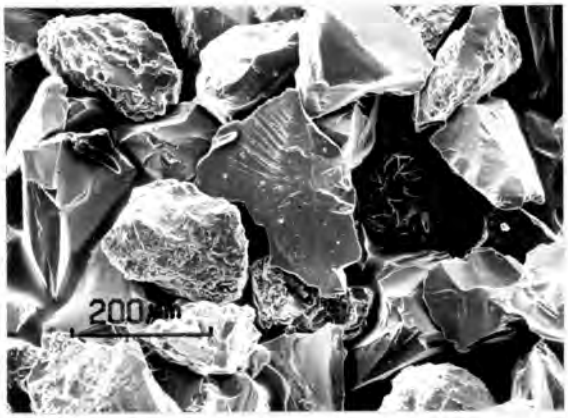

Fig.4.14 As received (unworn) 500-250μm

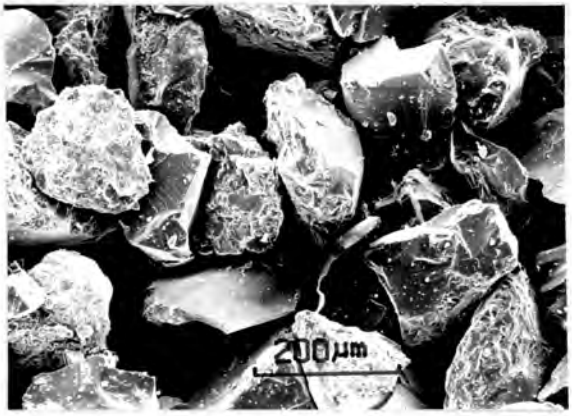

Fig.4.15 Worn particles 500-250μm

4.3.3 Concentration and flow rates

South African gold mines typically pump slurries at relative densities of 1.65 to 2.1 g/cm^3 (12).

At concentrations exceeding 2.0 g/cm^3, the slurries, particularly the milled waste, became unstable hydraulically in the laboratory test rig pipeline. Consequently all testing was performed on slurry densities below 2.0 g/cm^3. Relative densities of 1.7 and 1.9 g/cm^3 representing 65% and 75% solid respectively, were pumped in the valve wear tests.

The concentration or specific gravity (SG) was simply determined by the mass ratio of the slurry to water for a given volume,

SG = mass of slurry/mass of water.

The procedure for calculating the specific gravity of the quartzite particles was determined according to the American Society of Testing and Materials (ASTM) standard C-128.

Increasing the concentration from a specific gravity of 1.7 to 1.9 g/cm^3, did not result in a greater volume of material flowing through the test cell. An increase in concentration is offset against a drop in the flow velocity (fig.4.16) as a result of the lower viscosity of the slurry. The net effect is that the same volume of solid passes through the valve per unit time, but at different slurry flow rates. A detailed account of flow rate measurement appears in appendix A.

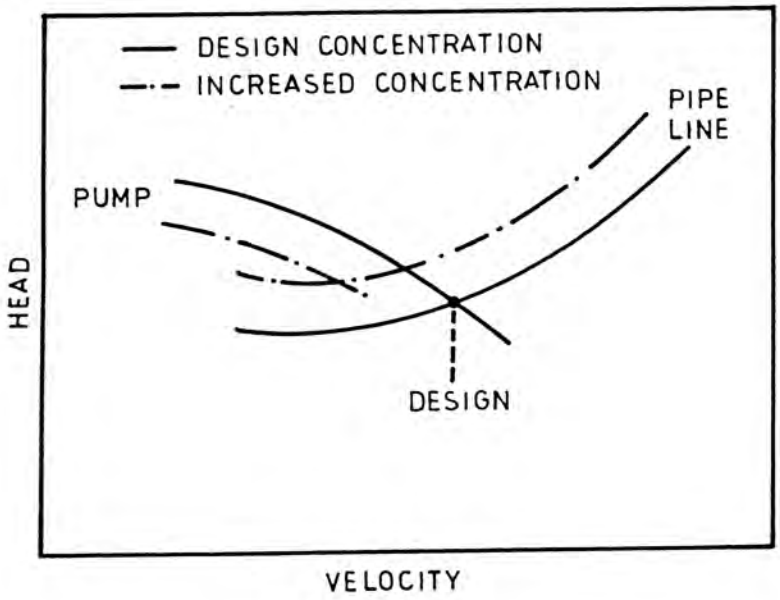

Fig.4.16 The effect of increased concentration in coarse particle transport with fixed speed centrifugal pump (4).

4.3.4 Assessment of flow erosion

A flow erosion test was performed on a relatively soft stainless steel AISI 316 valve poppet and seat (200 HV30), to assess the effect erosive wear on wear patterns and mass loss measurements.

Milled waste slurry was pumped through an open valve at a specific gravity of 1.9 g/cm^3 for a continuous period of 90 minutes. The valve showed no appreciable erosive wear losses during this period. The contribution of erosive wear to the total wear of the valve is small in comparison to the other wear modes, and therefore has been omitted from this study.

4.3.5 Valve closure velocity and characteristics

Typical inlet or suction valve closure velocities in service were found to be 1.72 ± 0.05 m/s (9).

The maximum closure velocity of the valve in the laboratory test rig was found to be 1.9m/s. Velocities of 1.3; 1.7 and 1.9 m/s were selected as a suitable range for investigating the effect of velocity on the wear behavior of the valve. A typical ocilloscope trace, at valve closure velocity of 1.9m/s, is illustrated in fig.4.17. Note the sudden deceleration or impact as the valve poppet strikes the seat or disc in the test cell.

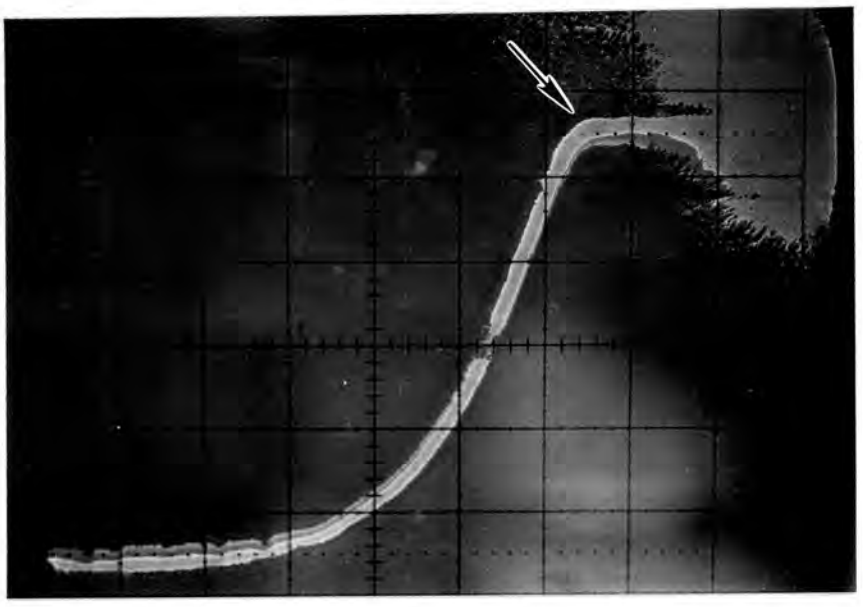

Fig.4.17 Valve closure (1.9 m/s). Note the the sudden impact. Horizontal scale 10 ms/DIV vertical scale 10 volts/DIV.

4.3.6 Valve frequency and test period

The Schwing disc poppet valve typically cycles at a rate of 15 strokes per minute in-situ (9). An accelerated test rate of 50 cycles per minute was selected for the purpose of testing, which was compatible with the compressor's capacity.

Valve wear was assessed at 500, 1500, 3000, 5000 and 10 000 closure cycles, corresponding to a maximum time in actual service of 11 hours.

4.3.7 Test parameters

The following parameters were kept constant for the valve tests.

(i) A maximum of 10 000 valve closures.

(ii) A cycling rate of approximately 50 closures/min.

(iii) All tests were carried out in the vertical orientation (inlet or suction valve).

(iv) All seats were heat treated to achieve a uniform hardness of 600 HV30.

(v) The pH range of the slurry was kept approximately constant at 7.1 - 7.5.

(vi) The milled waste slurry was replenished after every 8 hours of service and the belt filter tailings after 12 hours.

4.4 Testing Programme

A testing programme was designed to establish the effect of material hardness, slurry constitution, valve angle and valve closure velocity on the wear of the poppet valves. Full details of the programme are shown in tabular form below (table 4.1).

	SPECIFIC GRAVITY (g/cm^3)	6mm slurry 1.7	6mm slurry 1.9	200μm slurry 1.7	200μm slurry 1.9
1	CONSTITUTION WEAR TEST Velocity 1.9m/s Valve angle 60°	A	B	C	D
2	VELOCITY WEAR TEST Velocity 1.7m/s Velocity 1.3m/s Valve angle 60°	E G		F H	
3	VALVE POPPET ANGLE Angle 45° Angle 75° Velocity 1.9m/s	I K		J L	

TABLE 4.1 : Test matrix

Each "block" in the matrix above, for example block A, represents four individual valve tests i.e. four different poppet hardnesses.

4.5 Reproducibility

A reproducibility test was performed using a milled waste slurry (6mm nominal particle size), a valve angle of 60° and bulk hardness of 450HV30 on three individual valve sets.

The reproducibility of the valve tests was found to be better than +/- 5 per cent for the valve poppets, and +/- 10 per cent for the seats or discs. These values were considered to be satisfactory for this type of test. The valve poppet and seat reproducibility as well as the cumulative wear loss reproducibility up to 10 000 closure cycles is plotted in fig.4.18.

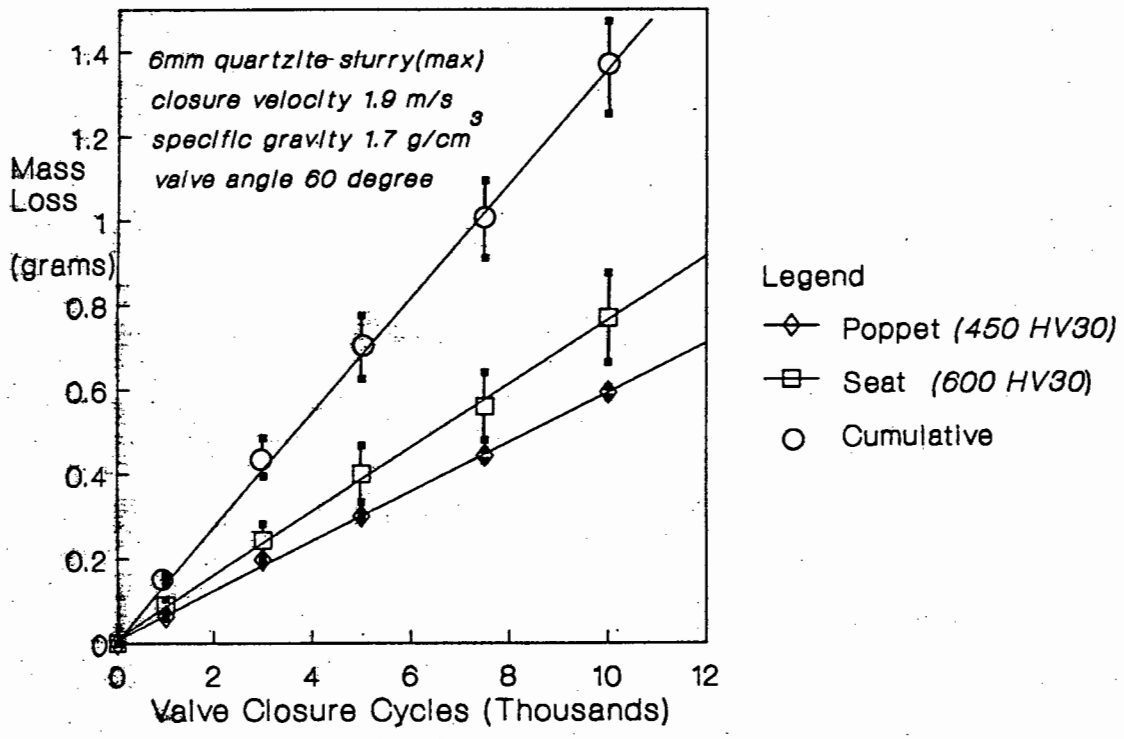

Fig.4.18 Showing mass loss with valve closure cycles; reproducibility error bars as shown.

4.6 Transferability

Having simulated the service conditions as closely as possible, correlation of the wear mechanisms for both the laboratory and the in-situ valve still remained.

A worn, surface hardened medium carbon steel Schwing valve with an service life of 80 hours was compared to a worn BS 817M40 laboratory valve of equivalent hardness and valve angle, after 3.3 hours of laboratory testing. Both the in-situ and the laboratory valve had been used to pump milled waste (6mm nominal particle size). Macroscopic wear patterns on the valve poppets and seats were found to be very similar. Both poppet valves were found to exhibit a seating line as illustrated in fig.4.19. A similar examination of the corresponding valve seats revealed close similarities in wear patterns, particularly on the inside face as illustrated in fig.4.20.

Fig.4.19 Worn valve poppet after 80 hours in-situ (a) and a worn laboratory valve (b) after 3.33 hours in the laboratory.

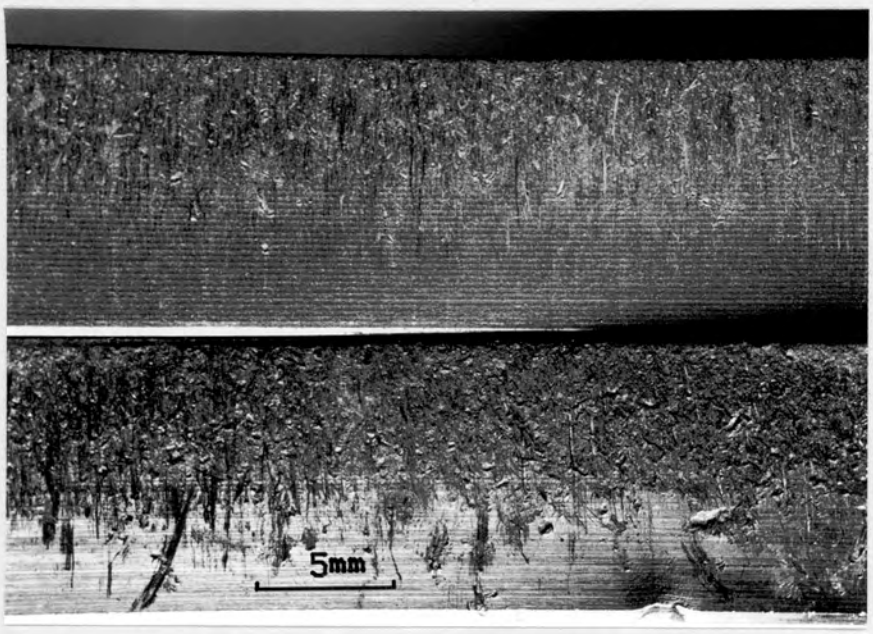

Fig.4.20 A worn laboratory valve disc or seat (a) and the in-situ seat (b).

The microscopic observations of the valves also confirmed a strong correlation in the nature of the wear mechanisms. Similarities in the size and shape of wear scars are clearly evident in figs.4.21 and 4.22. The in-

situ and the laboratory valve both showed evidence of multiple impacts and severe abrasive wear.

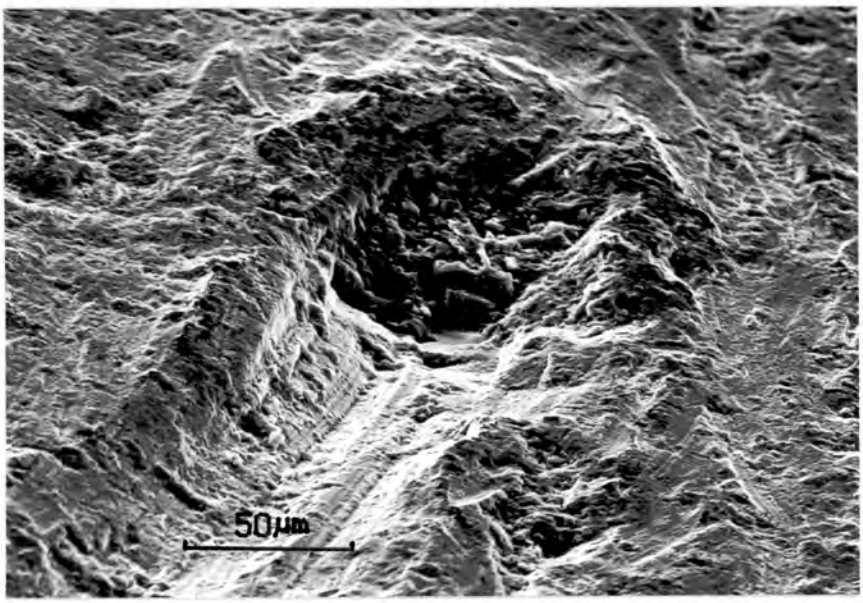

Fig.4.21 Showing embedding of a abrasive particle at the end of a short wear track on the in-situ poppet.

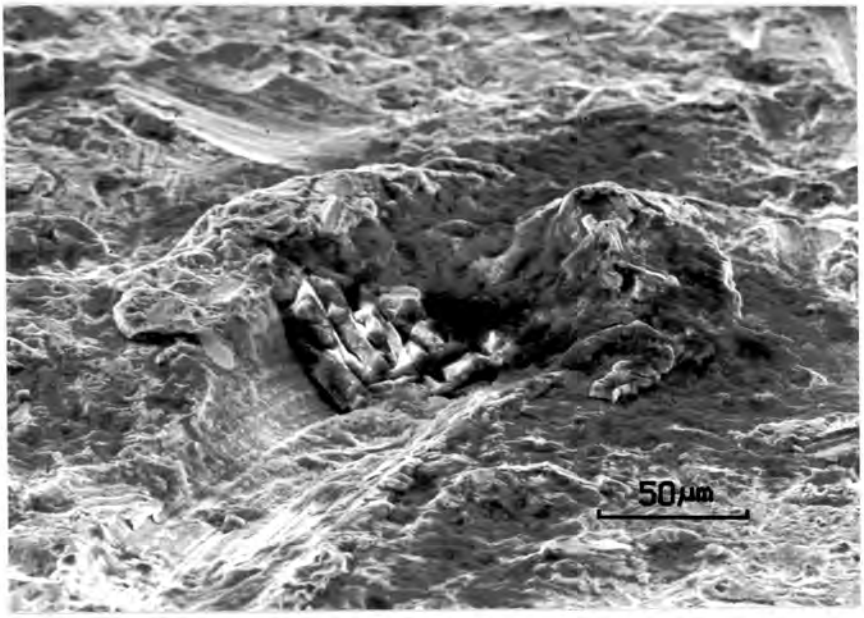

Fig.4.22 An embedded particle at the end of a short abrasive wear track on a laboratory test valve poppet. Note the particle has fractured due to the high load on both valves.

5. EXPERIMENTAL TECHNIQUES

5.1 Materials

A medium carbon, low alloy steel conforming to BS 817M40 was selected as the disc poppet valve and seat material. The chemical analyses are shown in table 1. Although a medium carbon, surface hardened steel is used as valve material in practice (7), it was considered that the through hardening steel BS 817M40 would provide more controllable and consistent material properties throughout wear testing.

	Poppet Material % m/m*	Seat Material % m/m
Carbon (C)	0.41	0.38
Manganese (Mn)	0.72	0.71
Silicon (Si)	0.09	0.10
Chromium (Cr)	0.99	0.99
Nickel (Ni)	1.47	1.45
Molybdenum (Mo)	0.31	0.29
Iron (Fe)	balance	balance

* mass by mass

TABLE 1: Chemical analyses of poppet and seat material.

5.2 Heat treatment

A heat treatment procedure similar to that recommended by British standards was adopted to determine the mechanical properties of BS 817M40 (En 24).

A series of Charpy V-notch specimens, as described in American Society of Testing and Materials (ASTM) standards En-23 (1985) and a series of type A Hounsfield tensile test specimens (gauge length 17.8mm) were taken parallel to the rolling direction of the bar and prepared for heat treatment. In an attempt to reduce decarburisation during heat treatment, specimens were first placed in a bed of cast iron swarf, and then placed in a furnace which had been purged with nitrogen gas. Austenitisation was carried out at 850 °C for 60 minutes, followed by an oil quench. These specimens were then tempered at intervals of 100°C between 100 and 500°C for one hour. The results of the heat treatments are shown in fig.5.1. Austenitisation was performed in a Naber 3.2 KW furnace and tempering in a fluidised bath.

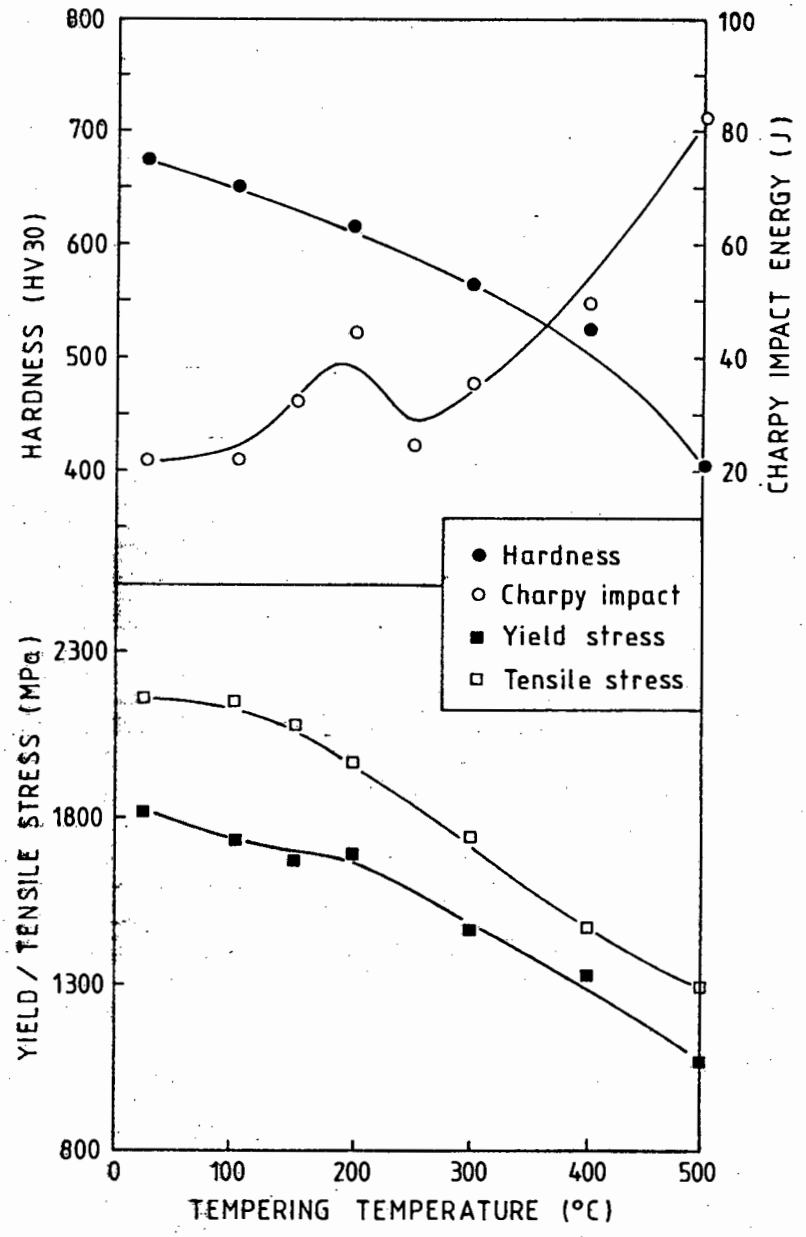

Fig.5.1 Tempering temperature versus hardness and toughness for BS 817M40.

5.2.1 Valve heat treatment

In an attempt to prevent decarburisation of the valves, several precautions were taken prior to heat treatment. First the poppet valve was coated with Aniscol, a commercially available protective ceramic paste. Only those faces which normally experience wear during service were coated since such coatings decrease quenching rates during heat treatment. Secondly the poppet was placed face down in a bed of cast iron swarf and the furnaces purged with dry nitrogen gas at a rate of 5cc/min. The poppet was pre-heated to 600°C and subsequently transferred to a second furnace and heated to an austenitising temperature of 850°C. A thermocouple was

used to monitor the rate of heating at the centre of the poppet (fig. 5.2).

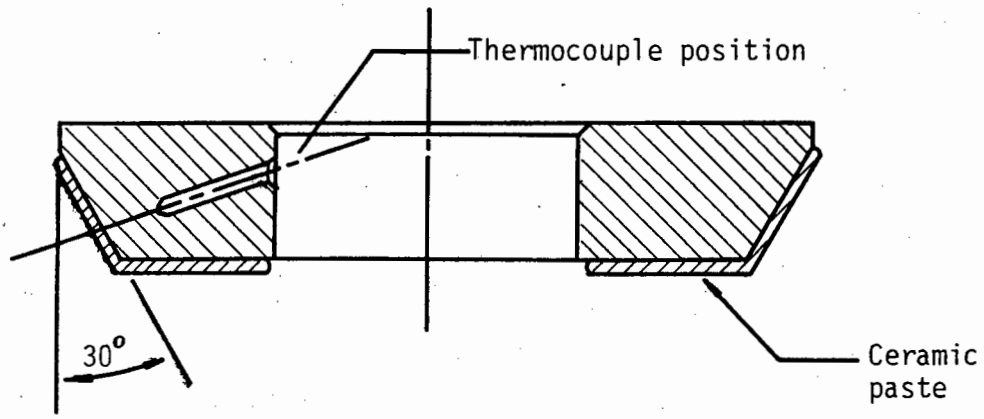

Fig.5.2 Valve poppet illustrating surface coated in ceramic paste and the location of the thermocouple.

From the information obtained (fig.5.3 and 5.4) it was decided to pre-heat the valves for 50 minutes and austenitise for 22 minutes. The valves were then quenched in Shell Volutte C oil. The same heat treatment schedule was adopted for the seats.

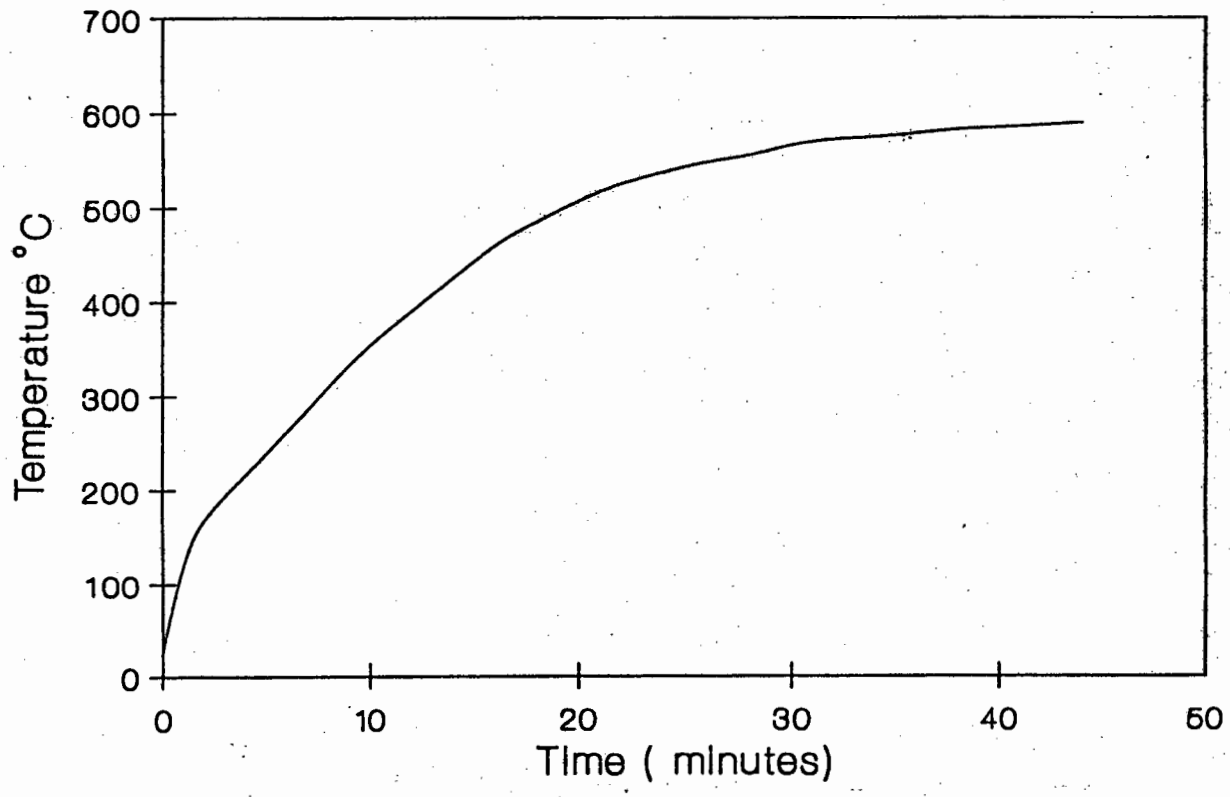

Fig.5.3 Valve poppet pre-heat (furnace 1)

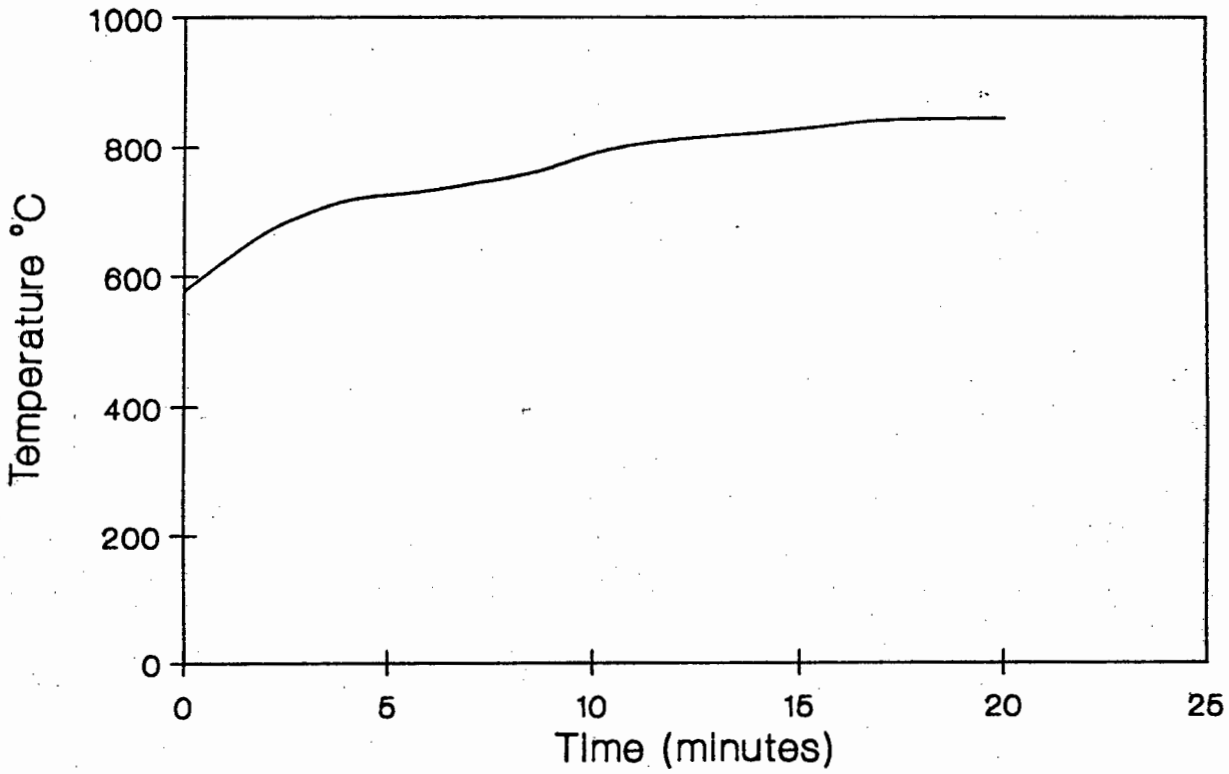

Fig.5.4 Austenitisation of the valve poppet in furnace 2.

5.2.1.1 Valve poppet

The valve poppets were tempered at four different temperatures after oil quenching from 850°C, to give a range of mechanical properties. This particular range (table 2) was selected in order to establish the effect of valve hardness on wear. Two Naber 3.2 KW furnaces were used for both austenitising and tempering.

Tempering Temp.(°C)	Hardness (HV)
100	650
150	620
300	550
450	450
as received	300

TABLE 2 : Poppet tempering temperatures and corresponding hardness values.

5.2.1.2 Valve Seats

To simplify the study, all the valve seats or discs were given the same heat treatment, consisting of an oil quench from 850°C followed by a tempering at 200°C for an hour.

A tempering temperature of 200°C was chosen for two reasons. Firstly, previous testing Barnett (8) had shown that wear decreased significantly at high hardness values. High hardness values are associated with low tempering temperatures (fig.5.1). Secondly, optimum toughness is developed at 200°C (fig.5.1). A high toughness is desirable for the valves because of the impact loading they experience during service.

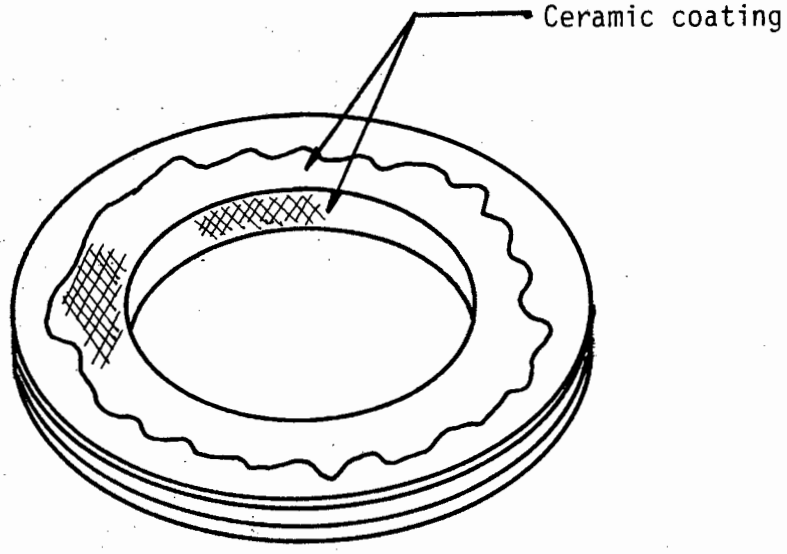

Fig.5.5 Illustration showing the faces on the valve seat which were coated in ceramic paste.

5.2.2 Evaluation of valve heat treatment

Heat treatment of the valve poppets and seats was generally found to be within ± 10 on the Vickers hardness scale, this was considered satisfactory.

The ceramic coating was largely responsible for the absence of decarburisation. Surfaces not coated with Aniscol prior to heat treatment developed a thin oxide layer during heat treatment and showed an appreciable decrease in surface hardness (20%). Since the ceramic coating greatly reduced the amount of decarburisation, valve faces were not final ground prior to testing but were rather lightly polished using 240 µm grit emery cloth.

5.4 Laboratory Methods

5.4.1 Hardness testing

Bulk hardness testing was measured using the Vickers diamond pyramid indentation method at 30Kg load on an Eseway harness tester. Microhardness measurements were made using a Shimadzu microhardness tester.

Microhardness measurements on quartzite samples were made using a load of 500g. Prior to indentation, the mounted quartzite particles were coated with a thin film (0.02μm) of gold palladium. The reflectivity of this surface facilitated the identification and measurement of the resulting impression. The hardness of the slurry particles was found to be 1168 ± 90 on the Vickers hardness scale.

This value is consistent with literature (40). The variation in hardness may arise from the heterogeneous nature of the grains i.e. grains typically consist of a variety of phases and minerals. The hardness of the quartzite was taken as 1168 HV for the purposes of this study.

5.4.2 Microstructural examination

Worn surface morphologies and subsurface deformation from various specimens tested in the laboratory were compared. A Nikon and a Reichert MeF2 microscope was used for optical microscopy.

Specimens were sectioned on a Microtom cut-off wheel and mounted in cold setting resin. A water wheel was used to polish the specimens in steps to 1200 grit carborundum. Finally, all specimens were polished using a 0.25μm diamond paste and etched in a 2.5% Nital solution for a few seconds prior to microscopic observation.

The study of the subsurface posed a particular problem because the edges of the specimen became rounded during the polishing procedure. This obscured the deformed areas that were of interest. The technique of electronickel plating was employed and proved to be effective in preventing rounding. Specimens were plated in a nickel sulphate, nickel chloride and boric acid solution with a nickel anode and a current density of 50-100 mA/cm^3 to a thickness of between 1 and 2 mm. For efficient plating it was necessary to ensure that the surfaces were clean before plating could commence.

The cleaning procedure was as follows :

1. The specimen to be plated was ultrasonically cleaned in alcohol for 5 minutes and rinsed in distilled water.

2. The specimen was then ultrasonically cleaned in a 20% solution of ammonia for 2 minutes and rinsed in water.

4. The specimen was afterwards dipped into a 25% solution of hydrochloric acid for 2-3 seconds and rinsed in water.

5. Finally the specimen was placed in the electroplating solution and plated at low current density.

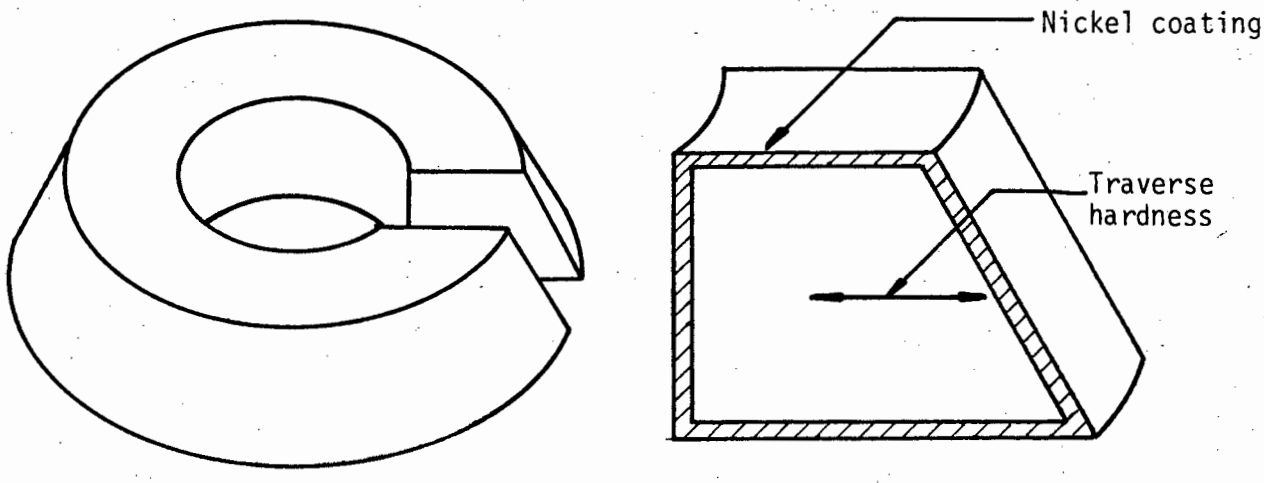

Fig.5.6 Location of specimen taken from the worn valve for nickel plating, In addition the illustration shows a specimen which has been plated and subsequently sectioned.

The subsurface deformation below the valve seating line was studied by cutting sections from the worn valve.

Prior to nickel plating the worn surfaces of both laboratory and in-situ valves were examined using a Cambridge S200 scanning electron microscope after they had been ultrasonically cleaned in alcohol. Sections were removed from the valve seats for examination (fig.5.6).

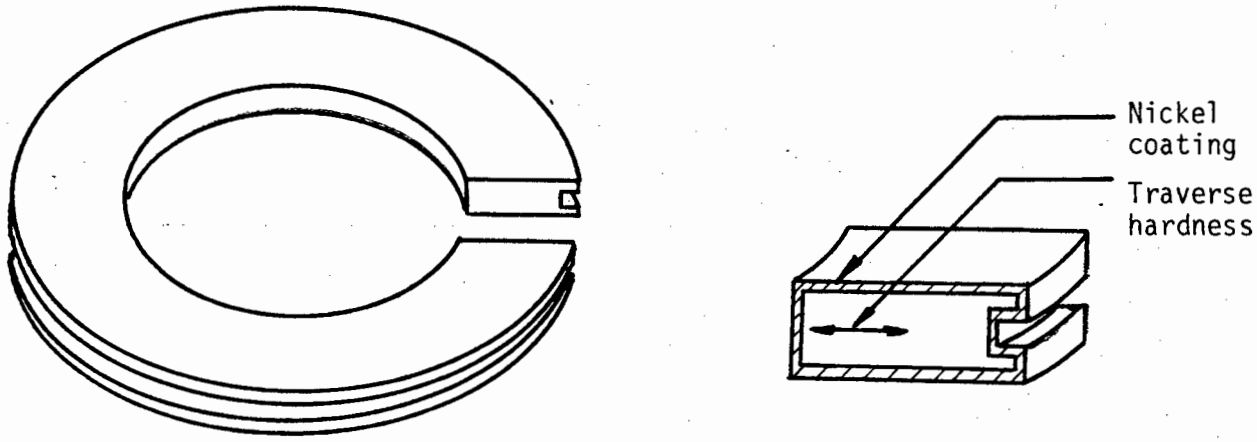

Fig.5.7 Illustration of the sectioned seat and a sectioned nickel plated specimen.

5.5 Specimen mass loss and presentation of results

The mass loss was monitored at regular intervals during testing by removing the valve, drying, cleaning and weighing. A Mettler PM 2000 balance, with an accuracy of 0.01 g, was used to determine mass loss.

Wear loss is dependent on particle abrasivity hence valve wear has been plotted as a function of relative hardness (Ha/Hm) where Ha is the abrasive hardness and Hm is the wearing material bulk hardness.

6. RESULTS

A complete set of slurry constitution, closure velocity and valve angle tests for both the milled waste and belt filter tailings will be presented, as set out in table 4.1. All the valve sets tested, exhibited a steady state wear loss with increasing closure cycles. In all cases the mass loss of the valves is reported for 10 000 closure cycles. The results are presented in graphical form, but are available in tabular form in appendix C.

6.1 Slurry Constitution

Wear tests were performed at specific gravities of 1.7 and 1.9 g/cm^3 for both the 6mm and 200µm nominal particle size slurries at a valve angle of 60° and a closure velocity of 1.9 m/s.

6.1.1 Milled Waste

Milled waste consisting of 6mm nominal particle size was used in the testing programme. The results of the milled waste valve wear tests are plotted in fig.6 for both slurry specific gravities and presented in tabular form in tables 1 and 2, appendix C.

A change in the wear rate or a transition point was found to exist on the relative hardness versus wear loss curve (fig.6). At a closure velocity of 1.9 m/s, the transition was identified as being approximately Ha/H = 1.9 for a slurry with a specific gravity of 1.7 g/cm^3 , where Ha is the hardness of the abrasive and H the poppet hardness. At the higher slurry density, a similar transition was found at a Ha/H value of 1.9 but it was far less pronounced than for the lower slurry density of 1.7 g/cm^3.

It is also worth noting that the mass loss for poppet valves of similar hardness is always higher when the valves are subjected to the higher density slurry despite the total throughput of solids being similar for both slurry densities (appendix A). The net difference in mass loss for the valves subjected to different slurry densities was slight below the transition point of Ha/H = 1.9, but became increasingly divergent as the value of relative hardness (Ha/H) increased above 1.9.

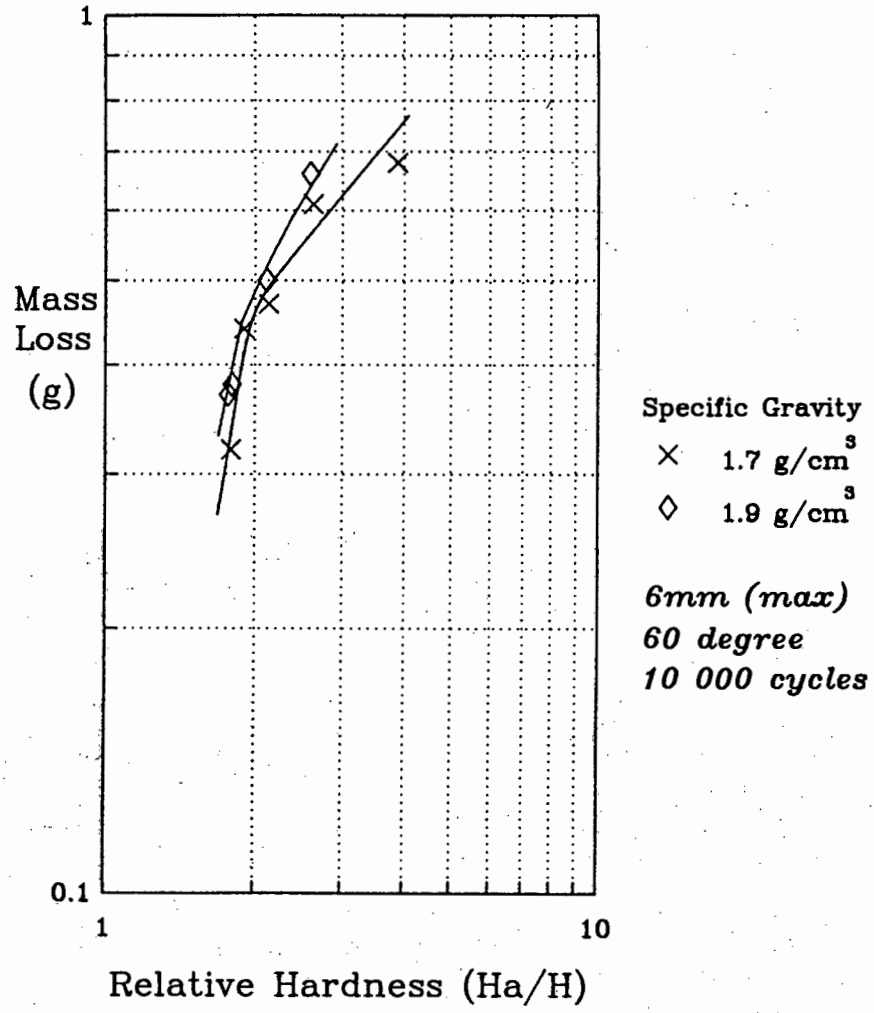

Fig.6.1 Shows the change in mass loss with change in relative hardness (Ha/H). Note the inflection around an Ha/H value of 2 for both specific gravities.

6.1.2 Belt Filter tailings

Belt filter tailings consisting of nominal particle size 200µm were used in the testing programme.

A plot of the relative hardness versus wear loss at 10 000 closure cycles can be seen in fig.6.2 superimposed on the results for wear loss using the 6mm nominal particle size slurry. These results are also presented in tabular form in tables 3 and 4, appendix C.

From fig.6.2 it can be seen that the finer slurry results in between 18 to 34 % less wear of the valve material than the coarser slurry at a specific gravity of 1.7 g/cm^3, depending on the poppet bulk hardness.

The wear rate increases significantly initially as the ratio of the hardness (Ha/H) increases, but gradually decreases at higher relative hardness values. The wear loss for the two different density slurries became increasingly divergent at higher hardness values. A similar trend was also observed with the milled waste.

Predictably, higher wear loss occurred at higher specific gravities which was similar to the result found with the milled waste (fig.6.2). The wear loss of the valve poppet at the higher specific gravity in the fine slurry, varies by between 8 to 24 %, depending on the valve poppets hardness.

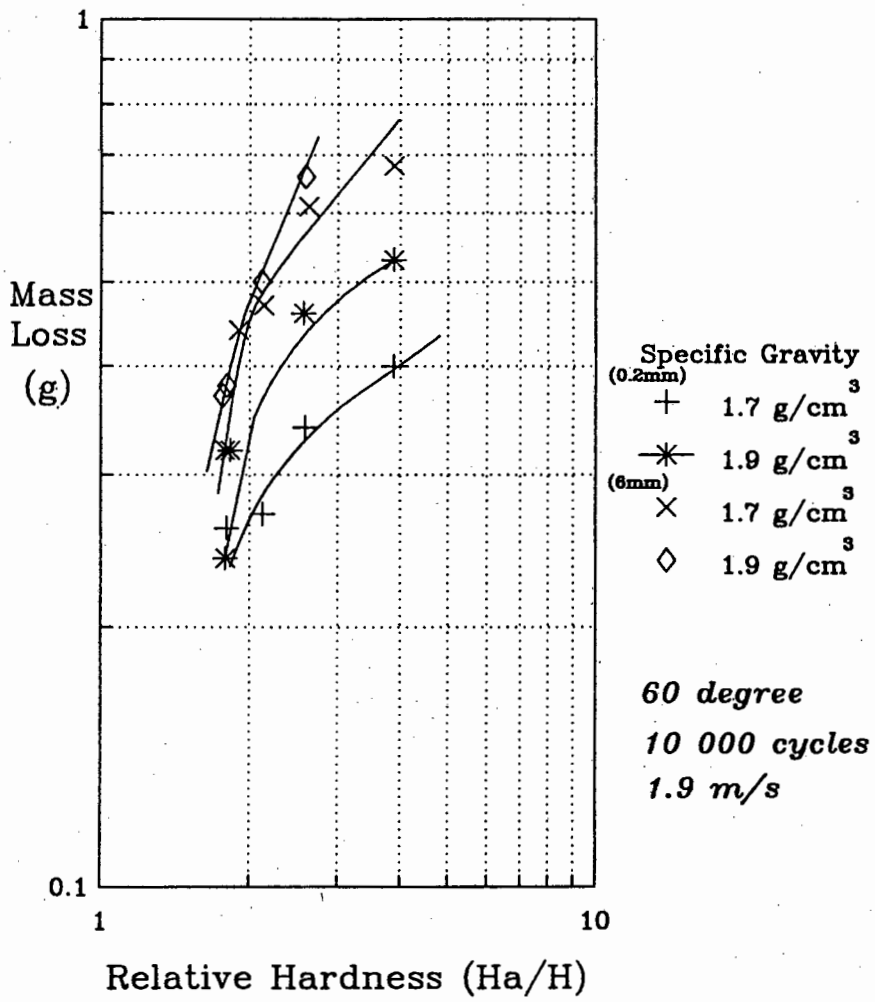

Fig.6.2 Shows the change in valve mass loss with change in relative hardness (Ha/H) using a 200µm nominal particle size slurry.

6.2 Valve Closure Velocity

Three valve closure velocities namely, 1.3, 1.7 and 1.9 m/s, were investigated for both the milled waste and the belt filter tailings at a valve angle of 60° and a slurry density of 1.7 g/cm^3. The results of the valve closure velocity tests for the milled waste and belt filter tailings are plotted in graphical form and presented in tabular form in tables 5 to 8, appendix C.

6.2.1 Milled waste

The results of the valve closure velocity tests which were carried out for velocities of 1.3, 1.7 and 1.9 m/s are presented in fig.6.3.

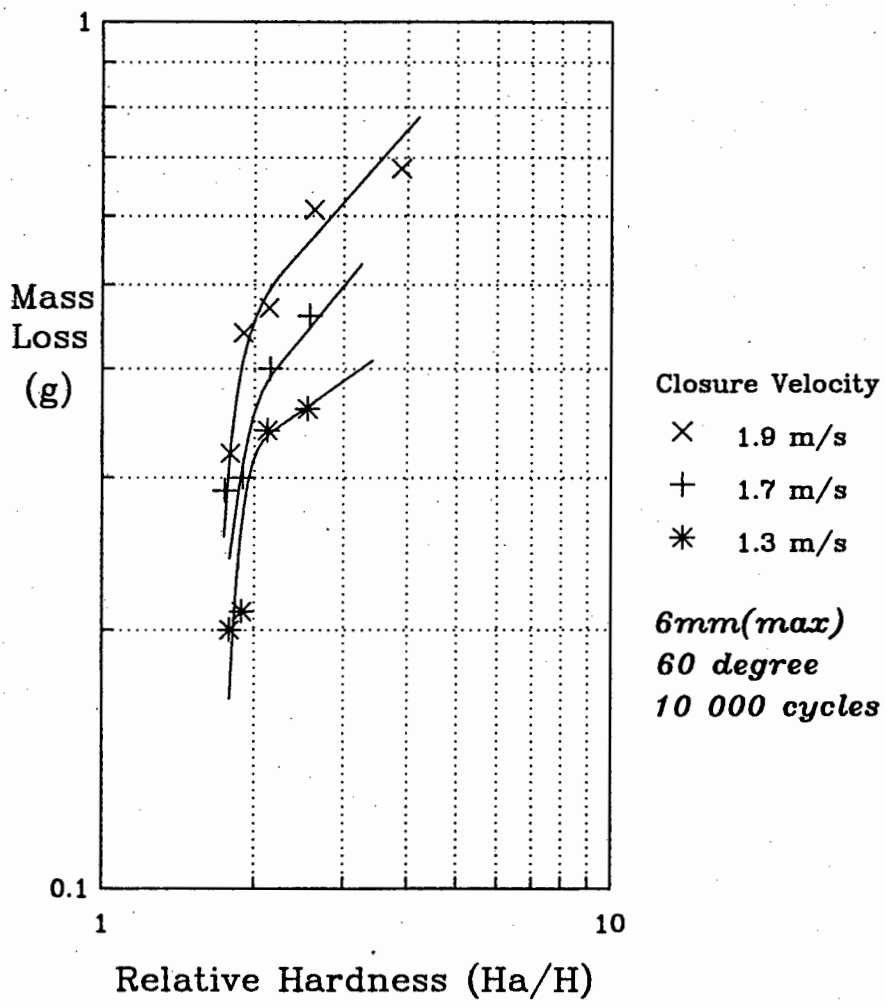

Fig.6.3 Showing the effect of valve closure velocity on mass loss with valves of differing Ha/H values (milled waste).

It is clear from fig.6.3 that increasing the valve closure velocity from 1.7 m/s to 1.9 m/s results in a 40 % greater mass loss for all valves regardless of the the relative hardness. The curves all display a transition in wear behavior which appears to shift marginally at lower closure velocities to higher relative hardness values.

In fig.6.4 a plot of wear loss versus valve closure velocity has been shown as a function of the valve poppet hardness. For the hardest valve poppets i.e. Ha/H = 1.79, the wear loss remains linear as the closure velocity increases. The initial wear loss appears to be linear for the softer materials but increases distinctly at velocities exceeding 1.7 m/s.

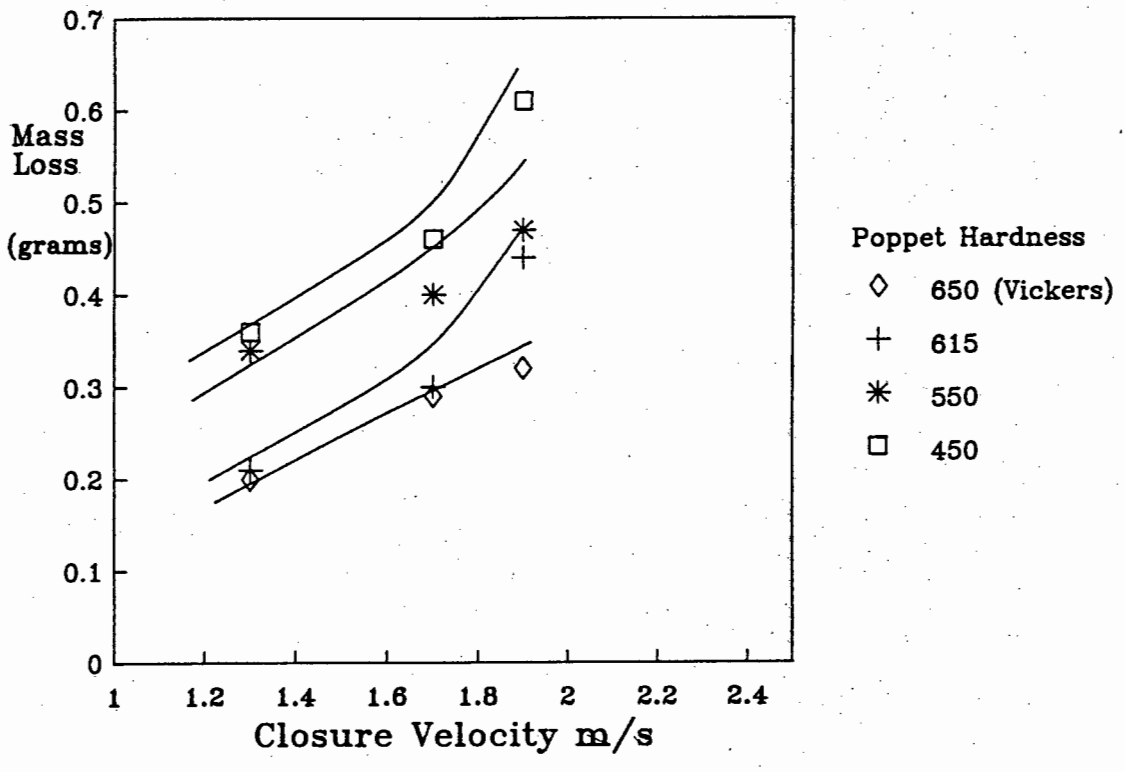

Fig.6.4 Showing the change mass loss with change in velocity (milled waste).

6.2.2 Belt Filter Tailings

The results of the belt filter tailing velocity tests are plotted in fig.6.5 for the 1.3, 1.7 and 1.9m/s closure velocities.

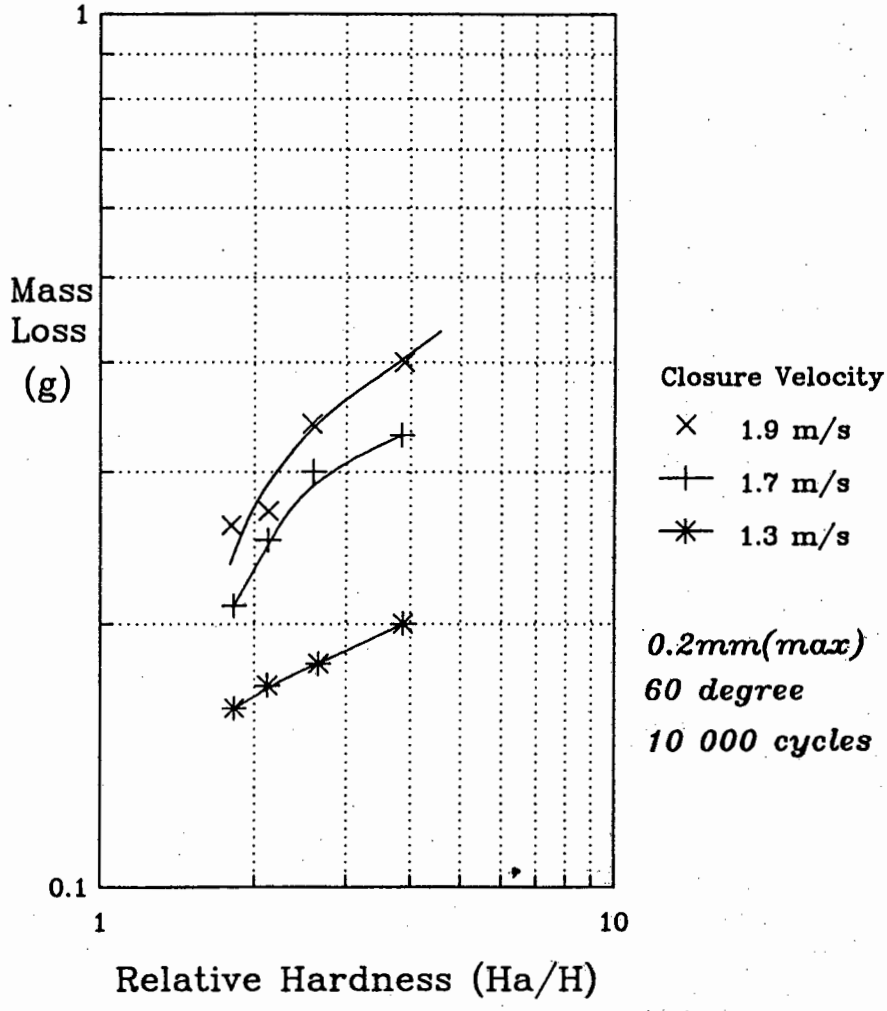

Fig.6.5 Showing the effect of valve closure velocity on the mass loss with valves of differing Ha/H values (belt filter tailings).

From fig.6.5 it is clear that wear loss increases with valve closure velocity and relative hardness (Ha/H) i.e. lower valve hardness. At closure velocities of 1.7 and 1.9 m/s the wear rate (fig.6.5) decreases with increase in relative hardness, as was observed in the milled waste velocity tests (fig.6.3), but at a velocity of 1.3 m/s, unlike the other curves, an increasing wear rate was observed with increase in relative hardness.

In fig. 6.6 a plot of wear versus valve closure velocity has been shown as a function of the valve poppet hardness. However, in contrast to the milled waste (fig.6.4), the belt filter tailings exhibit a linear increase in wear loss with an increase in valve closure velocity, irrespective of the valve poppet hardness (fig.6.6).

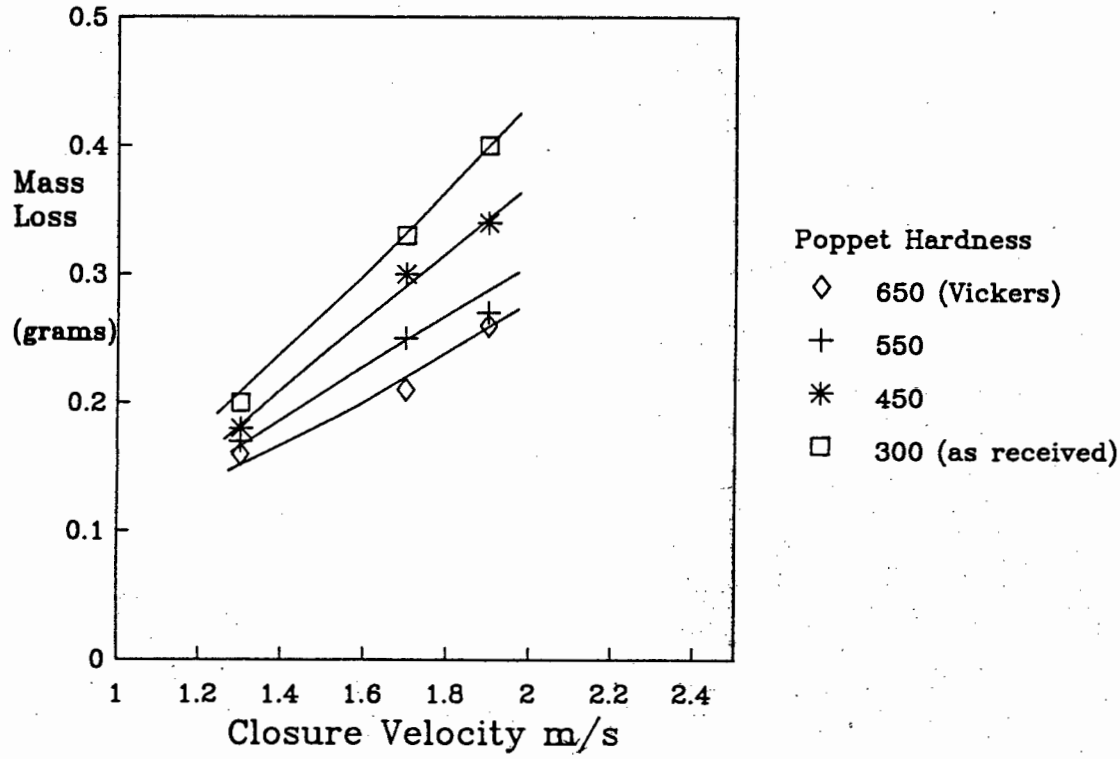

Fig.6.6 The effect of mass loss on closure velocity (belt filter tailings)

6.3 Valve Angle

Three valve angles namely, 45°, 60° and 75° were tested using both the 200µm and 6mm nominal particle size slurries at a constant closure velocity of 1.9 m/s and and a slurry density of 1.7 g/cm^3. The results of the valve angle wear tests are presented tabular form in tables 9 to 12.

6.3.1 Milled Waste

The results of the 6mm comminuted waste rock tests are shown in fig.6.7 for 10 000 cycles. With the exception of the hardest poppet i.e. 650HV, all the valves show a linear increase in wear with an increase in the valve angle and a decrease in hardness. The hardest valve appears to suffer slightly less wear at 60° than at 45° or 75°.

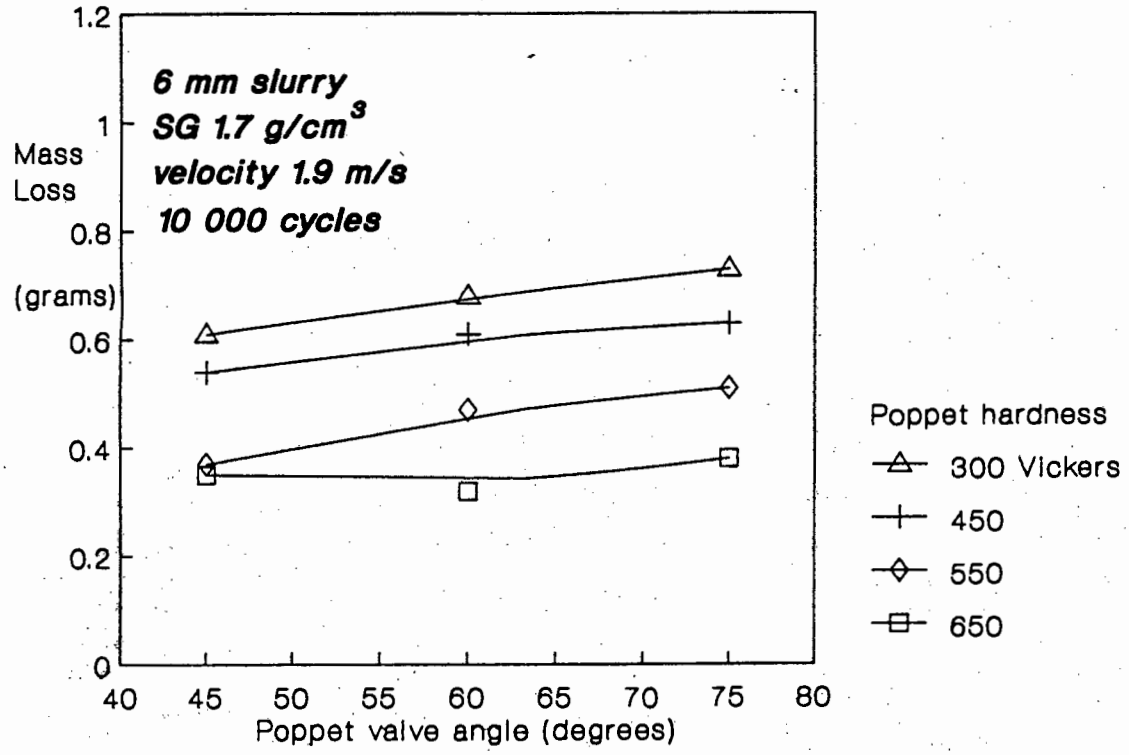

Fig.6.7 The effect of valve angle on the mass loss of valves with different hardnesses.

6.3.2 Belt Filter Tailings

The results of the 200μm comminuted waste rock tests are presented in fig.6.8 at 10 000 valve closures. The two softer steels exhibit a linear increase in wear with a increase in valve angle, a result similar to that shown by the milled waste (fig.6.7). However, in contrast to the milled waste, the two harder steels tested in the belt filter tailings, exhibited a lower wear loss at a valve angle of 60° than either the 45° or the 75° valve angles (fig.6.8).

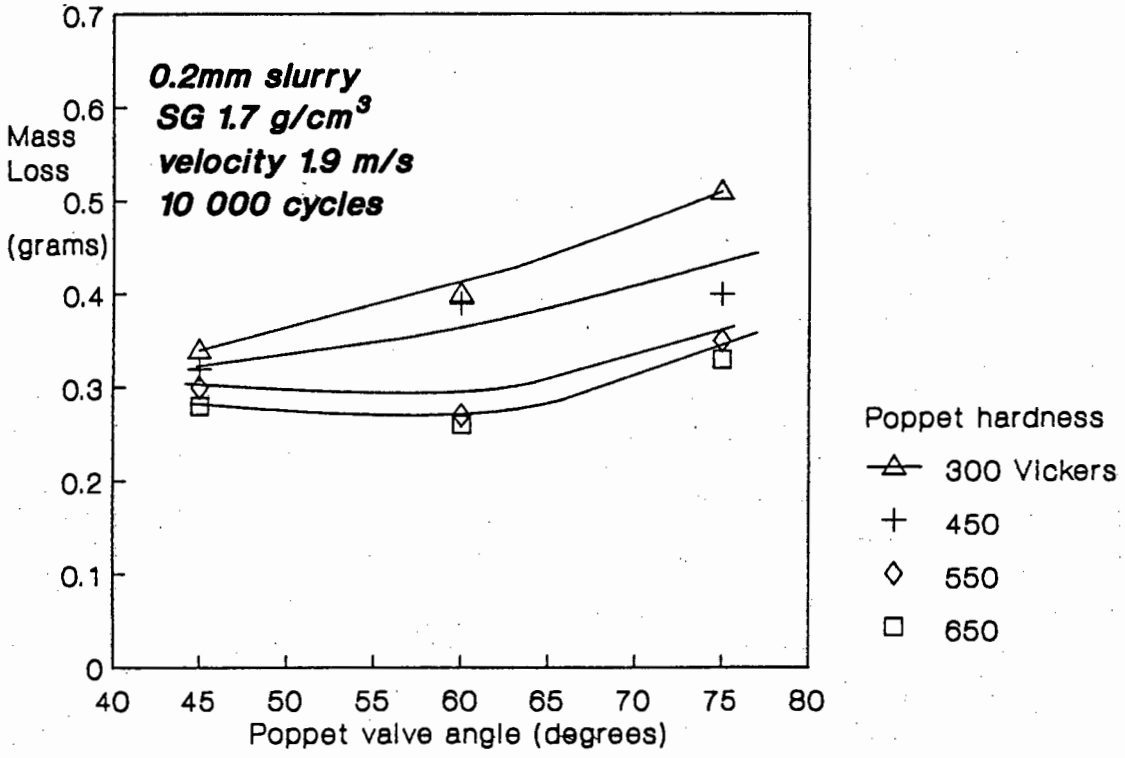

Fig.6.8 The effect of valve angle on the mass loss of valves with different hardnesses.

6.4 Cumulative Wear Loss

The wear on a valve poppet cannot be considered in isolation since it is only one component of the complex wear couple. The cumulative wear loss of the valve assembly i.e. the sum of the seat and poppet losses, are present in tables 1 to 12, appendix C.

The cumulative wear loss was found to generally increase with a decrease in poppet hardness. This is shown in fig.6.9 as a function of the hardness of the poppet, the seat having a similar hardness value in all the tests (600 HV30). However a number of valves exhibited a moderate decrease in cumulative wear at between 450 and 550 HV30 in both the milled waste and belt filter tailings as illustrated in fig.6.10.

The valve poppet's contribution to the cumulative wear relative to the seat, was found to increase as the valve poppets hardness decreased for the series of tests performed. The lowest volume loss, irrespective of the valve closure velocity, slurry density or valve angle, was always found to be at the highest valve hardness figure of 650 HV30. No apparent trend could be found to

describe the seats wear behaviour as a function of the poppets bulk hardness.

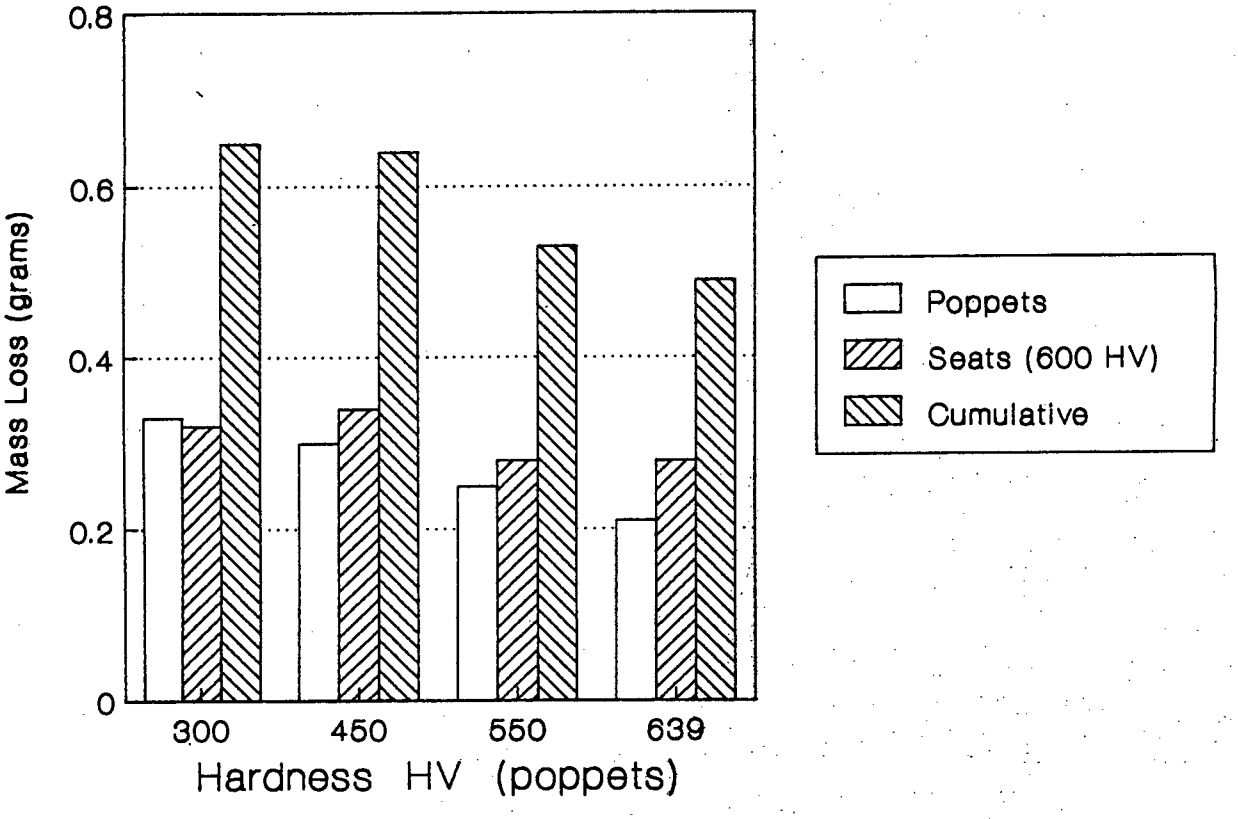

Fig.6.9 The cumulative wear loss as a function of the valve poppet hardness. (belt filter tailings, closure velocity 1.7 m/s, specific gravity 1.7 g/cm^3)

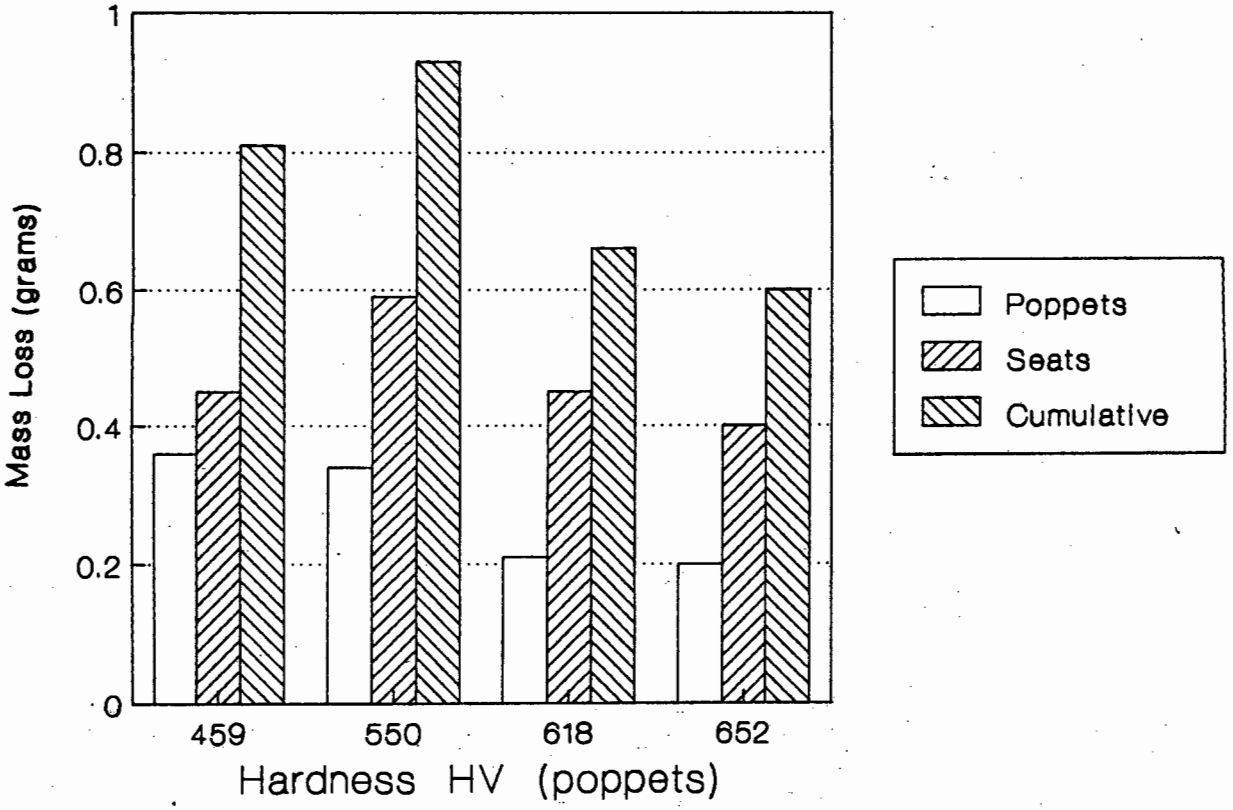

Fig.6.10 The cumulative wear loss as a function of the valve poppet hardness. Note the decrease in cumulative wear at a valve poppet hardness of 459 HV30. (milled waste, closure velocity 1.3m/s, specific gravity 1.7 g/cm)

6.5 Metallographic Examination

An examination of the worn surface morphologies was performed in an attempt to interpret the wear data.

6.5.1 Valve poppets

An examination of the worn valve poppets revealed that the wear patterns of valves tested in coarse slurry differed considerably from those tested in the fine slurry as illustrated in figs.6.11 and 6.12 respectively.

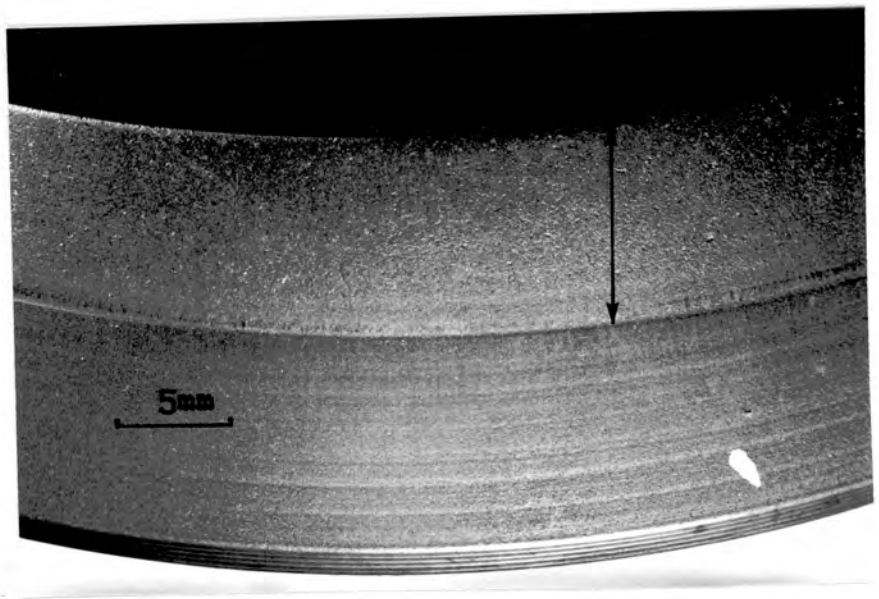

Fig.6.11 Worn valve poppet tested in the coarse slurry, Note the broad wear zone. (specific gravity 1.7g/cm3, velocity 1.7 m/s, 450 HV30).

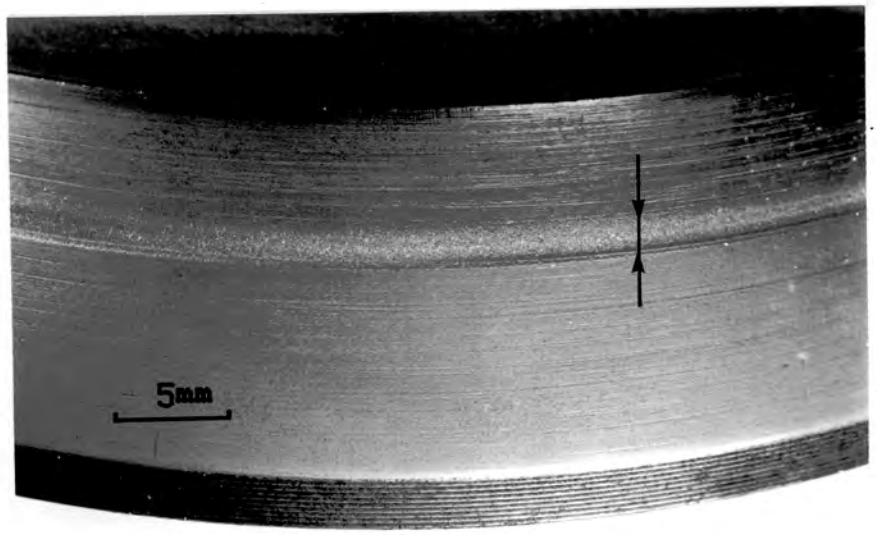

Fig.6.12 Worn valve poppet tested in the fine slurry, Note that wear is confined to a narrow band. (specific gravity 1.7g/cm3,velocity 1.7 m/s, 450HV30).

In contrast to the milled waste valves, which experience wear at the seating line and over the majority of the face below the seating line, belt filter tailing valves exhibit more localised wear around the seating line. This seating line appears to show three distinct wear zones as illustrated in fig.6.13 , particularly in those valves tested in the fine slurry or belt filter tailings.

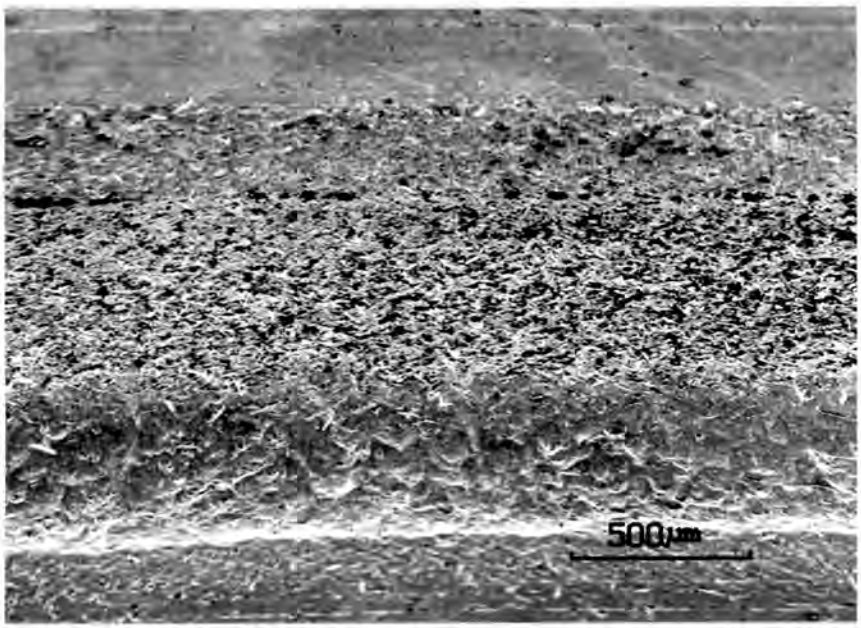

Fig.6.13 Showing the wear zones around the valve seating line

Zone 1 consisted of relatively unworn valve material adjacent to the seating line. Zone 2 (fig.6.14) consisted of an area where the material had been deformed and displaced laterally as a result of multiple impacts leaving a deep groove. In contrast to Zone 2, Zone 3 (fig.6.15) showed definite signs of abrasive wear in which quartzite particles had ploughed out wear tracks. This was particularly evident with the coarse slurry. In addition there was evidence that impacting quartzite particles were also responsible for surface deformation in this area. The actual size of these zones was found to vary, depending on the bulk hardness and angle of the valve. Harder valves resulted in smaller zones in contrast to higher valve angles (75°) which resulted in bigger zones.

Zone 2 rarely exceeded 500μm in width, whilst Zone 3 was found to be directly dependent on the slurry size. Zone 3 was found to be less than 500μm when tested with the fine slurry but as large as 4mm when tested with the coarse milled waste slurry.

In addition, the worn groove in zone 2 appeared to be more severe in the finer slurries.

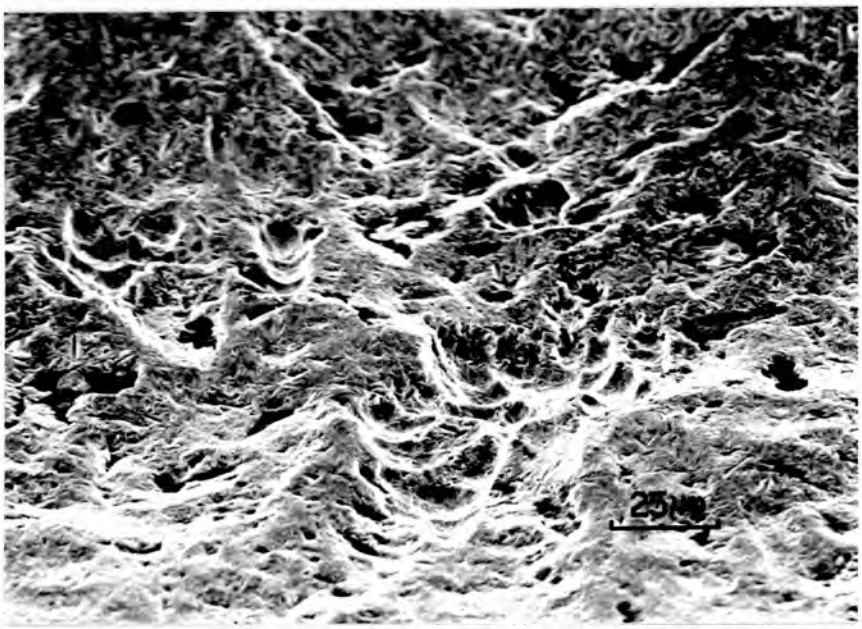

Fig.6.14 Seating line Zone 2, with multiple impact sites (tested in belt filter tailings, valve angle 60°).

Fig.6.15 Zone 3, Impact and abrasive wear damage. Note the embedded quartz particle. (tested in belt filter tailings, valve angle 60°).

6.5.2 Seat

The wear patterns on the valve disc or seats were found to differ vastly in the two different slurries as illustrated in figs.6.16 and 6.17.

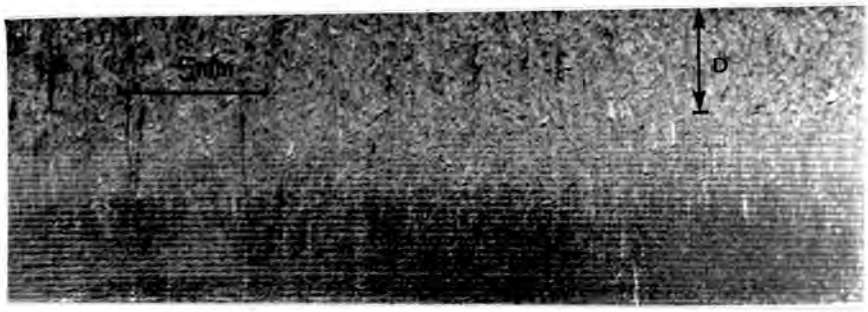

Fig.6.16 Worn seat or disc, Note the wear extends well down the seat. (6mm nominal particle size slurry, specific gravity 1.7g/cm3, 600HV30).

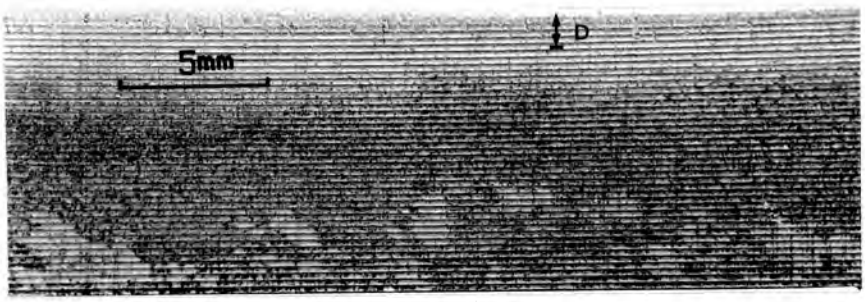

Fig.6.17 Wear is confined to the seat edge, (200µm nominal particle size, specific gravity 1.7g/cm3, 600 HV30).

Wear on the valve seats tested in the 200µm nominal particle size slurry, was confined to a narrow band in the region of the valve edge as indicated in fig.6.18. In sharp contrast, wear on the seat tested in the 6mm nominal particle size slurry was found to extend considerably further down the inside face (fig.6.18). This distance (D), was found to be a function of the poppet valve angle. In addition these seats showed evidence of impact wear on the seat edge as well as deep parallel abrasive tracks down the inside face (fig.6.19).

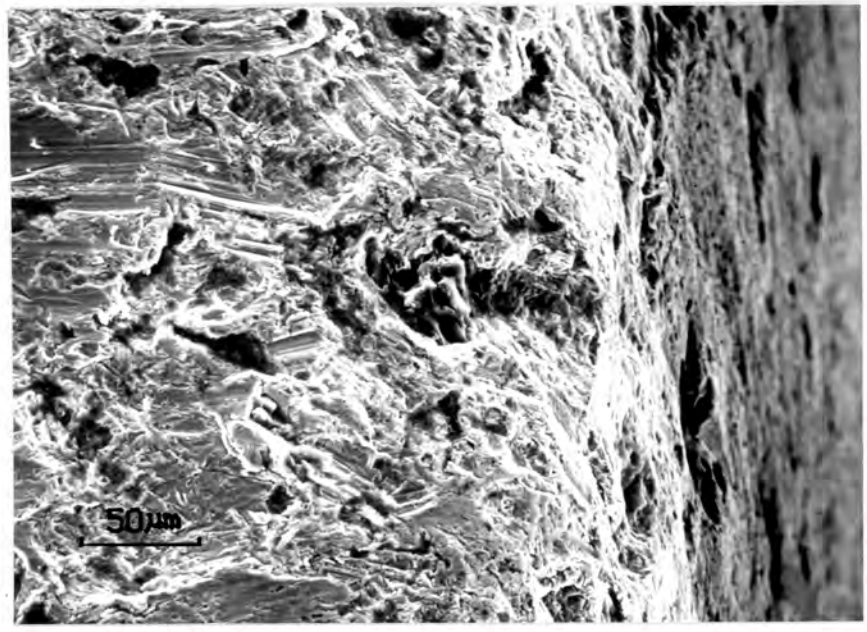

Fig.6.18 A view of the seat edge showing two regions (1) impacts (2) abrasion on the inside face.

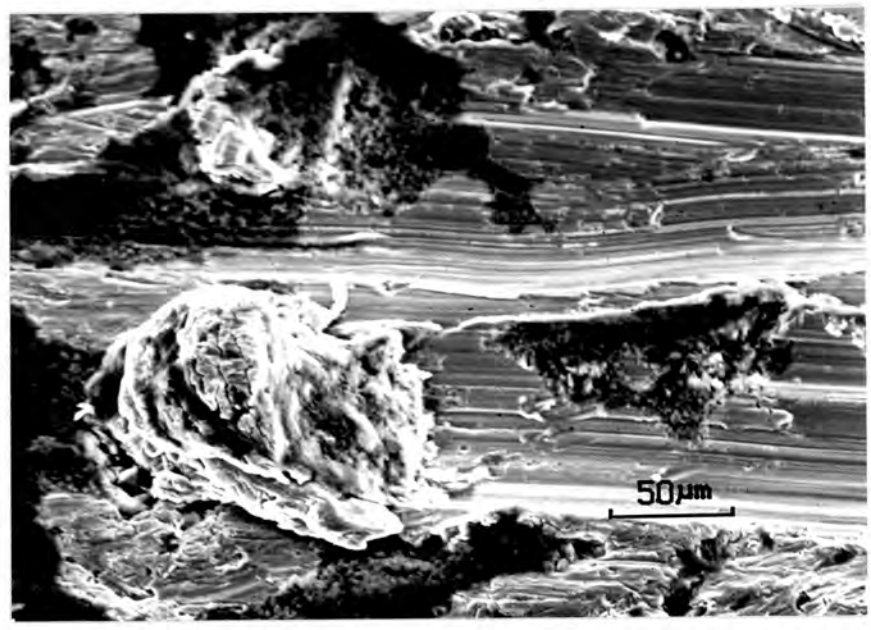

Fig.6.19 Ploughing by abrasive particles on a seat tested using milled waste. Note the embedding of the particle and the severe accompanying plastic deformation.

An examination of this wearing subsurface revealed three distinct subsurface layers as shown in fig.6.20.

1. The undeformed or undisturbed base material.
2. A plastically deformed region.
3. A surface region which differed morphologically from the base material (Zone 1 and Zone 2), being homogeneous and very finely structured.

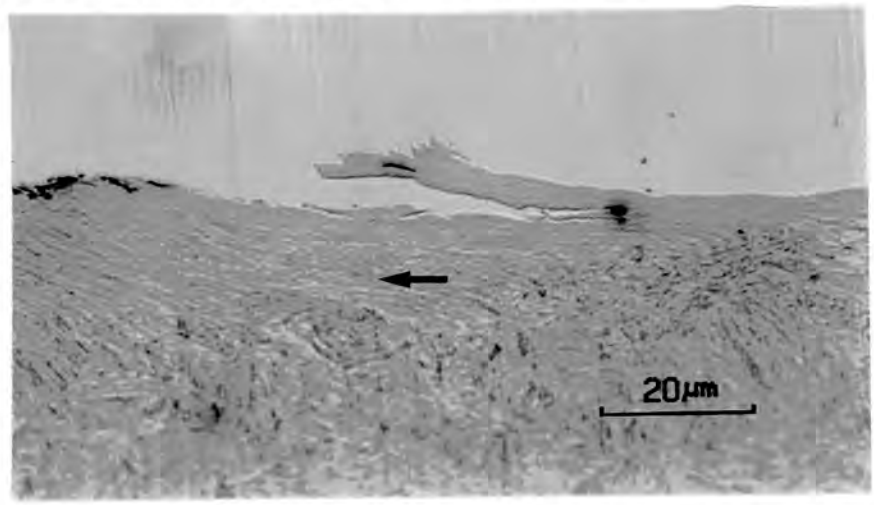

Fig.6.20 A cross section through the worn seat surface. The depth at which flow begins can clearly be seen as well as the sliding direction.

Zone 3 was found to be approximately 240 Vickers harder than the base material. Evidence was also found to suggest that in addition to microcutting and microploughing, delamination of the highly workhardened zones occurred as result of crack and void formation of the subsurface zones, as described by Rice (67). No well defined surface zones were observed on the valve poppets.

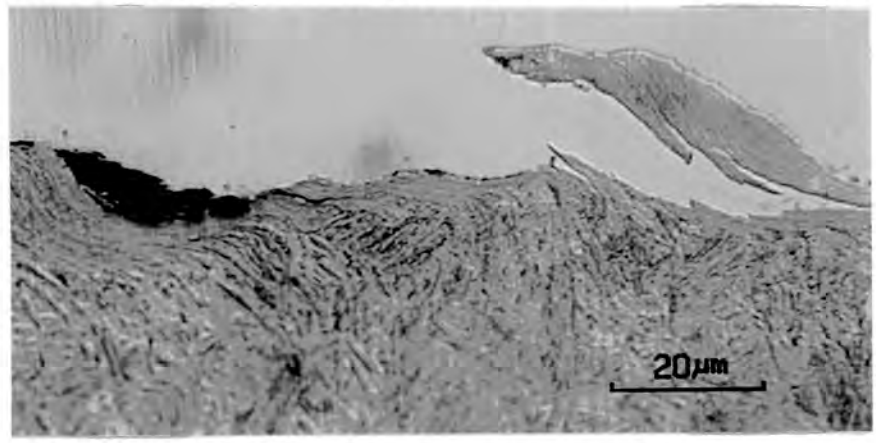

Fig.6.21 Delamination of the surface material on a seat tested in 6mm nominal particle size slurry. Note the impact site and the fractured embedded quartzite particle.

In contrast to the seat tested in milled waste, the wear on the valve seat, tested in the belt filter tailings was found to be almost entirely due to impact damage or microspalling as illustrated in fig.6.22 and 6.23. The absence of subsurface zones is clearly visible in fig.6.24.

Fig.6.22 Impact wear on a seat tested in fine slurry (200µm nominal particle size).

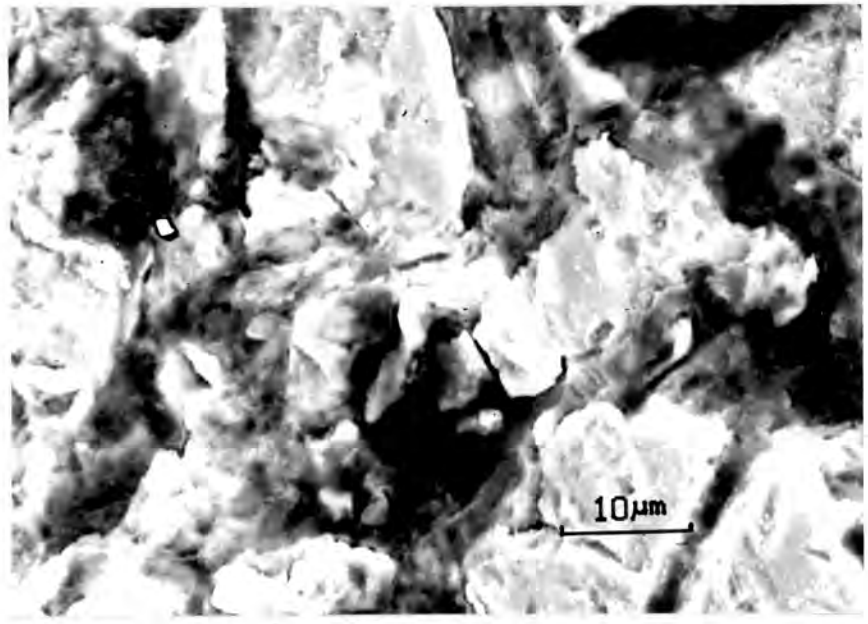

Fig.6.23 Showing impact wear on the seat tested in fine slurry (200µm nominal particle size).

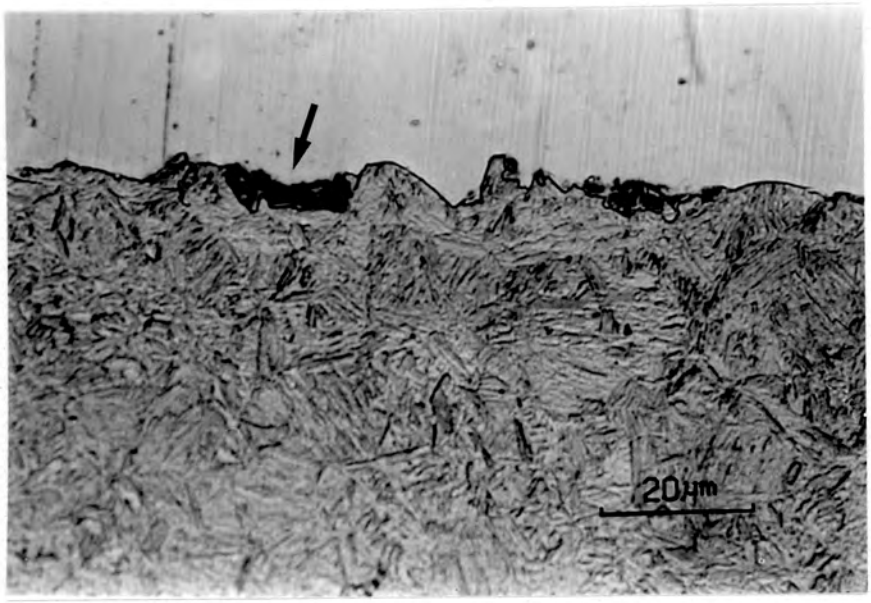

Fig.6.24 A cross section through a worn seat tested in 200µm nominal particle size slurry. Note the absence of sliding deformation and surface zones. In addition note the entrapped quartzite particles.

6.6 Microhardness

The microhardness traverse across a selected number of valve poppets was used to assess the extent of subsurface deformation. All the valve poppets examined, exhibited maximum workhardening near the surface with a decrease in hardness across the strained region to the bulk level.

Increasing the slurry density from 1.7 g/cm^3 to 1.9 g/cm^3 for both the milled waste and belt filter tailings, was found to increase the workhardening value near the surface. A typical example is shown in fig.6.25.

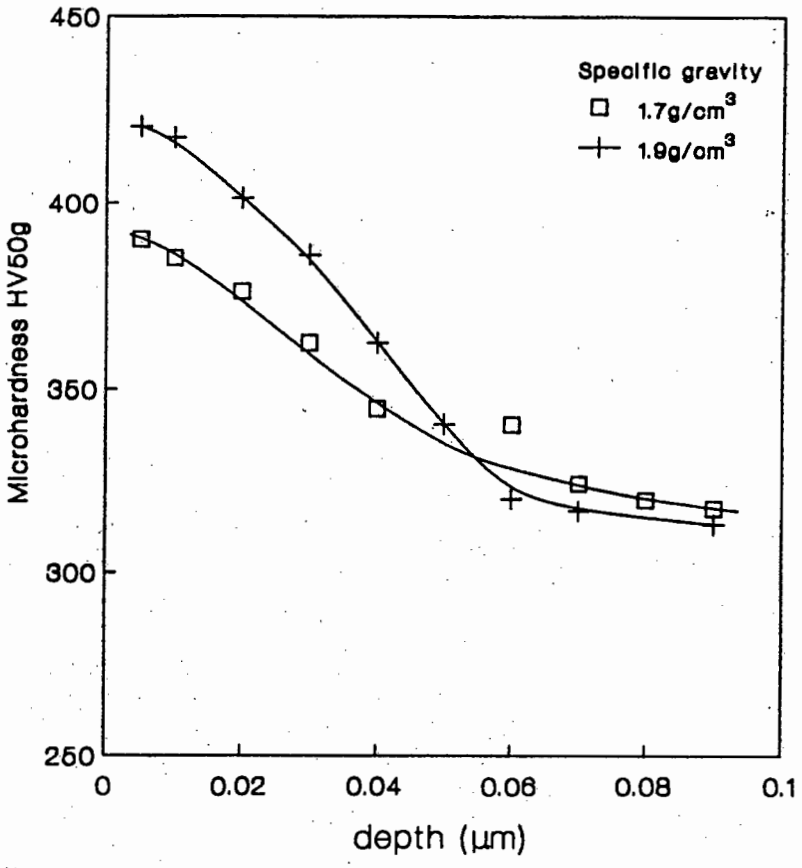

Fig.6.25 Showing an increase in workhardening at a higher slurry concentration for two valve poppets tested in the as received condition, (belt filter tailings, 10 000 closure cycles, valve angle 60°, 1.7 m/s)

Increasing closure velocity from 1.3 to 1.9 m/s resulted in a substantially greater workhardening near the surface as illustrated in fig.6.26. Furthermore increasing closure velocity was found to result in greater depths of workhardening, particularly above 1.3 m/s. Lower valve angles (45°) exhibited greatest workhardening near the surface (fig.6.27).

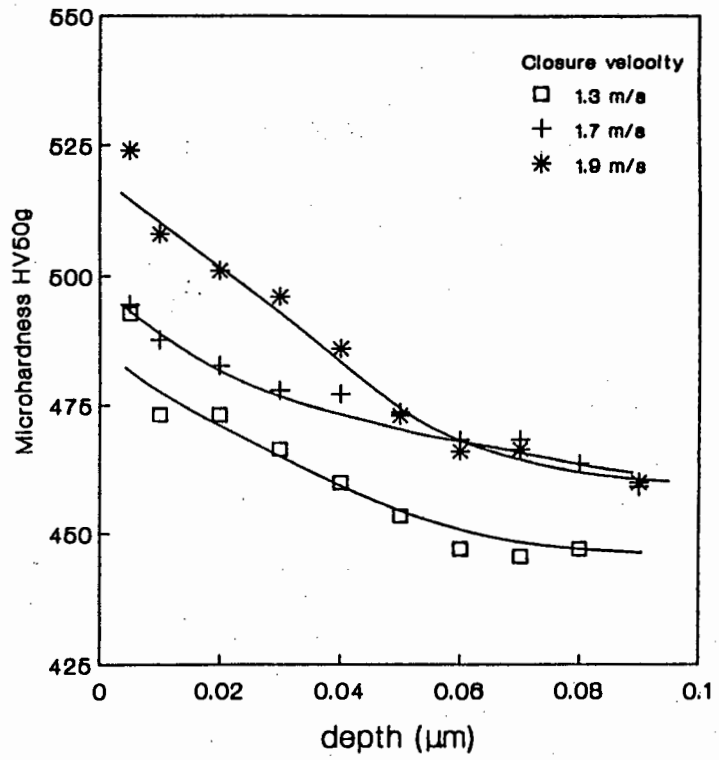

Fig.6.26 Showing reduced workhardening at lower closure velocities, (valve poppets OQ 850°C, tempered 450°C, belt filter tailings, 10 000 closure cycles, 60° valve angle).

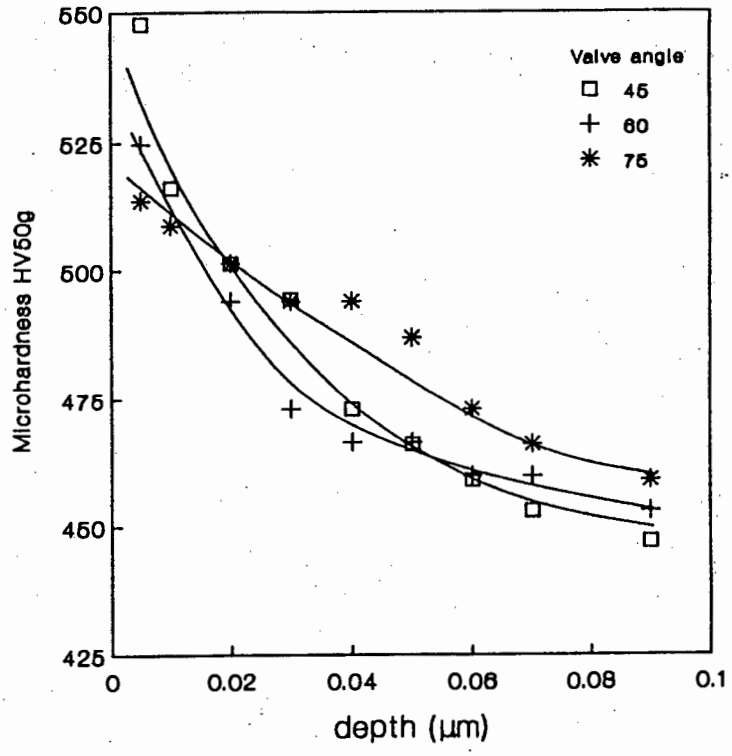

Fig.6.27 Showing increased workhardening at lower valve angles. (valve poppets OQ 850°C, tempered 450°C, milled waste, 10 000 closure cycles, 1.9m/s).

7. DISCUSSION OF RESULTS

In order to interpret the wear data, an understanding of the wear mechanisms which operate during the pumping of slurries is a prerequisite.

7.1 The Wear Mechanism in General

During the suction stage of the pumping operation, slurry is drawn into the valve chamber through the open disc poppet valve.

As the valve begins to close rapidly the larger particles in the slurry are trapped between the valve poppet and the seat (fig.7.1). The particles indent the surface and are crushed under the high load, resulting in impact damage to both the valve poppet and seat. This zone of impact damage on the valve poppet is confined to the seating line area and the area directly below. The impact damage on the seat is usually restricted to a small area on the the edge of the seat.

The impacts result in the formation of craters and material is extruded around the impacting particles causing work hardening of the surface material (fig.7.2). Multiple impacts eventually lead to micro-cracking and micro spalling of the surface layers (fig.7.3).

As the gap between the valve poppet and seat decreases further during closure large trapped abrasive particles are forced to move across the valve and seat surface. This movement results in further deformation and/or microcutting of the metal surfaces through three body abrasive wear (fig.4.20). Delamination of the surface material in the seats may also occur (fig.6.20).

The superposition of both impact and abrasive wear can be seen in fig.7.4.

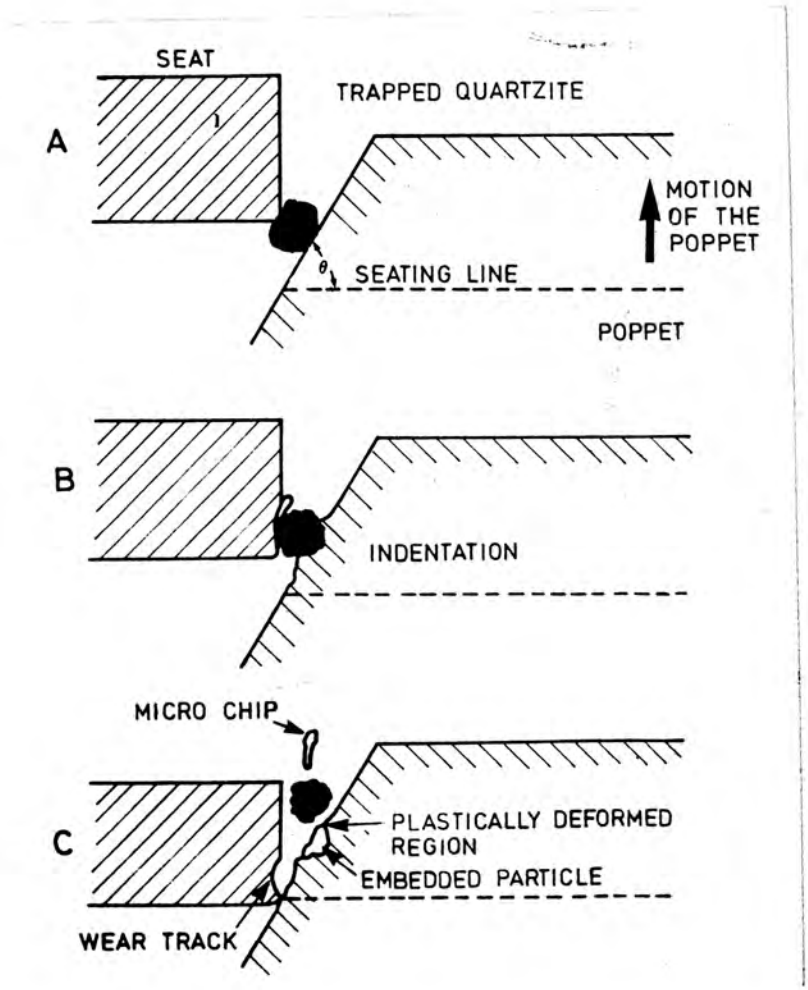

Fig.7.1 Diagrammatic illustration of the sequence leading to wear of the poppet and seat.

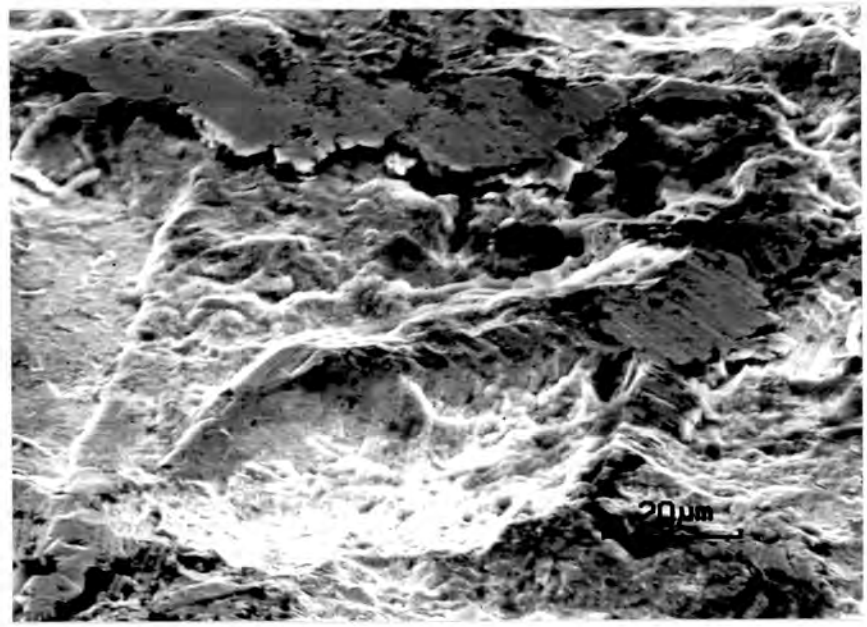

Fig.7.2 Multiple impacts and the formation of wear debris at crater ridges (valve angle 60°).

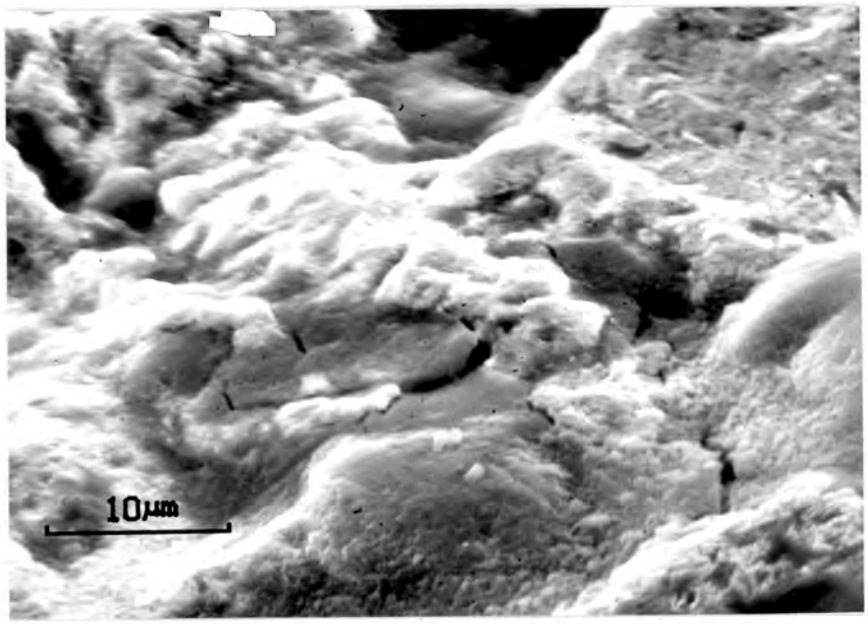

Fig.7.3 Showing micro-cracking of the surface and the formation of a platelet as a result of the impact (valve angle 45°).

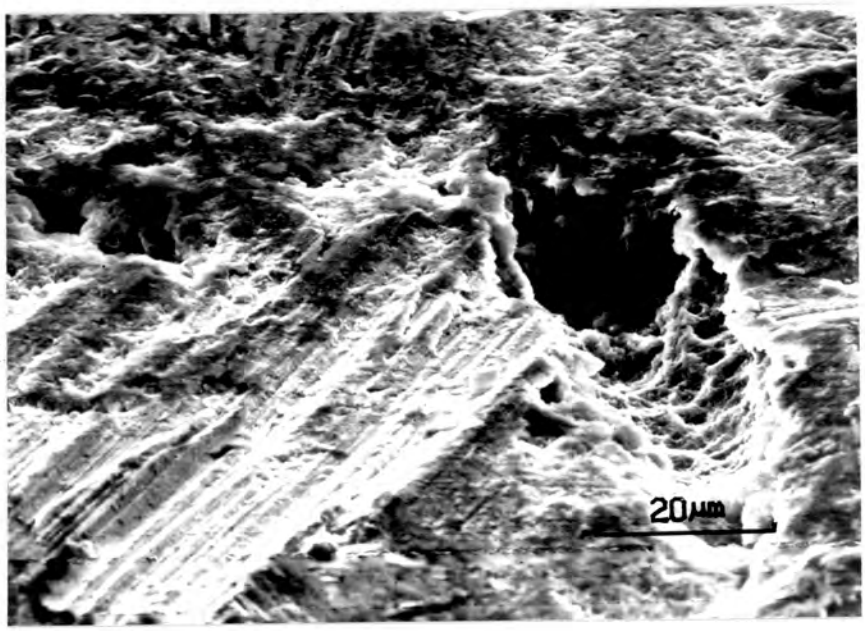

Fig.7.4 The two principle mechanisms, abrasion and impact are visible on this valve poppet. Note the superposition of the abrasive wear track over the impact crater (valve angle 60°).

7.2 Slurry Constitution

7.2.1 The effect of increasing solid concentration

Increasing the slurry density from 1.7 to 1.9 g/cm^3 at a closure velocity of 1.9 m/s is seen to increase the mass loss during testing by 15 % in fine slurries, and by 8 % the coarse slurries, at a poppet bulk hardness of 450 HV30. Whilst the volume of solids flowing through the test cell did not alter with an increase in slurry density, (appendix A), due to a drop in the flow velocity, more particles are likely to be trapped between the valve and seat on closure resulting in a greater number of particles available for impact and abrasion at the valve interface and hence larger mass losses.

The effect of increasing concentration on two valves of equivalent hardness can be seen in fig.7.5 and 7.6. It is apparent from figs.7.5 and 7.6 that increasing the concentration results in greater surface deformation. This in turn results in greater workhardening, particularly near the surface (fig.6.25).

Fig.7.5 Showing the wear on a valve poppet at a specific gravity of 1.7 g/cm^3. Note the embedded quartzite particle.(200µm nominal particle size slurry, 10 000 closure cycles, closure velocity 1.9m/s, 60°).

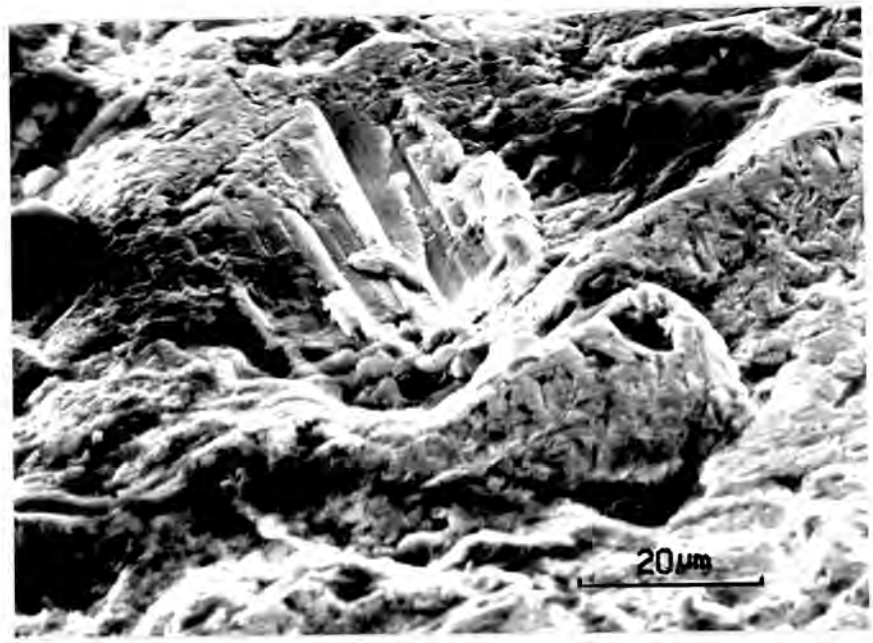

Fig.7.6 Showing the wear on a valve poppet at a specific gravity of 1.9 g/cm^3. Note the massive surface deformation. (200µm nominal particle size slurry, 10 000 closure cycles, closure velocity 1.9m/s, 60°).

7.2.2 Milled waste

This work has established that as the bulk hardness of the valve is increased, the mass loss of the steel decreases, regardless of the valve closure velocity, valve angle and slurry density. Furthermore, an improvement in excess of 50 % in wear resistance, at a specific gravity of 1.7 g/cm^3 and a closure velocity of 1.9 m/s, was obtained when the poppet hardness was increased from 301 HV30 to 652 HV30 (fig.6.1 and 6.3).

In the present situation where quartzite is the transported material, the hardness of the steel should be in excess of approximately 600 HV30 giving a relative hardness of Ha/H = 1.9. Such a result is in agreement with Khruschov (35) and Elkholy (16) who both found a similar transition value for sand/water slurries. It also parallels the results of Richardson (70), who found that for a relative hardness in excess of 2 (Ha/H > 2), relative wear resistance was almost independent of the hardness of the metal matrix.

This change in wear behaviour is believed by many workers to be due to a change in the abrasive wear mechanism from a predominantly ploughing to predominantly cutting mode, with increase in hardness or loss of ductility (58). Hence, the change in wear behavior is explicable in terms

of the abrasion component of the impact/abrasion mechanism.

Valve poppets heat treated to a relative hardness Ha/H of less than 1.9 are considerably harder and less ductile than valves with a relative hardness 1.9. The poor ductility or conversely the high hardness results in reduced penetration of the surface during impact and abrasion by the quartzite particles, hence favouring the cutting mode during abrasion rather than the ploughing mode which is more prevalent at lower hardness values (25). Consequently, less surface material is displaced at high hardness values which in turn leads to lower wear losses. Observation of the worn valve surfaces confirms that there is a noticeable decrease in the severity of the surface deformation caused by the abrasive component at higher valve hardness values, which would substantiate this argument. This is illustrated in figs. 7.7 and 7.8.

Although valve poppets exhibit a greater impact resistance above the transition point, this improved impact resistance is offset against an appreciable decrease in hardness (fig.5.1). The increased ductility of the material results in greater penetration of the surface and consequently in the formation of larger impact craters and boundary peaks. These surface protrusions are subsequently microcut and/or ploughed off by the abrading particles.

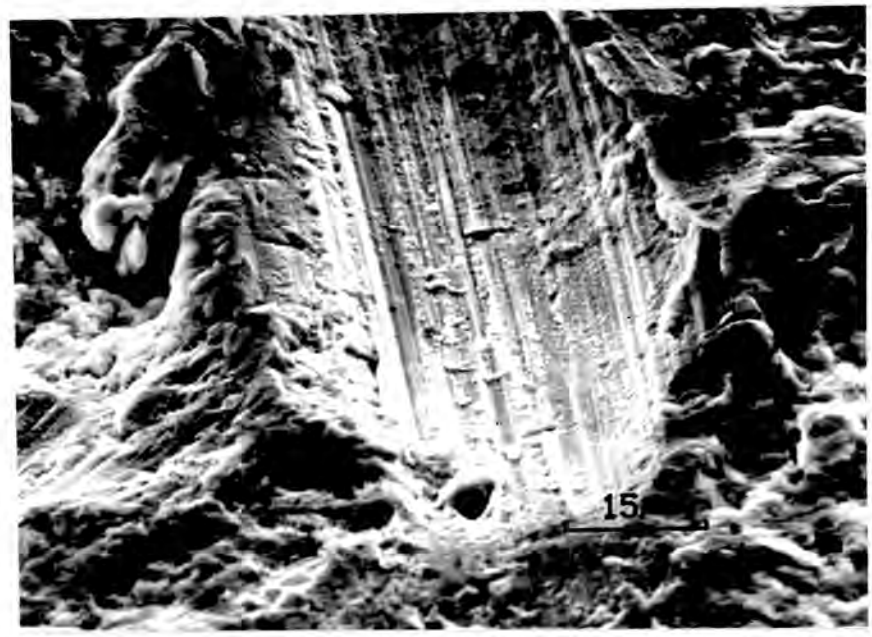

Fig.7.7 Showing predominantly ploughing of the relatively soft valve poppet (450 HV30,closure velocity 1.9 m/s, specific gravity 1.9 g/cm3, valve angle 60°).

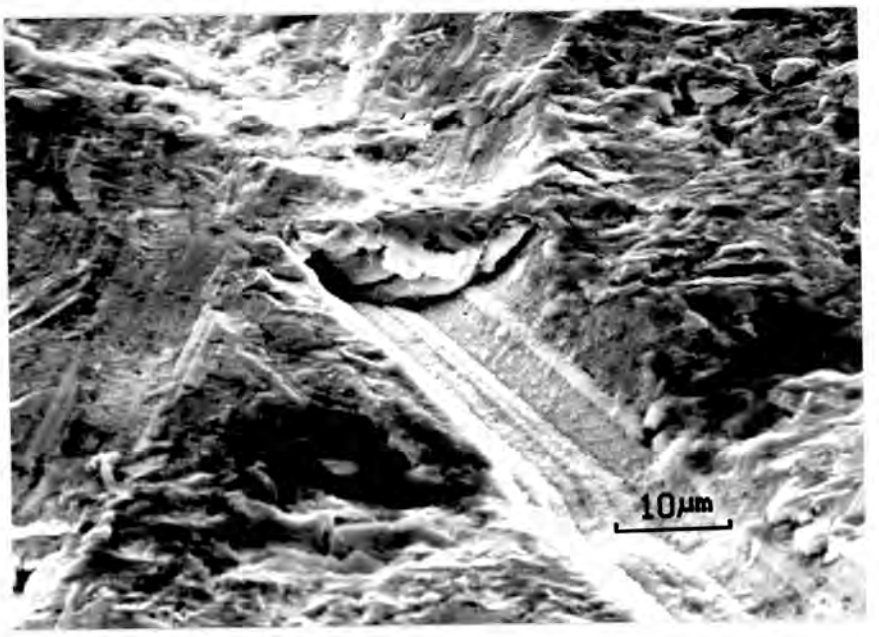

Fig.7.8 Showing predominantly cutting of the relatively hard valve poppet (650 HV30). Note the superposition of the impact mode.(valve closure velocity 1.9 m/s, specific gravity 1.9g/cm3, valve angle 60°).

In summary, when pumping 6mm nominal particle size slurry, the two mechanisms of impact and abrasive wear are responsible for material removal on both the poppet and seat (fig.6.16). As the hardness of the valve poppet increases, cutting wear becomes more predominant compared to surface deformation and ploughing. The transition from ploughing to cutting wear mode manifests itself in a change in the shape of the the mass loss versus hardness curve.

At higher slurry densities, the impact and abrasion mechanisms become more severe above the transition point resulting in a less distinct transition point. In contrast reduced closure velocity has the opposite effect.

7.2.3 Belt filter tailings

In the course of this work it was established that the wear rate of a valve tested in belt filter tailings (200µm nominal size particle slurry) was between 18 to 34 % lower than a valve of an equivalent hardness tested under the same operating parameters in the milled waste slurry. This result is in agreement with Miller (38) who observed that accelerated wear of disc poppet valves occurs in service when the abrasive particles exceed 2mm in diameter.

With reference to fig.6.12, the absence of any abrasive wear tracks and the predominantly micro-spalling of the surface, suggests that the wear caused by the 200µm slurry can almost entirely be attributed to the impact wear mechanism, irrespective of the poppet hardness as illustrated on figs.6.23 and 7.09.

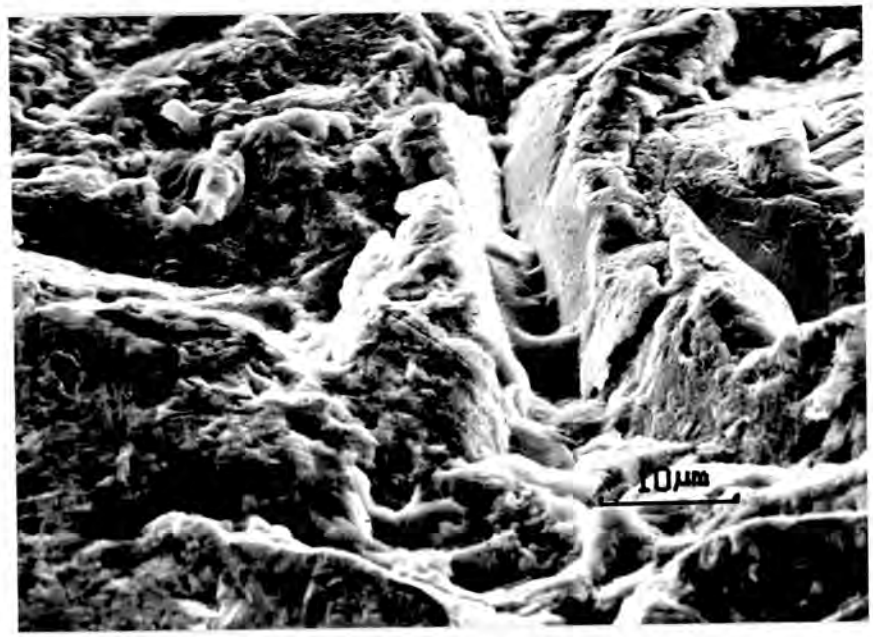

Fig.7.9 Showing impact wear on a poppet tested in 200µm slurry.

As was found in the milled waste, the size and depth of the impact craters appears to be a function of the hardness i.e. more material is displaced in the softer valves resulting in increased surface deformation. However it is not recommended that crater volume be used as an indication of wear because material may not necessarily be removed as a result of an impact but may be displaced plastically to the crater ridges (76). Furthermore, the large particle size distribution in both the slurries produces a broad range of indentation, making a comparison of crater volumes very difficult (fig.7.10).

Although considerably less wear occurs in finer slurries, the nature of the wear is such that it is more localized around the seating line than in the coarse slurries i.e. it develops a deeper seating groove which could result in premature failure due to subsequent flow erosion.

Fig.7.10 Showing a high density of small impacts and a range of different impact crater diameters (tested in 200µm slurry, valve angle 60°). Note the rotational flow and the incorporation of the fractured quartzite and oxide surface as described by Levi (41).

7.3 Valve Closure Velocity

The higher wear with increased valve closure velocity for both the 6mm and 200µm nominal particle size slurries, may be attributed to the larger component of impact force, since more kinetic energy is available ($K_e=\frac{1}{2}mv^2$) per impact, resulting in greater penetration of the quartzite particles in the valve and seat, and consequently both in greater depth and surface workhardening as illustrated in fig.6.26. This ultimately leads to greater material losses. Increasing the closure velocity from 1.3 to 1.9 m/s using the milled waste slurry, results in an increase of between 37 to 40 % in the wear loss at a specific gravity of 1.7 g/cm^3, depending on the poppet bulk hardness. Jahanmir (29) has shown that this wear rate is dependant on the depth of microvoid nucleation and crack propagation and hence on the velocity of impact.

Furthermore, higher velocities are known to decrease abrasive wear resistance (54). Noel (61) has attributed this decrease in wear resistance at higher velocities to a deterioration in the materials dynamic properties as well as, greater particle loading and flow effects of the contacting particles.

7.4 Valve Angle

The effect of valve angles on the impact and abrasive mechanism will be considered individually.

7.4.1 Impact mechanism

The increase in wear rates with increase in valve angle can be explained on the basis of the tangential component of impact which causes deformation and wear ahead of the impacting particles, as illustrated in fig.7.11.

The size of the tangential component of impact and hence the wear rate is determined by the angle of impact (θ) i.e Lower angles of impact lead to greater extrusion of material compared to 90 degree impact angles, as shown in fig.7.11. A similar behaviour was observed by Bitter (10) in ductile materials (fig.3.20).

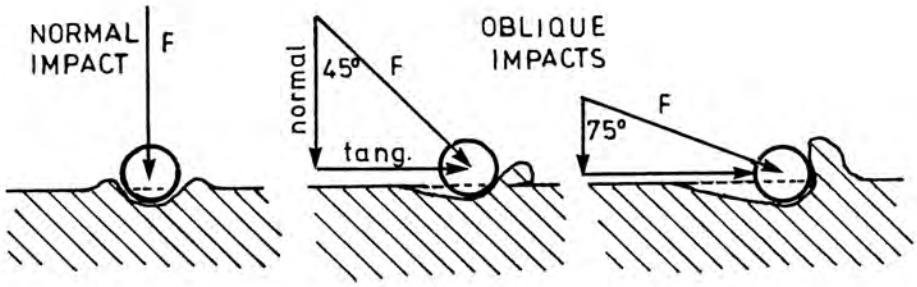

Fig.7.11 The effect of particle impact angle on the magnitude of the tangential force and the subsequent surface deformation.

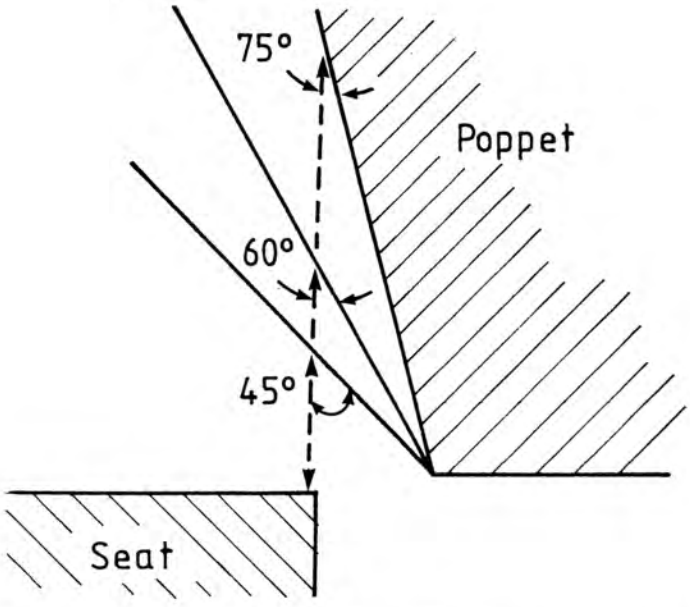

Fig.7.12 Illustration showing the position of the valve poppet in relation to the seat or disc at different valve angles.

From fig.7.12 it is clear why impacts are predominantly normal on the seat irrespective of the slurry size or valve angle. From fig.7.12 it can also be appropriated why more wear occurs at higher valve angles (to the vertical). The effect of impact angle is shown in figs.7.13 to 7.15 for three different valves of comparative hardness tested under the same experimental parameters.

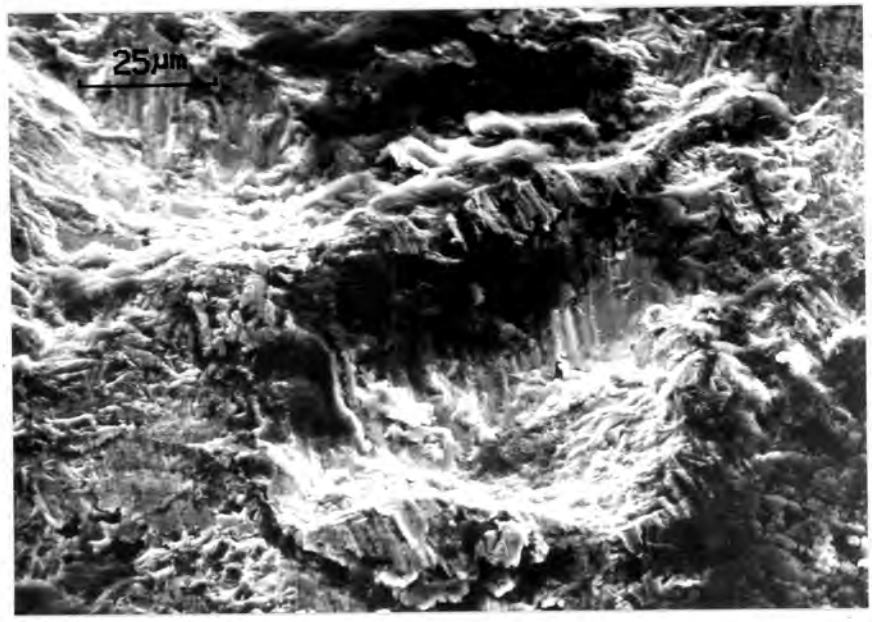

Fig.7.13 Valve angle 45 degrees. (Tested in milled waste, closure velocity 1.9m/s, specific gravity 1.7g/cm3).

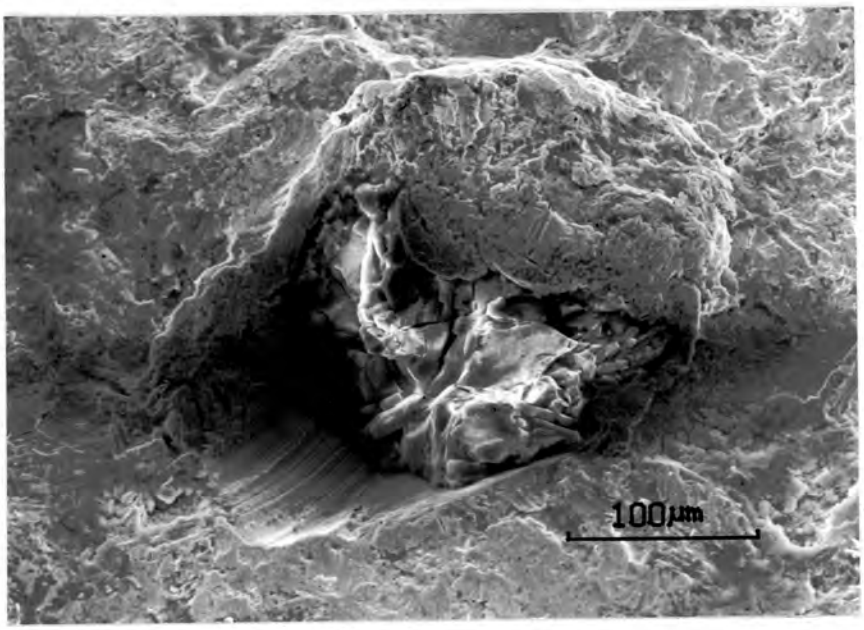

Fig.7.14 Valve angle 60 degrees. Note the cutting and deformation ahead of the quartzite particle (tested in milled waste, closure velocity 1.9m/s,.specific gravity 1.7g/cm3.

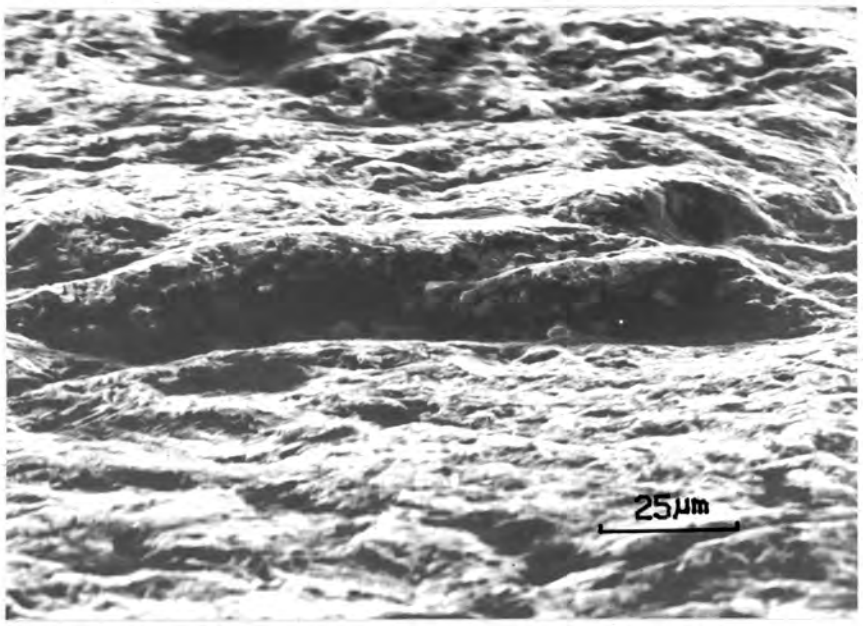

Fig.7.15 Valve angle 75 degrees. Note the undercutting of the plastically deformed region ahead of the crater (tested in mill waste, closure velocity 1.9m/s, specific gravity 1.7g/cm).

The apparent poor performance of the harder 45 degree

valve poppets (figs.6.7 and 6.8) may be attributed to microspalling of the hard material as a result of the high angles of impacts and hence the large normal component of impact i.e a 45 degree valve has a larger normal component of impact than a 60 or 75 degree valve as illustrated in fig.7.11. This is confirmed by the higher workhardening values found near the surface at lower valve angles (fig.6.27).

Multiple impacts lead to the formation of subsurface micro-cracking and microspalling as shown in fig.7.3. Sare (74) suggested these subsurface cracks may develop and propagate during each impact cycle after fracturing of the inherently brittle carbide phase in the steel matrix as a result of shock waves which accompany impacts (fig.7.16).

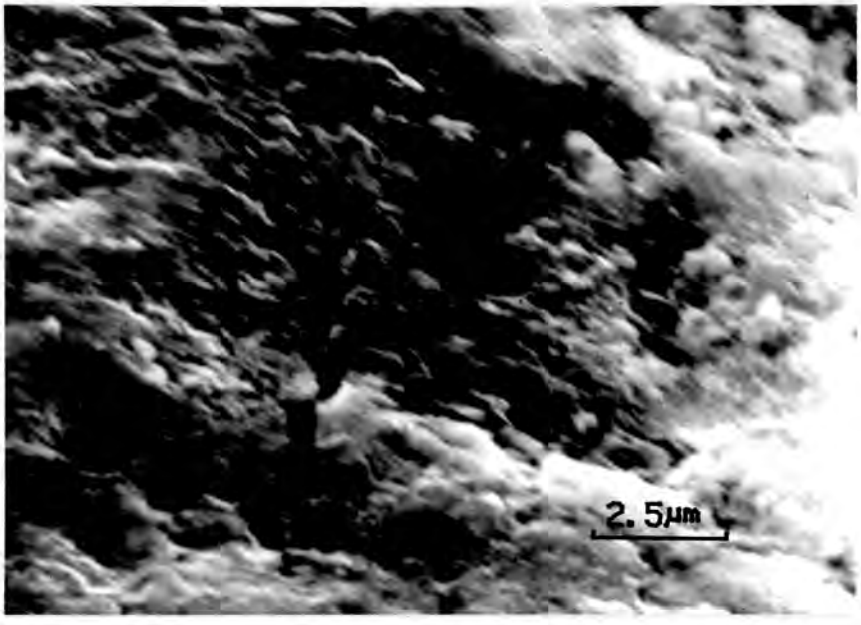

Fig.7.16 A micro-crack intersecting the surface of a valve poppet. The crack appears to be growing progressively around surface obstacles.

Jahanmir (29), suggests that the impacts and the accompanying workhardening results in a certain amount of subsurface strain with the subsequent formation of cracks and production of wear debris as illustrated in fig.7.17 and 7.18.

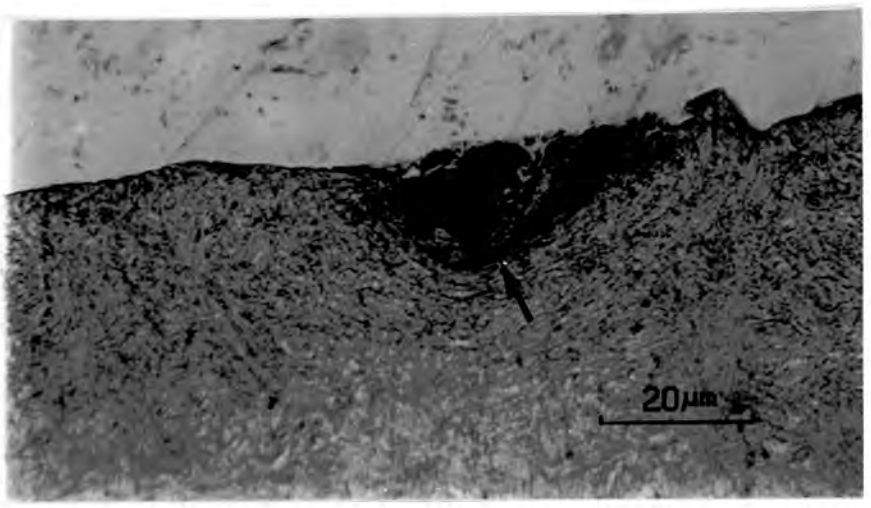

Fig.7.17 Subsuface cracking below the impact sites Note the entrapped quartzite particle.

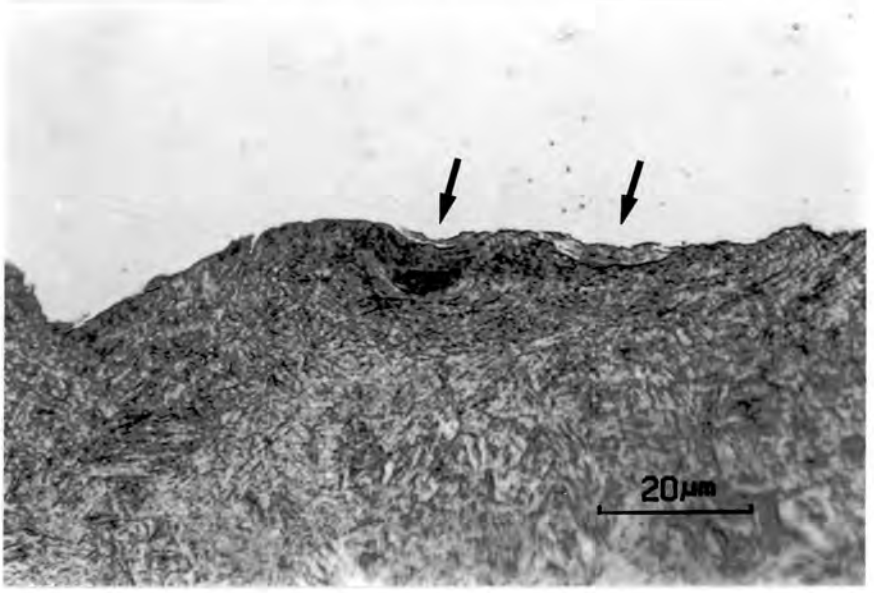

Fig.7.18 A cross section of a valve poppet showing a subsurface crack and the formation of exfoliations below impact sites. The micrograph shows the orientation and formation of two subsurface cracks (valve angle 45°).

Evidence has clearly been found to support both these theories of crack formation. However, a third possibility may exist i.e a combination of the two theories. The subsurface strain which accompanies an impact may reduce the threshold stress required to nucleate cracks in the brittle carbides and hence aid the formation and propagation of these cracks. This would also account for the preferential formation of cracks directly below the impact i.e where maximum surface strain and impact stress occur (fig.7.18).

Although micro-cracking and micro-spalling are not exclusive to the 45 degree valves, they occur sooner at 45° than at higher angles because of the larger normal component, which is responsible for the majority of subsurface strain directly below an impact. The onset of micro-cracking and micro-spalling in valves tested in the fine slurry (200μm nominal particle size) at 45 degrees occurs sooner. This can be attributed to the fact that wear is almost completely an impact event in these slurries and thus very little energy is directed into the abrasion component and thus a large normal component can be expected.

7.4.2 Abrasive mechanism

As mentioned previously, the mechanism leading to metal loss appears to be predominantly abrasion for the milled waste slurry only. The abrasion mechanism is particularly severe at high angles to the vertical (i.e. valve angle 75 degrees), and progressively less severe at lower angles (i.e. 45 degrees). A similar effect was found for the corresponding seats. The increase in abrasive wear at high valve angles can be attributed simply to the the valve geometry. The gap between the seat and poppet is considerably smaller for a 75 degree valve than a 45 degree valve, resulting in deeper gauging of the valve poppet and seat when particles are trapped between the surfaces.

7.5 Seating line

The formation of a seating line on the valve poppets (figs.6.11 and 6.12) may be almost entirely attributed to the impact mechanism. Repetitive percussive loading results in the formation of a seating line at the valve interface.

From Fig.7.19 it can be seen that impacts are normal above the seat and oblique below. Although the seating line is found on poppets using the coarse slurry, it is particularly severe when testing with belt filter tailings (200μm slurry), because of the impact dominated mechanism.

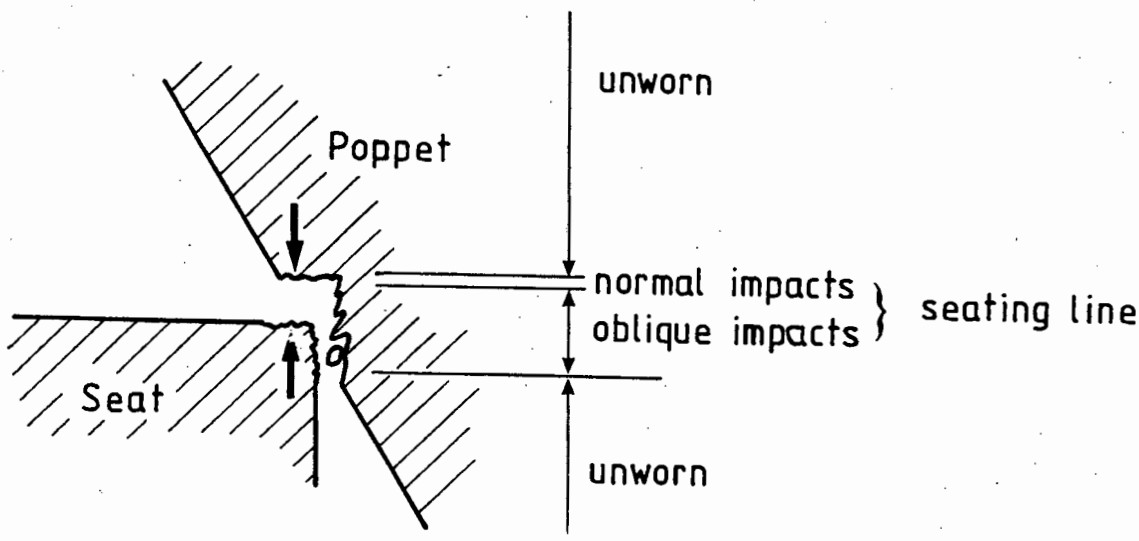

Fig.7.19 Showing the formation of a seating line.

7.6 Cumulative wear loss

An interesting trend, irrespective of the slurry constitution, valve closure velocity or valve angle, is that the contribution by the valve poppet to the total wear loss of the system i.e. the cumulative loss of the poppet and seat, usually increases as the poppet hardness decreases in relation to the seat. The notable exceptions were the 75 degree valves tested in milled waste, which shows accelerated abrasion of the seats due to the geometry of the valve.

In an attempt to understand why the seat's contribution to the cumulative wear should generally decline or conversly the poppets contribution to the cumulative wear should increase as poppet hardness decreases, two hypothetical valve couples will be considered for a given impact load.

As the valve closes there is an equal but opposite reaction on both the poppet and seat. When the poppets hardness (Hh) marginally exceeds the seats hardness (Hs) i.e. Hh > Hs, the probability of penetration by the quartzite particle is equally likely on both wearing surfaces (fig.7.20). However, if the poppet hardness (Ht) of the valve couple, is considerably lower than that of the seat hardness (Hs) i.e.Ht << Hs, the probability of penetration by the quartzite during impact will be much greater on the poppet than the seat due to the lower flow stress of the material (fig.7.21). The net effect will be that the seats contribution to the cumulative loss

relative to the poppet will decline at lower poppet hardness values, as illustrated in fig.6.9 and 6.10.
It can be seen from figs.7.20 and 7.21 that although the ability of the valve couple to absorb energy is considerably greater at a lower poppet hardness value, this increase is offset by a reduced poppet flow stress which results in greater penetration of the surface and hence greater wear rates.

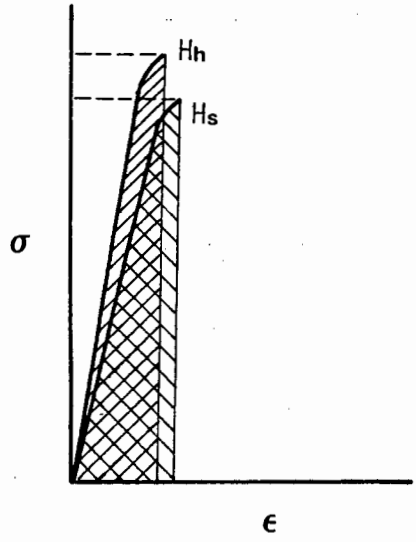

Fig.7.20 A hard poppet(Hh), hard seat(Hs).

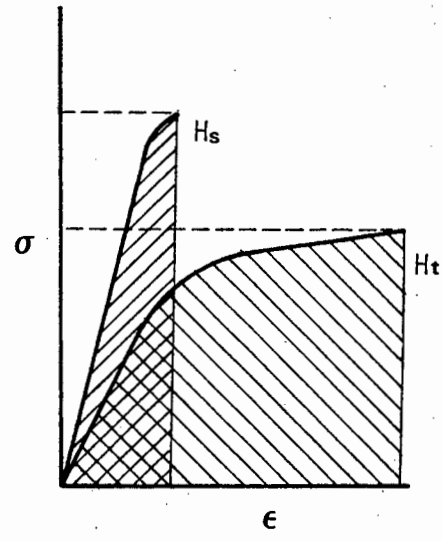

Fig.7.21 A relatively soft poppet(Ht), hard seat(Hs).

However, it would appear from the results, that the rate at which the poppets contibution to the cumulative loss increases, is unique in each valve system, and depends strongly on the complex interaction of the different operating parameters. It is this complex interaction between the valve couple and the operating environment which determines whether the valve system shows a moderate decline in cumulative wear at poppet hardnesses between 450 and 550 HV30.

8. CONCLUSION

The following conclusions have been reached in this study:

1. The wear of the poppet valve is dependant on hardness, slurry size, slurry concentration, valve closure velocity and valve angle.

   a) Valve poppets perform better at higher hardness values irrespective of slurry constitution, valve closure velocity and valve angle.

   b) A transition point on a relative hardness versus wear loss curve for valve poppets was identified at Ha/Hm≈1.9 for the 6mm nominal particle size slurries. This transition point remains the same when the specific gravity is increased from 1.7 to 1.9 g/cm^3.

   c) Coarser slurries (milled waste) result in much greater weight losses than finer slurries (belt filter tailings) on both the poppet and seat.

   d) Increasing specific gravity (concentration) results in more wear by both the belt filter tailings and milled waste slurries. The increase in wear is particularly severe in the softer valves at higher concentrations.

   e) The lowest wear occurs at the lowest closure velocity i.e. the valves suffer the least wear at 1.3m/s for both the 200μm and 6mm nominal particle size slurries.

   f) A significant increase in the wear loss appeared to occur at closure velocities exceeding 1.7 m/s for a relative hardness in excess of 1.79 in coarse slurries.

   g) For valve poppets tested in the coarse slurry, the lowest wear occurs at a valve angle of 45 degrees and the highest at 75 degrees, with the exception of valves harder than 550 Vickers. These valves experience their lowest wear at a valve angle of 60 degrees.

   h) For valves poppets tested in the fine slurry, the lowest wear occurs at a valve angle of 45 degrees and the highest at 75 degrees, with the exception of valves harder than 450 vickers. These valves experience their lowest wear at a valve angle of 60 degrees.

2. The general mechanism of wear was found to be a combination of high stress three body abrasion and impact wear. The mechanism of wear was found to be a function of the valve hardness, slurry size, slurry concentration, valve closure velocity and valve angle.

   a) Valves tested in the 200μm nominal particle size slurry suffered mainly impact wear on both the poppet and seat.

   b) Valves tested in the 6mm nominal particle size slurry suffered a combination of abrasion and impact wear on the seat and poppet.

   c) The transition from a cutting to ploughing wear mode manifests itself in a change in the shape of the mass loss versus hardness curve for the coarse slurry.

   d) Deformation and cutting wear as a result of oblique impacts on the poppet valve were found to be responsible for the high wear loss at high valve angles i.e. 75 degrees, particularly in the fine slurry. Severe abrasive wear was also found to be responsible in the coarser slurry because of geometrical constraints between the valve poppet and seat.

   e) The apparent poor performance of the hard 45 degree valve poppet may be attributed to the microspalling of the hard material as a result of the high angles of impact.

9. RECOMMENDATIONS

The effect of corrosion on the valve and any possible synergistic effects have not been investigated but should be considered in the final valve material selection. Based on the findings of this study, service life may be extended up to 100% if the following recommendations are adhered to:

1. Valve angle should be maintained at 60 degrees.

2. Finer slurries and lower specific gravities should be pumped. However in reality, specific slurry consistencies are pumped to develop optimum strength during backfilling, with the result that valve wear is of secondary importance in these instances .

3. The closure velocity should be reduced. To prevent a drop in the tonnage pumped, an hydraulic controller could be used to slow the valve down just prior to impact, thus maintaining the pumping rate.

4. A valve poppet with a through hardness in excess of 600 Vickers should be used with a corresponding seat or disc with a through hardness in excess of 600 Vickers. The suitable material should also exhibit good corrosion resistance in South African mine waters.

Until recently, the service-life of a disc poppet valve in reciprocating slurry pumps in South African gold mines has been between 30 and 40 hours. The considerable financial losses incurred as a consequence of this downtime led to the initiation of this project. In an attempt to access the results, a suction valve consisting of a poppet (650 HV30) and a seat (600 HV30) made from BS 817M40 was installed in a pump. At the time of compilation of this thesis, the valve had been in service for 112 hours. This shows adequately that the prime objective of this work, to recommend a suitable material which will extend the service life has been realized.

It is considered that even greater improvements can be achieved if the material hardness can be extended beyond those hardnesses used in this work, which is in agreement with Fehn (19). The use of hard inserts such as ceramics may also increase valve life (45).

References

1. Allen C., Protheroe B.E and Ball A., The selection of abrasion corrosion resistant material for gold mining equipment, Journ. of South African inst. of Min. and Met, (1981)289-297.

2. Angus H.T., The significance of hardness, Wear, **54**, (1979)33-78.

3. Avery H.S., An analysis of the rubber wheel abrasion test, Wear of materials, ASME publ., (1981)367-377.

4. Baker P.J. and Jacobs B., A guide to slurry pipeline systems, BHRA Fluids Engineering, (1979)34.

5. Ball A., On the importance of workhardening in the design of wear resistant materials, Wear, **92**, (1983)201-207.

6. Barnett K., Suggested UCT Materials Eng. Dept. involvement in COMRO's slurry backfilling research, Mat. Eng. dept. report UCT, (1985).

7. Barnett K., Fundamentals of slurry pump valve design, Mat. Eng. Dept. report, University of Cape Town, (1986)March.

8. Barnett K., Fundamentals of slurry pump valve design, Mat. Eng. Dept. report, University of Cape Town, (1986)May.

9. Barnett K., Fundamentals of slurry pump valve design, Materials Engineering Department Report, University of Cape Town, (1986)August.

10. Bitter J., A study of erosive phenomena, Wear **6**, (1963)169-190.

11. Brown R., Jun E. and Edington J.W., Mechanism of solid particle erosive wear for 90° impact on copper and iron, Wear, **74**, (1981-1982)143-156.

12. Chamber of Mines Research Organisation of South Africa Annual Report, (1986)21-22.

13. Diesburg D.E. and Borik F., Optimizing abrasion resistance and toughness in steels and irons for the mining industry, Mat. for Mining Ind., (1974)Industrial symposium.

14. Engel P, Lyons T.H. and Sirico J.L., Impact wear model for steel specimens, Wear **23**, (1973)185-201.

15. Engel P., Percussive impact wear: a study of repetitively impacting solid components in engineering, Trib.Int., **11**(3), (1978)169-176.

16. Elkholy A., Prediction of abrasion wear for slurry pump materials, Wear , **84**, (1983)39-49.

17. Eyre T.S., Wear resistance of metals, Treatise on Material Science and Technology, **13**, (1979)363-441.

18. Faddick R.R., Proceedings of the 8th International conference on hydraulic transport of solids in pipelines, Hydrotransport 8, Johannesburg, chp.**10**, (1982).

19. Fehn B., Two cylinder piston pumps with hydraulic drive: technical characteristics and application options, 9th Int.Conf. on Hydraulic Trans. of Solids in Pipes, Rome, (1984).

20. Feld H. and Walters P., Contribution to the understanding of mineral/hard metal abrasive wear, Powder Metall. Int, **7**(4), (1975)188-190.

21. Finnie I., The mechanism of erosion of ductile metals, Proc. 3rd U.S. Natl.Cong.of Applied Mechanics, ASME, New York (1958), 527.

22. Fogel G., The influence of microstructure on abrasive wear resistance wear , Msc Thesis, Univ. Cape Town, Dept. Material Eng.(1981).

23. Garrison W.M. and Garriga R.A., Ductility and the abrasive wear of an ultrahigh strength steel, Wear, **85**, (1983)347-360.

24. Garrison W.M., Abrasive wear resistance: The effect of Ploughing and the removal of ploughed material, Wear, **114**(2), (1987)239-247.

25. Hokkingawa K. and Li Z.Z., The effect of hardness on the transition of abrasive wear mechanisms of steel, Wear of materials ,**1** ,(1987)585-593.

26. Hovis S.K., Talia J. and Scattergood R.O., Erosion mechanisms in aluminum and Al-Si alloys, Wear, **107**, (1986)175-181.

27. Hutchings I.M., A model for the erosion of metals by spherical particles at normal incidence, Wear, **70**, (1981)269-281.

28. Jackson L.D.A., Slurry abrasion, Candanian Inst. of Min. and Met. and the mining society of Nova Scotia Trans., **70**, 1967.

29. Jahanmir S., The mechanics of subsurface damage in solid particle erosion, Wear **61**, (1980) 309-324.

30. Kar J.N., Investigation of the role of microstructures of the two body abrasive wear resistance of steels, Wear of materials, (1981)415- 425.

31. Kashcheev V.N., Some aspects of improving abrasive resistance, Wear, 89, (1983)265-272.

32. Kayaba T., Hokkirgawa K. and Kato K., Analysis of the abrasive wear mechanism by successive observations of wear processes in a scanning electron microscope, Wear, **110**, (1986)419-429.

33. Keiser J., Heidersbach R., Dobbs D. and Oliver W., Characteristics of individual impact craters on selected aluminum alloys, Wear, **124**, (1988)105-118.

34. Khruschov M.M and Babichev M.A., Resistance to abrasive wear of structurally heterogeneous materials, Friction and Wear in Machinery, **12**, (1958)12-26.

35. Khruschov M.M., Principles of abrasive wear, Wear, **28**, (1974)69-89.

36. Krause H. and Senuma T., A contribution towards improving the applicability of laboratory wear tests to practice, Wear, **74**, (1981-1982)67-83.

37. Kwok C.K. and Thomas G., Microstructural influence on abrasive wear resistance of high strength, high toughness medium carbon steels, Wear of materials, (1983)140-147.

38. Larsen-Badse J., The abrasion resistance of some hardened and tempered carbon steels, Trans. Metall. Soc. AIME, **236**,(1966)146.

39. Larsen-Badse J. and Mathews K.G., Influence of structure on the abrasive resistance of a A1040 steel, Wear, **14**, (1969)199-206.

40. Larsen-Badse J. and Premaratne B., Effect of relative hardness on the transition in abrasive wear mechanisms, Wear of materials, (1983)161-166.

41. Levy G. and Morri J., Impact fretting in CO_2 based environments, Wear, **106**, (1985)97-138.

42. Levy A.V., The platelet mechanism of erosion of ductile metals, Wear, **108**, (1986)1-21.

43. Liu Y.J, Yand R.L., Cheng K.Q and Deng H.J, Wear of metallic materials under dynamic loading, Wear of materials, (1980)390-395.

44. Mc Queer J.I., Abrasion resistance of a series of vanadium white cast irons, MSc Thesis, Univ. Cape Town, Dept. Materials Eng., (1985).

45. Miller J.E., Reciprocating pumps for slurry service, (ASLE) Lubrication Eng., **41**(6), (1985)356-360.

46. Miller J.E., The Mechanics of Wear in Slurry pumping, (ASME) International symposium on slurry flows,**38**, (1986)181-187.

47. Misra A. and Finnie I., A classification of three body abrasive wear and design of a new tester, Wear, **60**, (1980)111-112.

48. Misra A. and Finnie I., An experimental study of three body abrasive wear, Wear of Materials, (1981)426-431.

49. Misra A. and Finnie I., On the size effect in abrasive and erosive wear, Wear, **65**, (1981)359-373.

50. Moore M.A., Richardson R.C.D. and Attwood D.G., The limiting strength of worn metal surfaces , Metallurgical Trans., **3**,(1972)2485-2491.

51. Moore M.A., Abrasive wear by soil, Trib. Int., (1975)105-110.

52. Moore M.A., Treatise on material science and technology, **13**, (1979).

53. Moore M.A., Abrasive wear, Metals in Engineering, **1**, (1978)97-109.

54. Moore M.A. and Mclees V.A., Effect of speed on the wear of steels and copper by bonded abrasive and soils, J.Agric.Eng.Res., **25**, (1980)37-45.

55. Moore M.A., Fundamentals of friction and wear of materials, Am. Soc. Metals, Material Science Seminar, (1980).

56. Moore M.A., Fundamentals of friction and wear, Amer. Soc. Metals, Materials Seminar (1980).

57. Moore M.A., Laboratory simulation testing for service abrasive wear environments, Fulmer Research Institute publ.(1986).

58. Murry M.J., Mutton P.J. and Watson J.D, Abrasive wear mechanisms in steels, Wear of materials ASME, (1979)257-265.

59. Mutton P.J and Watson J.D., Some effects of microstructure on the abrasion resistance of metals, Wear, **48**, (1978)385-398.

60. Ninham A., The effects of mechanical properties on erosion, Wear of materials, **2**, (1987).

61. Noel R.E.J., Abrasive-corrosive wear behaviour of Metals, MSc.thesis Dept. Materials Engineering, University of Cape Town, (1981).

62. Prasad N. and Kulkarni S.D., Relations between microstructure and abrasive wear of plain carbon steels, Wear, **63**, (1980)329-338.

63. Quirke S.J., Abrasive wear testing of steels in soil, MSc Thesis, Univ. Cape Town, Dept. Materials Eng., (1987).

64. Rabinowicz E., Dunn L.A. and Ruseell P.G., A study of abrasive wear under three body conditions, Wear, **4**(5), (1961)345-355.

65. Rabinowicz E., The wear equation for erosion of metals by abrasive particles, Proc. Int. Conf. on erosion by Solid and Liquid impact, **38**,(1979)1-5.

66. Rice S.L., Variation in wear resistance due to microstructural condition in high strength steel under repetitive impact, Trib.Int., (1979)25-29.

67. Rice S.L., Nowotny H. and Wayne S.F., Characteristics of metallic subsurface zones in sliding and impact wear, Wear of material, (1981)47-52.

68. Richardson R.C.D., The maximum hardness of strained surfaces and the abrasive wear of metals and alloys, Wear, **10**(5), (1967)353-382.

69. Richarson R.C.D., The wear of metallic materials by soil, Agric. Eng. Res., **12**(1), (1967)22-39.

70. Richardson R.C.D., The wear of metals by relatively soft abrasives, Wear , **11**, (1968)245-274.

71. Rickerby D.G. and Macmillan N.H., The erosion of aluminum by solid particle impingement at normal incidence, Wear, **60**, (1980)369-382.

72. Rickerby D.G. and Macmillan N.H., The erosion of Aluminum by solid particle impingement at oblique incidence, Wear, **79**, (1982)171-190.

73. Salesky W.J and Thomas G., Design of medium carbon steel for wear applications, Wear, **75**, (1982)21-40.

74. Sare I.R., Abrasion resistance and fracture toughness of white cast iron, Metal technology, **6**(11), (1979)412-418.

75. Sare I.R., Repeated impact-abrasion of ore crushing hammers, Wear, **87**, (1983)207-225.

76. Sarkar A.D., A study of crater volumes produced by single particles at low impact velocities, Wear, **87**, (1983)181-190.

77. Spurr R.T., The abrasive wear of metals, Wear, **68**, (1981)272-282.

78. Suh N.P., Delamination theory of wear, Wear, **25**, (1973)111-124.

79. Sundararajan G., An empirical relation for the volume of the crater formed during high velocity oblique impact Tests, Wear, **97**, (1984)9-16.

80. Torrance A.A., An explanation of hardness differential needed for abrasion, Wear , **68**, (1981)263-266.

81. Uetz H., Sommer K. and Khosiawi M.A., Correlation between model and workshop using abrasive wear operation procedure, Wear, **69**(1), (1981)25-41.

82. Verkerk, C.G., The current status of hydraulic backfill techniques in South Africa, Bulk solids handling, **3**(1), (1983)93-94.

83. Vingsbo O., Wear and wear mechanisms, Wear of materials (ASME publ.), (1979)620-635.

84. Wang Q., Wear resistance of steels under wet abrasive erosive conditions, Wear, **112**, (1986)207-216.

85. Wayne S.F., Rice S.L., Minakawa K. and Nowothy H., The role of microstructure in the wear of selected steels, Wear, **85**, (1983)93-106.

86. Yingjie L., Xingui B. and Keqiang C., A study on the formation of wear debris during abrasion, Trib. Int., (1985)107-110.

87. Zum Gahr K.H. and Mewes D., Severity of material removal in abrasive wear of ductile metals, Wear of Materials, ASME, (1979)130-139.

88. Zum Gahr K.H., Formation of wear debris due to abrasion of ductile metals, Wear, **74**, (1981-1982)353-373.

89. Zum Gahr K.H. and Mewes P., Severity of material removal in abrasive wear of ductile metals, Wear of materials, ASME, (1983)130-139.

90. Zum Gahr K.H., Modeling of two body abrasive wear, Wear, **124**, (1988)87-103.

APPENDIX A : FLOW CALCULATIONS

Calulations to determine the solid flow rate through the test cell

The time taken for a container of known volume to fill with slurry to a predetermined level was recorded for specific gravities of 1.7 and 1.9 g/cm^3. These specific gravities representing concentrations of 65 and 75 % solid respectively (fig.19).

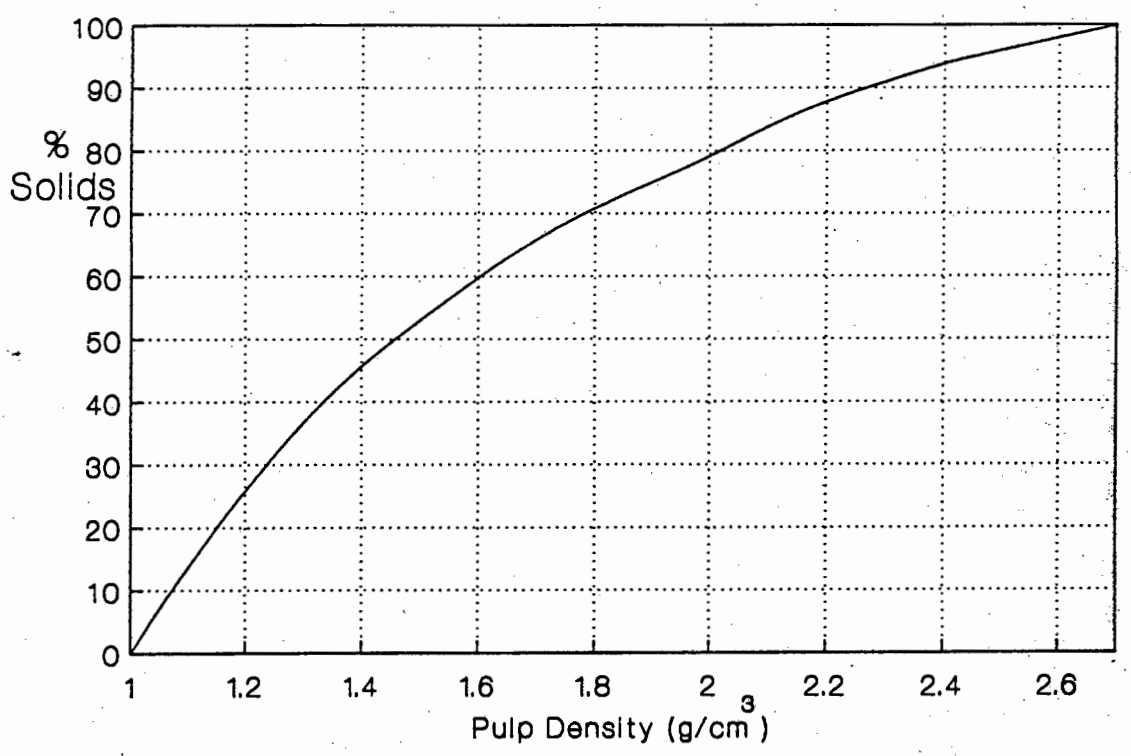

Fig. 1 Percentage solid versus specific gravity

Volume of the Container

The volume of the container may easily be calculated if the density of water is assumed to be 1 g/cm^3.

mass of container and water		1189g
mass of the container	-	84
mass of the water		1105g

Volume of the container = 1105 cm^3

Specific Gravity 1.7 g/cm^3

average time to fill container Xt_1= 2.186 sec

if the volume = V

The slurry flow rate = V/Xt_1 = V*0.457 cm^3/sec
but 65% of the slurry is solid
therefore flow rate of the solid = V*0.457*0.65
= 0.297V cm^3/sec

Specific Gravity 1.9 g/cm^3

average time to fill container Xt_2 =2.538 sec

container volume = V

The slurry flow rate = V/Xt_2 = V*0.3956 cm^3/sec
but 75% slurry is solid (fig.1)
therefore flow rate of the solid = V*0.396*0.75
= 0.297V cm^3/sec

Therefore the same volume of solid flows through the valve but at different flow velocities.

APPENDIX B : TESTING PROCEDURE

The testing procedure described below, was developed to minimize pipeline blockages during testing.

1. Clean the valve poppet and seat ultrasonically in alcohol and weigh, prior to testing.

2. Switch the compressor on. Periodically open the compressor tap to release condensate. If this is not performed, "jerky" reciprocation may occur during testing.

3. Clean the test cell with the air hose, prior to fitting the poppet and seat. Fit the seat O-ring and the cell O-ring. Clamp the test cell closed and attach the rubber inlet hose using the hose clamps.

4. Open and close the valve manually to ensure there are no obstructions in the test cell, and ensure the pneumatic exhaust is on before switching the air delivery on.

5. Turn the supply water line on and ensure the test valve is open. This is usually automatic.

6. Start the rotary agitator and the mixer pump. If the agitator motor labours, provide additional agitation with the aid of the air lance by probing the slurry.

7. One problem that materialised was that it was necessary to "wet" the pipeline before a high concentration slurry could be pumped along it. This was achieved by pumping water or dilute slurry ahead of the concentration slurry. Isolate the test cell circuit with the aid of the valve on the test cell line. Turn the water supply on allow it to flow through the by-pass pipeline. Turn the peristaltic pump on, slowly open the slurry supply tank valve. This releases slurry into the flow. Reduce the water flow simultaneously until only slurry from the supply tank is feeding the pump.

8. Slowly open the isolation valve and allow the slurry to flow through the test cell as well. This should be performed carefully because it is at this point that the slurry usually becomes hydraulically unstable.

9. For the coarse slurries (6mm nominal particle size), regulate the concentration by allowing the excess water to flow out of the slurry tank. The addition of fresh water to the fine slurry (200µm nominal particle size) is minimized to avoid losing the finely suspended slurry particles.

10. When the desired slurry concentration or specific gravity has been reached, begin the test i.e. cycling of the poppet valve.

11. On completion of a test, the flow must be returned to fresh water and the slurry supply tank valve must be closed. It is important to flush the system after each test.

12. Ensure the pneumatic circuit is off before opening the test cell. Remove the test specimen and clean immediately in alcohol, and weigh.

13. In the event of a blockage, the following procedure is recommended.

i) Stop the test valve cycling.

ii) Determine which line is blocked.

iii) If the test cell pipeline is blocked, isolate it with the aid of the pipeline valve and then flush the pipeline using the fresh water supply, without stopping the bypass slurry flow.Restart the test once the blockage has been removed.

iv) If the main pipeline is blocked, the entire system must be stopped and flushed before re-starting.

APPENDIX C : **VALVE WEAR EXPERIMENTAL DATA**

Table 1: Valve wear test data, 6mm nominal particle size, specific gravity 1.7 g/cm^3 , closure velocity 1.9 m/s and valve angle 60°.

VALVE SET	POPPET	SEAT	HARDNESS (HV30)	TIME PUMPED (Min.)	MATERIAL LOSS (grams)	MATERIAL LOSS RATE (g/hour)
1	X		301	200	0.68	0.20
		X	602	200	0.60	0.18
2	X		446	200	0.61	0.18
		X	602	200	0.85	0.26
3	X		547	200	0.47	0.14
		X	602	200	0.78	0.23
4	X		614	200	0.44	0.13
		X	602	200	0.88	0.26
5	X		652	200	0.32	0.10
		X	605	200	0.59	0.18

Table 2: Valve wear test data, 6mm nominal particle size, specific gravity 1.9 g/cm^3 , closure velocity 1.9 m/s and valve angle 60°.

VALVE SET	POPPET	SEAT	HARDNESS (HV30)	TIME PUMPED (Min.)	MATERIAL LOSS (grams)	MATERIAL LOSS RATE (g/hour)
6	X		452	200	0.66	0.20
		X	602	200	0.88	0.26
7	X		554	200	0.50	0.15
		X	602	200	1.29	0.39
8	X		648	200	0.38	0.12
		X	605	200	0.90	0.27
9	X		661	200	0.37	0.11
		X	605	200	0.82	0.25

Table 3: Valve wear test data, 200μm nominal particle size, specific gravity 1.7 g/cm^3 , closure velocity 1.9 m/s and valve angle 60°.

VALVE SET	POPPET	SEAT	HARDNESS (HV30)	TIME PUMPED (Min.)	MATERIAL LOSS (grams)	MATERIAL LOSS RATE (g/hour)
10	X		301	200	0.40	0.120
		X	598	200	0.30	0.090
11	X		452	200	0.39	0.117
		X	602	200	0.34	0.102
12	X		550	200	0.27	0.081
		X	605	200	0.29	0.087
13	X		648	200	0.26	0.078
		X	598	200	0.29	0.087

Table 4: Valve wear test data, 200μm nominal particle size, specific gravity 1.9 g/cm^3 , closure velocity 1.9 m/s and valve angle 60°.

VALVE SET	POPPET	SEAT	HARDNESS (HV30)	TIME PUMPED (Min.)	MATERIAL LOSS (grams)	MATERIAL LOSS RATE (g/hour)
14	X		298	200	0.53	0.159
		X	598	200	0.42	0.126
15	X		457	200	0.46	0.138
		X	602	200	0.37	0.111
16	X		638	200	0.32	0.096
		X	604	200	0.34	0.102
17	X		652	200	0.24	0.072
		X	605	200	0.39	0.117

Table 5: Valve wear test data, 6mm nominal particle size, specific gravity 1.7 g/cm^3 , closure velocity 1.3 m/s and valve angle 60°.

VALVE SET	POPPET	SEAT	HARDNESS (HV30)	TIME PUMPED (Min.)	MATERIAL LOSS (grams)	MATERIAL LOSS RATE (g/hour)
18	X		652	200	0.20	0.060
		X	602	200	0.40	0.120
19	X		618	200	0.21	0.063
		X	602	200	0.45	0.135
20	X		550	200	0.34	0.102
		X	598	200	0.59	0.177
21	X		459	200	0.36	0.108
		X	594	200	0.45	0.135

Table 6: Valve wear test data, 6mm nominal particle size, specific gravity 1.7 g/cm^3 , closure velocity 1.7 m/s and valve angle 60°.

VALVE SET	POPPET	SEAT	HARDNESS (HV30)	TIME PUMPED (Min.)	MATERIAL LOSS (grams)	MATERIAL LOSS RATE (g/hour)
22	X		666	200	0.29	0.087
		X	598	200	0.60	0.180
23	X		614	200	0.30	0.090
		X	598	200	0.68	0.204
24	X		543	200	0.40	0.120
		X	602	200	0.53	0.159
25	X		454	200	0.46	0.138
		X	602	200	0.64	0.192

Table 7: Valve wear test data, 200μm nominal particle size, specific gravity 1.7 g/cm^3 , closure velocity 1.3 m/s and valve angle 60°.

VALVE SET	POPPET	SEAT	HARDNESS (HV30)	TIME PUMPED (Min.)	MATERIAL LOSS (grams)	MATERIAL LOSS RATE (g/hour)
26	X		639	200	0.16	0.048
		X	602	200	0.17	0.051
27	X		550	200	0.17	0.051
		X	610	200	0.20	0.060
28	X		439	200	0.18	0.054
		X	598	200	0.17	0.051
29	X		302	200	0.20	0.060
		X	602	200	0.24	0.072

Table 8: Valve wear test data, 200μm nominal particle size, specific gravity 1.7 g/cm^3 , closure velocity 1.7 m/s and valve angle 60°.

VALVE SET	POPPET	SEAT	HARDNESS (HV30)	TIME PUMPED (Min.)	MATERIAL LOSS (grams)	MATERIAL LOSS RATE (g/hour)
30	X		639	200	0.21	0.063
		X	602	200	0.28	0.084
31	X		550	200	0.25	0.075
		X	606	200	0.28	0.084
32	X		449	200	0.30	0.090
		X	606	200	0.34	0.102
33	X		304	200	0.33	0.099
		X	594	200	0.32	0.096

Table 9: Valve wear test data, 6mm nominal particle size, specific gravity 1.7 g/cm^3 , closure velocity 1.7 m/s and valve angle 45°.

VALVE SET	POPPET	SEAT	HARDNESS (HV30)	TIME PUMPED (Min.)	MATERIAL LOSS (grams)	MATERIAL LOSS RATE (g/hour)
34	X		644	200	0.35	0.105
		X	602	200	0.60	0.180
35	X		554	200	0.37	0.111
		X	610	200	0.52	0.156
36	X		454	200	0.54	0.162
		X	606	200	0.70	0.210
37	X		314	200	0.61	0.183
		X	602	200	0.64	0.192

Table 10: Valve wear test data, 6mm nominal particle size, specific gravity 1.7 g/cm^3 , closure velocity 1.7 m/s and valve angle 75°.

VALVE SET	POPPET	SEAT	HARDNESS (HV30)	TIME PUMPED (Min.)	MATERIAL LOSS (grams)	MATERIAL LOSS RATE (g/hour)
38	X		644	200	0.38	0.114
		X	606	200	0.82	0.246
39	X		543	200	0.51	0.153
		X	598	200	0.80	0.240
40	X		454	200	0.62	0.186
		X	598	200	0.82	0.246
41	X		317	200	0.73	0.219
		X	602	200	1.10	0.330

Table 11: Valve wear test data, 200µm nominal particle size, specific gravity 1.7 g/cm^3 , closure velocity 1.7 m/s and valve angle 45°.

VALVE SET	POPPET	SEAT	HARDNESS (HV30)	TIME PUMPED (Min.)	MATERIAL LOSS (grams)	MATERIAL LOSS RATE (g/hour)
42	X		639	200	0.28	0.084
		X	610	200	0.27	0.081
43	X		554	200	0.30	0.090
		X	602	200	0.36	0.108
44	X		452	200	0.32	0.096
		X	606	200	0.39	0.117
45	X		229	200	0.34	0.102
		X	602	200	0.30	0.090

Table 12: Valve wear test data, 200µm nominal particle size, specific gravity 1.7 g/cm^3 , closure velocity 1.7 m/s and valve angle 75°.

VALVE SET	POPPET	SEAT	HARDNESS (HV30)	TIME PUMPED (Min.)	MATERIAL LOSS (grams)	MATERIAL LOSS RATE (g/hour)
46	X		639	200	0.33	0.099
		X	602	200	0.45	0.135
47	X		547	200	0.35	0.105
		X	606	200	0.45	0.135
48	X		452	200	0.40	0.120
		X	590	200	0.49	0.147
49	X		295	200	0.51	0.153
		X	602	200	0.40	0.120

APPENDIX D : SPECIMEN GEOMETRY - POPPET VALVE

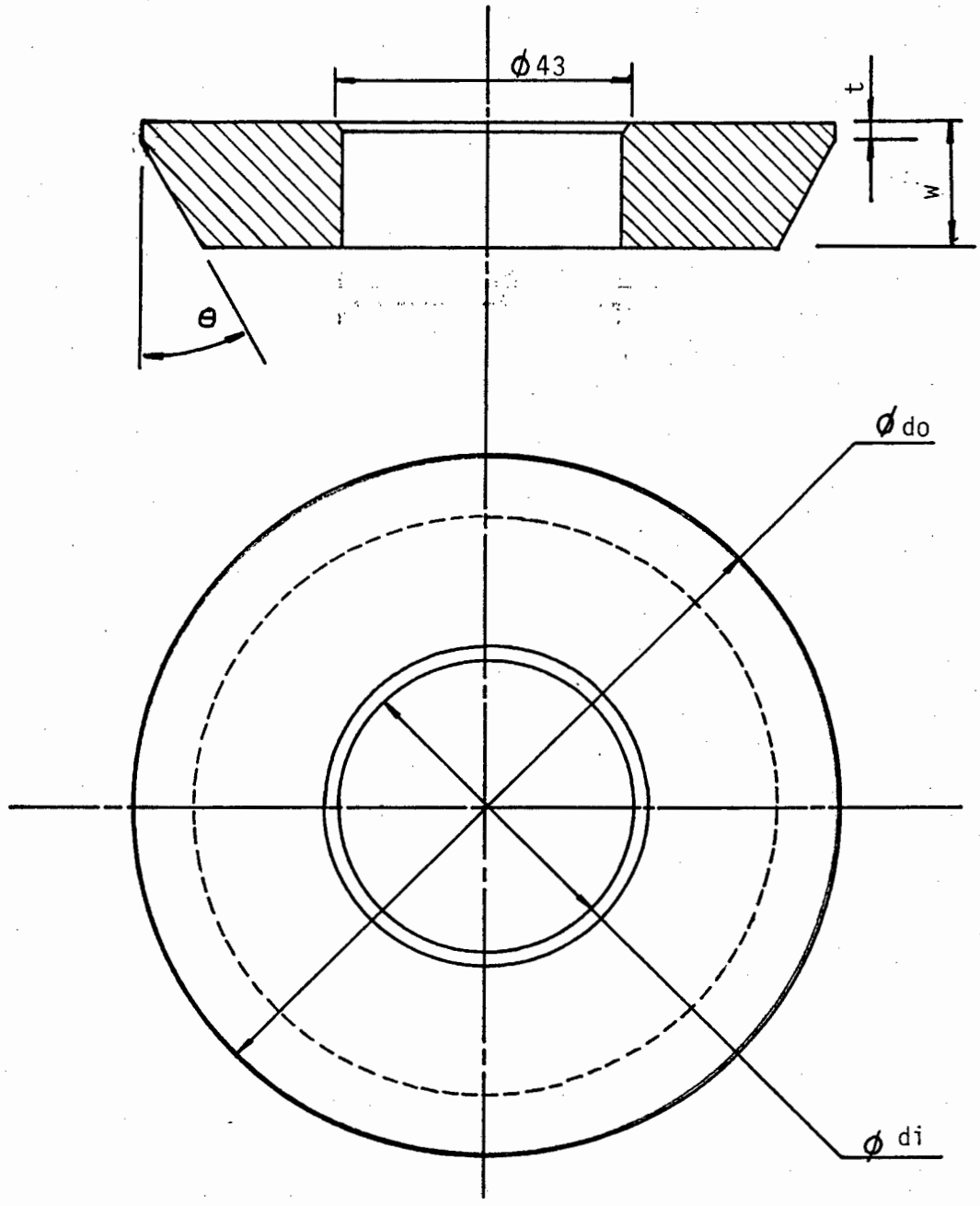

Dimensions in millimeters Scale : 1:1

θ	t	W	do	di
45°	3	17	100	40
60°	3	17	100	40
75°	0	17	93	40

SPECIMEN GEOMETRY - SEAT

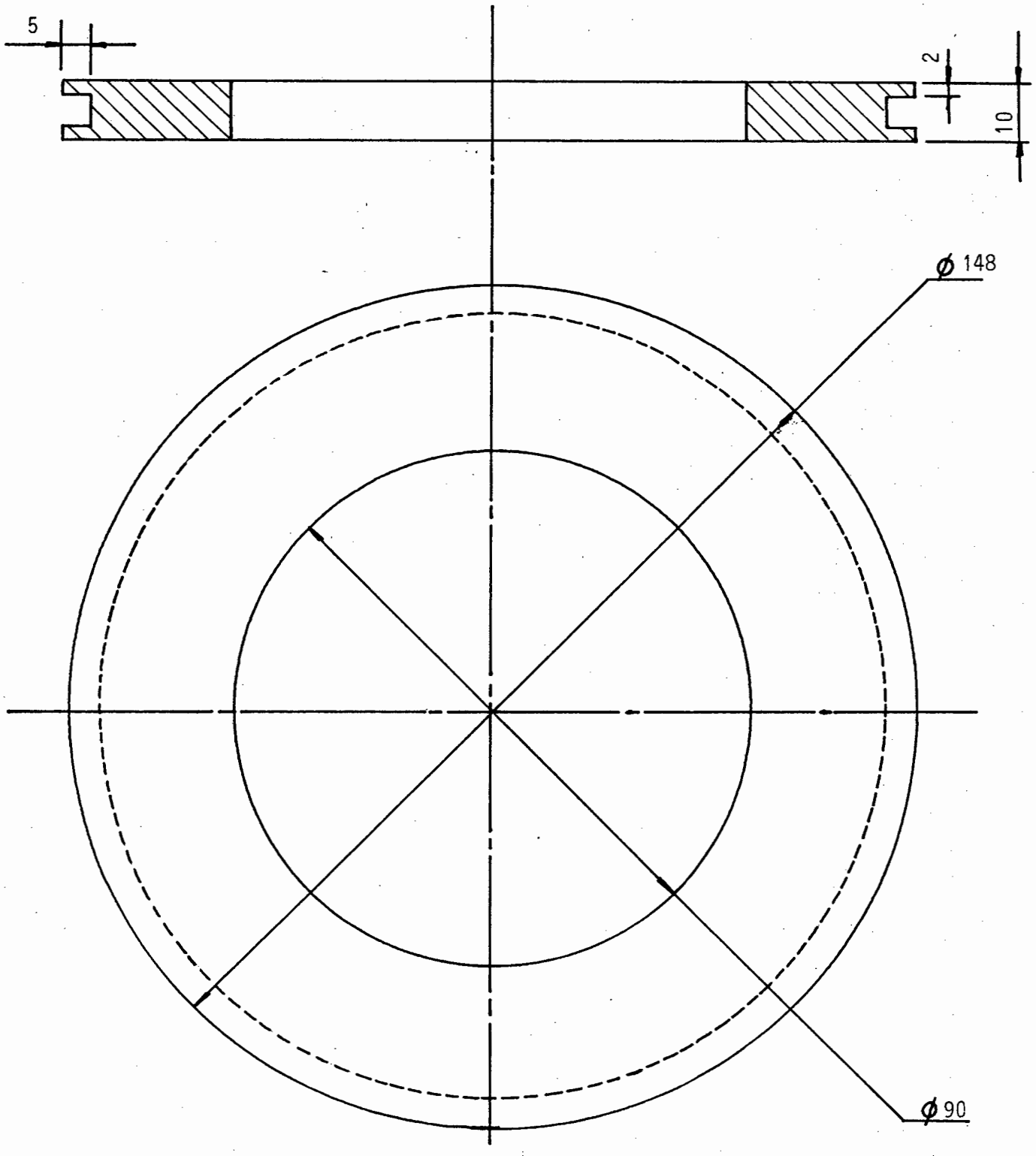

Dimensions in millimeters Scale : 1:1

APPENDIX E : PAPER SUBMITTED TO ANTIWEAR 1988

THE WEAR OF VALVES IN SLURRY PUMPS

S.H.D. Joffe and C. Allen
Department of Materials Engineering
University of Cape Town
South Africa

SYNOPSIS

Disc poppet valves which are similar to those used in reciprocating slurry pumps have been subjected to a laboratory wear test in quartzitic slurries which simulates actual working conditions. Wear has been studied as a function of valve hardness, valve closure velocity, slurry density and valve angle. It has been shown that large decreases in the wear rate can be achieved by control of operating parameters. An explanation for such behaviour has been made based on the mechanisms of impact and abrasive wear, which predominate during operation of the valves.

INTRODUCTION

The Chamber of Mines Research Organization (COMRO) is currently developing backfilling systems for use in deep level South African gold mines. One type of backfilling system involves the return of comminuted waste rock, by hydraulic transport, to the working face or stope to provide underground support, so improving mining conditions.

The comminuted waste rock consists primarily of quartzite which has been crushed to a diameter of 6 mm and less (fig. 1). Water is then added to the crushed rock to produce a slurry containing approximately 80 per cent solids. The slurry is pumped at high pressure and low velocity for distances of over a kilometre.

Positive displacement or reciprocating pumps, originally designed to pump concrete, are typically used to pump backfill slurries. The valve assembly of a reciprocating pump is illustrated in fig. 2. It is a hydraulically driven twin-cylinder pump. The two pumping pistons reciprocate, i.e. while one piston draws in fresh slurry, the other piston pushes the medium into the pressure line. The slurry flow is controlled by means of disc poppet valves.

Each pumping cylinder has one suction and one pressure or delivery valve. The poppet valves are actively controlled, being operated in such a manner that on the side of the intaking piston the suction valve is opened and the pressure valve is closed. During the pumping stroke the suction valve is closed and the pressure valve open. At the end of a stroke, reversal of the valves ideally takes place in such a way that the formerly open valves are closed before the closed valves are re-opened.

Although similar pumps are used abroad to pump backfill (1,2) it would appear that the service life of valve bodies and discs in pumps used to transport South African backfill slurries is considerably lower due to the highly abrasive nature of the quartzite slurry. Experience to date has shown that failure of the valve poppet and seat can occur after only 30 hours, corresponding to 700 tonnes of dry solids (3). A valve is usually classified as a failure when an

excessive loss in pumping pressure occurs due to improper sealing of the worn valve. The delivery or pressure valve reportedly wear much faster than the suction valves. One example of such a valves failure can be seen in fig. 3 where both abrasive and erosive wear is evident.

Particles are trapped between the valve and its seat on valve closure. The hard quartzite particles indent the valve material leading to surface deformation and material removal. With progressive wear, the valve is unable to seal completely. Any uneven wear, coupled with the high differential pressure across the valve, causes slurry to flow rapidly through the gap which forms, resulting in flow erosion of the valve material.

This paper is an attempt to establish the important operating parameters controlling the life of disc poppet valves in pumps used for the transportation of quartzite slurries, through an investigation of operating parameters and valve design, and to correlate the valve wear resistance with microstructural parameters. The overall objective is to suggest modifications to the design of reciprocating or positive displacement pumps to maximise wear resistance.

EXPERIMENTAL PROGRAMME

Test Rig

Ideally the wear behaviour of materials should be monitored in-situ. However, it is not always practical or feasible to mount such an operation and as a consequence laboratory tests which attempt to simulate the real operating conditions are preferable to field tests. In the present instance, it was considered that a laboratory rig could successfully reproduce the in-situ working conditions and allow process variables such as valve closure velocity, slurry constitution and valve design to be altered. Consequently a laboratory rig was built in which full size valves could be tested under similar operating conditions and slurry densities as pump valves operating in the gold mines. A diagram of the rig test cell is shown in fig. 4.

A peristaltic pump delivers fresh slurry from an agitated supply tank to the test cell at a predetermined constant flow rate. The closed loop system allows the slurry to be cycled continuously for the duration of the test. Fresh slurry is used for each complete test.

In order to ensure that the slurry conditions during testing were kept relatively constant a slurry degradation test was performed in which slurry was pumped continuously through the working system for a period of eight hours. Samples were taken at regular intervals and examined for shape and size changes.

The slurry degradation test over a continuous period of eight hours showed that there was little alteration in the morphology and size distribution of the quartzite particles. A sample taken initially was compared to a similar sample which had undergone testing. Several different size ranges were analysed from 63 m to 6 mm. No substantial changes in the morphology of the particles were observed except for a slight blunting of the cutting edges for the large particles. Typical results are illustrated in figs. 5 and 6. Similarly the particle size fractions did not change substantially during the eight hour period other than a small discrepancy for particles less than 0.5 mm (fig. 1). This discrepancy was considered to be due to sampling technique or to the possibility that part of these fractions were washed away prior to the system being closed at the beginning of the test.

A pneumatic control system permits easy adjustment of the valve closure velocity, the number of impacts and the frequency of impacts. A LVDT in conjunction with an oscilloscope was used to determine these process characteristics.

Materials

A medium carbon, low alloy steel conforming to BS 817M40 was selected as the disc poppet valve and seat material. The chemical analyses are shown in Table 1. In practice a surface hardened steel is used for the valve and seat material. However, it was considered that the through hardening steel BS 817M40 would provide more controllable and consistent material properties throughout wear testing.

Heat Treatment

Following machining, the valve components were heat treated in an air muffle furnace. Decarburisation of the surfaces was minimised by the use of ceramic paste and by employing dry nitrogen gas flowing through the furnace. The components were austenitised at 850°C for thirty minutes and quenched into oil. Afterwards the valves were tempered for one hour between 100°C and 450°C to achieve a range of hardness values between 650HV30 and 450HV30 respectively. Typically the surface hardness of carburised steel valves was approximately 700HV30. All the valve seats were tempered for one hour at 200°C to give a hardness of approximately 600HV30.

Hardness Testing

Bulk hardness testing of the valves was carried out on a Eseway hardness machine using a load of 30 Kg.

Microhardness measurements on quartzite samples were made using a Shimadzu microhardness tester and a load of 500 g. Prior to indentation the mounted quartzite particles were coated with a thin film of gold palladium. The reflectivity of this surface facilitated the identification and measurement of the resultant impression. The hardness of the slurry particles was found to be 1168 ± 90 on the Vickers hardness scale. The variation in hardness arises from the various phases and minerals which constitute a single slurry particle.

Wear Testing

Wear testing was carried out using 6 mm diameter comminuted waste quartzite particles with a diameter of 6 mm and less at densities of 1.7 gcm^{-3} and 1.9 gcm^{-3}. Tests were conducted for closure velocities from 1.3 ms^{-1} to 1.9 ms^{-1}, valve angles from 45° to 75° (see fig. 12) and for four poppet valve hardnesses between 650HV30 and 450HV30. The following parameters were kept constant for all the tests.

i) 10 000 valve closures
ii) cycling rate approximately 50 closures/min.
iii) all tests in the vertical orientation (inlet or suction valve)
iv) seat or disc heat treatment uniform i.e. 600±10 HV30
v) pH range of slurry approximately 7.1 - 7.5

Prior to testing the valve faces were polished lightly using 240 grit emery paper and weighed on a Mettler balance to an accuracy of 0.01 g. The mass loss was monitored at regular intervals during testing by removing the valve, drying and weighing. The reproducibilty of the test was found to be better than ±5 per cent which was considered to be satisfactory for this type of testing.

RESULTS

The results of the wear testing carried out on poppet valves of varying hardnesses with change in valve angle and closure velocity are shown in figs. 7 - 10. In all cases the mass loss of the valve is reported for 10 000 cycles.

Valve Hardness

It is apparent that the mass loss in all tests is a function of material bulk hardness. As the hardness of the valve increases the mass loss decreases and the wear resistance increases. Fig. 7 indicates that the effect of bulk hardness on wear resistance is not linear. At bulk hardnesses greater than 600HV30 the mass loss, using the 1.7 gcm^{-3} slurry, is seen to decrease more rapidly with increase in hardness. This trend is not as significant with the higher density slurry (1.9 gcm^{-3}). It is also noticeable that the mass loss for valves of similar hardness is higher when subjected to the higher density slurry despite the total throughput of solids being similar for both slurry densities.

The sharp decrease in mass loss for valve hardnesses in excess of 600 HV30 can be seen more clearly in fig. 8 which is a log-log plot of mass loss against the relative hardness Ha/H, where Ha = slurry hardness and H = bulk hardness of the poppet valve. There appears to be an inflection on the relative hardness versus mass loss curve. At a closure velocity of 1.9 ms^{-1} this transition is approximately 1.9 Ha/H for a slurry specific gravity of 1.9 gcm^{-3}. At the higher slurry density a similar transition is found at a Ha/H value of 1.9 but is much less pronounced than for the lower slurry density of 1.7 gcm^{-3}.

Valve Closure Velocity

The results of the valve closure velocity tests which were carried out for velocities of 1.3 ms^{-1}, 1.7 ms^{-1} and 1.9 ms^{-1} for a slurry density of 1.7 gcm^{-3} and at a valve angle of 60° are presented in fig. 9. It is clear from fig. 9that increasing the valve closure velocity results in a greater mass loss for all valves regardless of relative hardness (Ha/H). The curves all display a transition in wear behaviour which appears to shift marginally at lower closure velocities to a higher relative hardness (Ha/H) value.

Valve Angles

Three valve angles, namely 45°, 60° and 75° were subjected to wear testing at a valve closure velocity of 1.9 ms^{-1} and a slurry density of 1.7 gcm^{-3}. The results of the 6 mm comminuted waste tests are shown in fig. 10 for 10 000 cycles. With the exception of the highest valve hardness i.e. 650HV30, all the valves show progressively more wear with an increase in valve angle and a decrease in hardness. The hardest valve appears to suffer slightly less wear at 60° than at 45° or 75°.

Metallographic Examination

Examination of the worn valves showed that generally wear had occurred solely around the seating line. There was no sign of significant wear on the majority

of the valve face. This seating line appeared to show three distinct wear zones as illustrated in fig. 11.

Zone 1 consisted of relatively unworn valve material adjacent to the seating line. Zone 2 consisted of an area where the material has been deformed and displaced laterally leaving a deep groove. In contrast to Zone 2, Zone 3 showed definite signs of abrasive wear in which quartzite particles had ploughed out wear tracks. In addition there was evidence that impacting quartzite particles were also responsible for surface deformation in this area. The actual size of these zones was found to vary depending on the bulk hardness of the valve. Harder valves resulted in smaller zones. Zone 2 rarely exceeded 500 m in width, whilst Zone 3 was approximately 4 mm in width.

DISCUSSION OF RESULTS

Clearly, in order to interpret the wear data, an understanding of the wear mechanisms which operate during the pumping of slurries is a prerequisite. It is considered that the wear loss suffered by the valves is due primarily to impact with the quartzite particles and to three-body abrasive wear.

As the valve begins to close rapidly, the larger particles in the slurry are trapped between the valve and the seat (fig. 12). The particles indent the valve surface and are crushed under the high load, resulting in impact damage to the valve. This zone of impact is confined to the seating line area. These impacts result in the formation of craters and material is extruded around the impacting particle causing work-hardening of the surface material. Multiple impacts eventually lead to microcracking and microspalling of the surface layers (fig. 13).

As the gap between the valve and seat decreases further during closure, any trapped abrasive particles are forced to move across the valve and seat surfaces. This movement results in further deformation and/or microcutting of the metal surfaces through three body abrasive wear.

The proportion of wear damage in the present case appears to be mainly due to impact rather than abrasion since particles, because of the geometric configuration of the valve and seat arrangement, do not move great distances across the valve surface.

This work has established that as the bulk hardness of the valve is increased the mass loss or alternatively the wear rate of the steel decreases, regardless of valve closure velocity, valve angle and slurry density. Furthermore, significant improvements in the wear resistance can be obtained at relative hardness values in excess of 1.9. In the present instance where quartzite is the transported material, the hardness of the steel used in such valves should be in excess of approximately 600HV30. Such a result is in agreement with the work of Elkholy (4) who found a similar transition value for sand/water slurries. It also parallels the results of Richardson and other workers (5,6) on abrasive wear testing who found that for significant increases in wear resistance the hardness of the material must be greater than eighty per cent the hardness of the abrasive.

This change in wear behaviour is believed by many workers to be due to a change in the abrasive wear mechanism with increase in hardness or loss of ductility (7). As the hardness increases, cutting wear becomes more prominent compared to surface deformation and ploughing which occurs for the softer materials. The

transition from ploughing to cutting wear manifests itself in a change in the shape of the mass loss versus hardness curve.

Whilst in the present case the hardness of the material at the transition point is lower than that postulated by Richardson, the surface hardness is likely to be harder than the bulk hardness as a result of work hardening. Furthermore, Richardson's work was based mainly on the abrasive wear process whereas in this instance impact wear makes a significant contribution to the total mass loss.

Increase in slurry density is also seen to increase the mass loss during testing. However, the effect on wear rate by changing the slurry density is not as pronounced as changing the valve hardness. Whilst the volume of solids flowing through the test cell did not alter with an increase in slurry density due to a drop in the flow velocity in these tests, more particles are likely to be trapped between the valve and the seat on closure, resulting in a greater number of impact points. This in turn will result in greater work hardening rates and a greater loss of material.

Similarly at higher closure velocities there is a greater component of impact force, greater penetration of the quartzite particles in the valve and seat,greater work hardening and greater material loss as a result. Furthermore high velocities are known to increase abrasive wear (8). Since the majority of damage to the working components appears to be due to impact the design of the pumps should clearly allow for low closure velocities regardless of the initial hydraulic ram speed.

The increase in wear rate with increase in valve angle can be explained on the basis of the tangential component of impact causing extrusion and deformation ahead of the impacting particle. Lower angles of impact lead to greater extrusion of material from the surface which can result in ductile tearing and greater loss of material than 90° impacts (fig. 14). Furthermore, such ridges are more easily removed through subsequent abrasive wear processes. Thus as the valve angle decreases from 75° to 45° there is a 10 per cent improvement in wear resistance for valves with similar hardness.

Whilst it is difficult to quantify precisely the increase in valve life resulting from changes in operating parameters it is clear that significant improvements can be made by careful control of operating parameters. For instance, decreasing the closure velocity from 1.9 ms^{-1} to 1.3 ms^{-1} results in a 50 per cent decrease in the mass loss for valves of similar hardness. Overall, it would appear that the life of disc poppet valves can be increased by at least 100 per cent on the basis of the results presented in this paper. However, care must be exercised in interpreting such data in isolation from the total wear within the system. In this case the total wear involves both the poppet and the seat. No attempt was made to improve the performance of the seat through recourse to material selection or design parameters. Improvements to the life of the seat could well result in further improvements to the life of the valve itself.

CONCLUSIONS

Significant improvements in the life of disc poppet valves in reciprocating slurry pumps can be achieved through increasing material hardness, reducing the actual closure velocity, slurry density and valve angle. In the present work it has been shown that at least 100 per cent improvement to the life of valves with similar hardness can be achieved though careful assessment of and attention to the operating parameters.

ACKNOWLEDGEMENTS

This paper reports work which has been undertaken for and suppported by the Chamber of Mines Research Organization of South Africa. Mrs AC Ball, Mrs H Bohm, Mrs S Betz and Mr B Greeves are thanked for their assistance in the preparation of the manuscript.

REFERENCES

1. B. Fehn, Two-cylinder Pumps with Hydraulic Drive, Hydraulic Transport of Solids in Pipe, 9th Int. Conf., Rome, (1984), 181-187.
2. J.E. Miller, Mechanics of Wear in Slurry Pumping, Int. Symp. on Slurry Flows, ASME, vol. 38, (1986), 181-187.
3. Private Communication - COMRO.
4. A. Elkholy, Prediction of Abrasion Wear for Slurry Pump Materials, Wear, 84, (1983), 39-49.
5. R.C.D. Richardson, Wear of Metals by Relatively Soft Abrasives, Wear, 11, (1968), 245-274.
6. M.A. Moore, Fundamentals of Friction and Wear of Materials, ASM, Materials Science Seminar, (1980).
7. M.J. Murray, P.J. Mutton and J.D. Watson, Wear of Materials, ASME, (1979), 257.
8. A. Misra and J. Finnie, An Experimental Study of Three Body Abrasive Wear, Wear of Materials, ASME, (1981), 426-431.

FIGURE CAPTIONS